Department Drilling and Completion Engineering

Master's Thesis

Comparison of Separation Factor Estimations based on Scenario Analysis

Robin Godot Richard Kühnast

Supervisor: Univ.-Prof. Dipl.-Ing. Dr.mont. Gerhard Thonhauser

Co-Supervisor: MSc Philip Bailey

Leoben, March 2015

Affidavit

I declare in lieu of oath, that I wrote this thesis and performed the associated research myself, using only literature cited in this volume.

Eidesstattliche Erklärung

Ich erkläre an Eides statt, dass ich die vorliegende Arbeit selbstständig verfasst, andere als die angegebenen Quellen und Hilfsmittel nicht benutzt und die den benutzten Quellen wörtlich und inhaltlich entnommenen Stellen als solche kenntlich gemacht habe.

Leoben, am …… (Unterschrift)

Acknowledgements

I would like to express my gratitude to the Chair of Drilling and Completion Engineering (Mining University Leoben) for the opportunity to write this thesis.

My special thanks are dedicated to Philip Bailey (Mining University Leoben) for the professional support and helpful comments during the entire development of this work.

Furthermore, I would like to thank Agilis Software Solutions Incorporated for the permission to use KellyDown™ and for the support in the launching phase of the software. In addition to that I want to thank Peter Fischbacher from Schlumberger for the supportive surveying material.

Finally, I want to thank my family, friends and life partner Pia Benedikt for the endless support and unconditional love.

Abstract

The growth of complex drilling activities worldwide demands reasonable practices to deal with uncertainties related to the wellbore position. The error associated to a measurement has been reviewed in great detail and advanced technology combined with sophisticated modeling allows the industry to manage the risk of wellbore collision incidents.

However, there is a huge variety in risk management applied by different companies. Separation or clearance factors are widely used, but a standard has not been defined. This can be blamed on the complexity of modeling uncertainty. The Industry Steering Committee on Wellbore Survey Accuracy (ISCWSA) published several models, suggestions and recommendations, but an explicit standard protocol has not been set.

The aim of this thesis is to reduce this lack of clarity and present a tool that can be used to compare ellipsoids of uncertainty and consequently separation distances and factors. A scenario was created that is built on a standard set of wellpaths published by the ISCWSA. Eleven different situations of a reference and an offset well are studied and all assumptions, limitations and calculations are described and analyzed. The results show the variety of calculation methods and can be used to recognize shortcomings and impairments. The suggestions made are based on typical real-world conditions and should therefore be more sensitive than general solutions. In addition to that, the estimation of separation factors is discussed in detail. It is recommended to use a standard separation factor that incorporates collision probabilities and allows for distinction between shallow and deep depths.

Kurzfassung

Die stetige Entwicklung komplexer Bohraktivitäten weltweit verlangt nach angemessenen Praktiken um mit Unsicherheiten im Zusammenhang mit der Position des Bohrlochs zu verfahren. Der Messfehler wurde von der Industrie bereits genau analysiert und das Zusammenspiel aus Spitzentechnologie mit anspruchsvoller Modellierung ermöglicht es heutzutage Risiken einer Bohrlochkollision zu verwalten.

Es gibt jedoch eine große Vielfalt im Risikomanagement verschiedener Firmen. Separations- oder Abstandsfaktoren sind im Gebrauch, aber bis jetzt wurde noch kein Standard definiert. Ein Grund für dieses Fehlen ist die Komplexität der Modellierung von Ungewissheiten. Das Industry Steering Committee on Wellbore Survey Accuracy (ISCWSA) hat verschiedene Modelle, Vorschläge und Empfehlungen publiziert, jedoch fehlt bei dieser Analyse auch eine eindeutige Lösung.

Aus diesem Grund soll die folgende Arbeit diese Unklarheit reduzieren und ein Werkzeug präsentieren, das benutzt werden kann um Ellipsoids of Uncertainty (EOU) und somit die Länge der Separation sowie Separationsfaktoren zu vergleichen. Es wurde ein Szenario mithilfe von Kellydown™ erstellt, welches auf elf verschiedene Situationen zwischen einer Referenzbohrung und einer Versatzbohrung eingeht und die Annahmen, Limitierungen und Berechnungen beschreibt und analysiert. Die Resultate bezeugen die hohe Variabilität verschiedener Berechnungsmethoden und können benutzt werden um Mängel und Defizite der eigenen Vorgehensweise aufzudecken. Die Vorschläge basieren somit auf typischen Bedingungen der realen Welt und sollten somit eine höhere Sensibilität gegenüber generellen Lösungsempfehlungen aufweisen. Zusätzlich wird die Erstellung von Separationsfaktoren genauer betrachtet und es wird aufgrund der Ergebnisse empfohlen einen Ansatz zu verwenden, der die Kollisionswahrscheinlichkeit miteinbezieht und somit eine Unterscheidung zwischen geringen und erheblichen Tiefen ermöglicht.

Table of Contents

Table of Figures

Nomenclature

A	azimuth angle
AW	Angular well
$B(s)$	build rate
B_x, B_y, B_z	magnetometer measurements
$[C]$	covariance matrix
CVM	center-vector method
d	diameter
d_s	diameter subject well
d_o	diameter offset well
D	center to center distance
DD	directional drilling
DDI	directional drilling index
dl	horizontal length of ds
DLS	dogleg severity
dp	change of measurement vector
dr	change of position vector
ds	small segment of a wellbore
dx, dy, dz	components of ds
δ	separation distance in pedal-curve method and center-vector method
ΔE	change in east direction
EOU	ellipsoid of uncertainty
e_i	i^{th} error vector
G	global
G_x, G_y, G_z	accelerometer measurements
HSE	health, safety and environment
HW	Horizontal well
I	inclination angle
I_1	inclination angle at survey station 1
I_2	inclination angle at survey station 2
IFR	in field referencing

k_s	separation factor for comparison of pedal-curve method to center-vector method
κ	curvature of the arc
ISCWSA	Industry Steering Committee for Wellbore Survey Accuracy
MCM	minimum curvature method
MD	measured depth
MDM	minimum distance method
ΔMD	change in measured depth
MWD	measurement while drilling
μ	mean value
ΔN	change in north direction
NEV	North East Vertical
OOW	Overlapping Opposite well
P	collision probability
$\underline{p_1}$	point of survey station 1
$\underline{p_2}$	position of survey station 2
PCM	pedal-curve method
PW	Perpendicular well
R	radius of curvature
R	random
RW	Reference well
S	systematic
S	center to center distance
s_1, s_2	radius of pedal-curve method or center—vector method
S_{12}	course length
Δs	segment of a wellbore
SF	separation factor
SOW	Short Opposite well
σ	standard deviation
σ_A	standard deviation of survey uncertainty well A

σ_B	standard deviation of survey uncertainty well B
σ_i	i^{th} error magnitude
$\sigma_N^2, \sigma_E^2, \sigma_V^2$	variances of the respective directions
$\sigma_N\sigma_E$, $\sigma_N\sigma_V$, $\sigma_E\sigma_V$	covariances of N, E and V
Δx, Δy, Δz	components of Δs
$\underline{t}$.	unit direction vector
$\underline{t_1}$	unit direction vector at survey station 1
$\underline{t_2}$	unit direction vector at survey station 2
$\mathrm{T}(s)$	turn rate
TC	travelling cylinder
V	Vertical
ΔV	change in vertical depth
W	well by well
z	true distance

1. Introduction

In the early years of the petroleum industry, it was common practice to drill wells vertically or with uncontrolled deviation. But with increasing complexity of the hydrocarbon systems, the drilling technology advanced and targets with a horizontal distance to the surface location became reachable. Directional drilling was introduced and can be defined as the process and all activities required to plan and drill a non-vertical well.

The development of this evolutionary technology was accompanied by the question of the exact location of the wellbore. Three technical terms describing the position of the well had to be established: the length of the wellbore (also called measured depth MD), the hole inclination angle (angle between hole and vertical) and the hole azimuth (direction from magnetic north). The theoretical location of the wellbore can be described from the three measurements. But the transformation into Cartesian coordinates has the potential to conceal the uncertainty related to sensor errors.

The uncertainty related to the wellbore position basically means that we are unsure on the exact position. But for many applications, such as collision-avoidance, target hitting, avoiding geo-hazards, it is essential to quantify this lack of clarity.

So the question is how can uncertainty be defined. One approach could be: *uncertainty is caused by an incomplete understanding about what we like to quantify,* but uncertainty cannot be tested against an irrefutable truth, so we will not know whether a quantification of uncertainty is either correct or the best possible (Caers 2011). Therefore, a model has to be created, which is based on statistical or physical defined terms, that describe the processes which lead to uncertainty.

The Industry Steering Committee for Wellbore Survey Accuracy (ISCWSA) was founded to cope with this task. Built on a rigorous mathematical framework a concept was presented by Williamson in 2000 for originally only MWD (measurement while drilling) surveys. This was extended with a gyro error model by Torkildsen et al. in 2004. Basically, the error model is a means to describe a survey error and evaluate how the wellbore position is affected by it.

When the error model is applied to survey data, an uncertainty estimate is generated, which is usually reported at a certain location in space as an ellipsoid with a specific confidence level. This ellipsoid allows the responsible persons to scan the subsurface for eventualities of a wellbore collision. There are several ways to describe the probability of such an extremely dangerous event to happen.

The aim of this study is to show how different ways of calculating separation factors, distances and probabilities can significantly influence resulting decisions. Clearance factors and distances between ellipsoids of uncertainty can be evaluated with various methods. But the oil and gas industry today does not have a standard procedure for this cause. This thesis will use therefore the standard set of wellpaths, published by the ISCWSA, to evaluate differences and deviations of separation factors. In order to cover real world scenarios, eleven offset wells will approach the reference well in eleven different ways. The different cases will be calculated and analyzed, giving the reader an overview on acceptable results for the respective wells. The calculations will be based on state-of-the-art error modeling methods to ensure outcomes that can work as a guideline for drillers and well planners who want to test their software tools.

Literature Review

The ISCWSA error model provides a rigorous mathematical concept that demonstrates how angular errors combine to produce uncertainty ellipsoids.

The basic concept for an uncertainty model was first introduced by Walstrom et al. (1969). The methods were based on the assumptions that surveyed coordinates are represented by random variables and that the measurement errors are mutually independent.

The results of this approach did not sufficiently match experiences gained in field. Truex (1971) mentioned discrepancies on observed surveys. The high inclination wells had a higher error than those expected from the Walstrom model.

The error ellipses calculated were too small and Wolff & De Wardt (1981) proposed a new way to evaluate uncertainty. The initial thought that errors vary randomly throughout a survey was proven wrong and it was demonstrated that systematic errors contribute the significant part to the borehole position error estimates. The evaluation of the borehole location was thereby dependent on error terms that were constant throughout a survey and stacked in the same direction, leading to a larger ellipse of uncertainty. The first draft recognized a compass error that summarized the deflection of the gyrocompass and the magnetic compass, a misalignment error, a true inclination error and a relative depth error. The predictions made matched the real world and this model was intensively used and commonly accepted by the oil and gas business.

In contrast to Walstrom's effort and to the following models, the equations do not include a confidence level. The lack of confidence level is a complex topic and will be discussed further when collision probabilities are of concern.

The fundamental approach to an overall MWD error model was delivered by Williamson (2000). His suggested tool was the first that combined the previous findings and mitigated various shortcomings. His theory is based on a rigorous mathematical framework and standard deviations of errors found by numerous experts and studies.

A similar attempt for gyroscopic tools was postulated by Torkildsen et al. (2008). The paper described a general method to determine wellbore position accuracies, applicable for all gyroscopic surveying tools and services.

Williamson (2000) and Torkildsen et al. (2008) provided the two models on behalf of the Industry Steering Committee for Wellbore Surveying Accuracy (ISCWSA) to create a standard for the industry.

During the past 15 years the main features of the model remained the same and only minor corrections were installed. Depth issues were addressed by Brooks et al. (2005). Reasonable quantification of measured depth uncertainty was the main objective of this paper and a set of error terms was introduced to reduce in particular formation evaluation incredibility.

Despite the progress in uncertainty modeling of the wellbore position, procedures to ensure proper data and measurement quality were still non-uniform. Ekseth et al. (2006) resolved this problem by listing all sources of errors and presenting internal data checks including limitations and operational recommendations.

Parallel to the development of accurate measurement error descriptions, the industry aimed to set up rules for proper collision-avoidance techniques. The risk was first quantified by Thorogood et al. in 1990, who based his analysis on the probability of collision. The risk management was then executed by means of a decision tree. A supplement by Williamson (1991) was published which further examined the calculation process of wellbore collision probability. The paper *An Improved Method for Computing Wellbore Position Uncertainty and its Collision and Target Intersection Probability Analysis* (Brooks & Wilson 1996) summarized the standard protocol to create ellipsoidal probability fields and showed a method to develop this uncertainty. The probability density function was then used to calculate the probability of intersection.

The next improvement was the switch to combinations of risk analysis management. The probability of a well collision was connected to the consequences that would follow from such an incident. Based on the severity of the outcome, risk levels were introduced that allowed drillers and other persons responsible to evaluate the respective procedure.

Williamson emphasised with his work (1998) that several main features were not yet sufficiently discussed. The topics were human error, the nature of survey errors distribution and distinction between real and modeled risk. The investigation showed that the normal distribution, even though fairly accepted by the industry, should be used with

caution. This difference is not further researched, but later Gjerde (2008) and Bang & Torkildsen (2009) identified magnetic errors to be inverse normal distributed and high latitudes to bear an enhanced error potential for magnetic measurements.

Several risk management methods were introduced to further improve probability-based decision making. Mcnair et al. (2005) presented an approach which would distinguish between shallow and deep zones, as each zone has a different potential for wellbore collisions. Poedjono et al. (2006, 2009) and Poedjono, Lombardo, et al. (2009) published papers that gave a detailed view on the evaluation, management and mitigation process of risk. The establishment of a standard industry-wide procedure was attempted and the advantages explained.

The consequences of damaged collision-avoidance rules are complex and will not be part of this thesis. The focus will be set on comparison of separation factors and probability of a wellbore intersection.

2. Overview

This chapter should give the reader a sufficient theoretical background on the concepts related to positional uncertainty, separation factor calculations and collision probability estimations.

2.1. Directional Drilling

Directional drilling (DD) can be defined as the process of directing the borehole along some trajectory to a target, which is horizontal offset to the surface location (Bourgoyne A. D., Chenevert M. E., Millhelm K. K. 1986). This implies that three coordinates have to be used to represent the wellbore position in a specific coordinate system. Figure 1 shows the straight segment of a well (Δs), which is commonly referred to as measured depth. The MD can be described in several ways by applying basic trigonometric relationships. The reference frame is commonly a NEV-coordinate system. Two important angles can be recognized in Figure 1. The inclination angle (I), referring to the angle between borehole and the vertical axis and the azimuth angle (A), referring to the angle between True North and the direction of the borehole.

Directional drilling offers a large variety of applications. Sidetracking can be used to create a new hole from an old one. This is primarily done to bypass a fish (or something else that has been stuck/lost in hole). DD is further needed to drill multiple wells from one location (offshore platform or drilling pad). This application is nowadays of great importance and used intensely throughout the industry. Straight hole drilling can also require directional control, if the formation tends to deviate the bit. Special tools are used to keep the inclination as low as possible. In addition to that, DD is performed to reach inaccessible sites, to avoid salt domes, to drill relief wells and to drill large horizontal sections (Carden & Grace 2007).

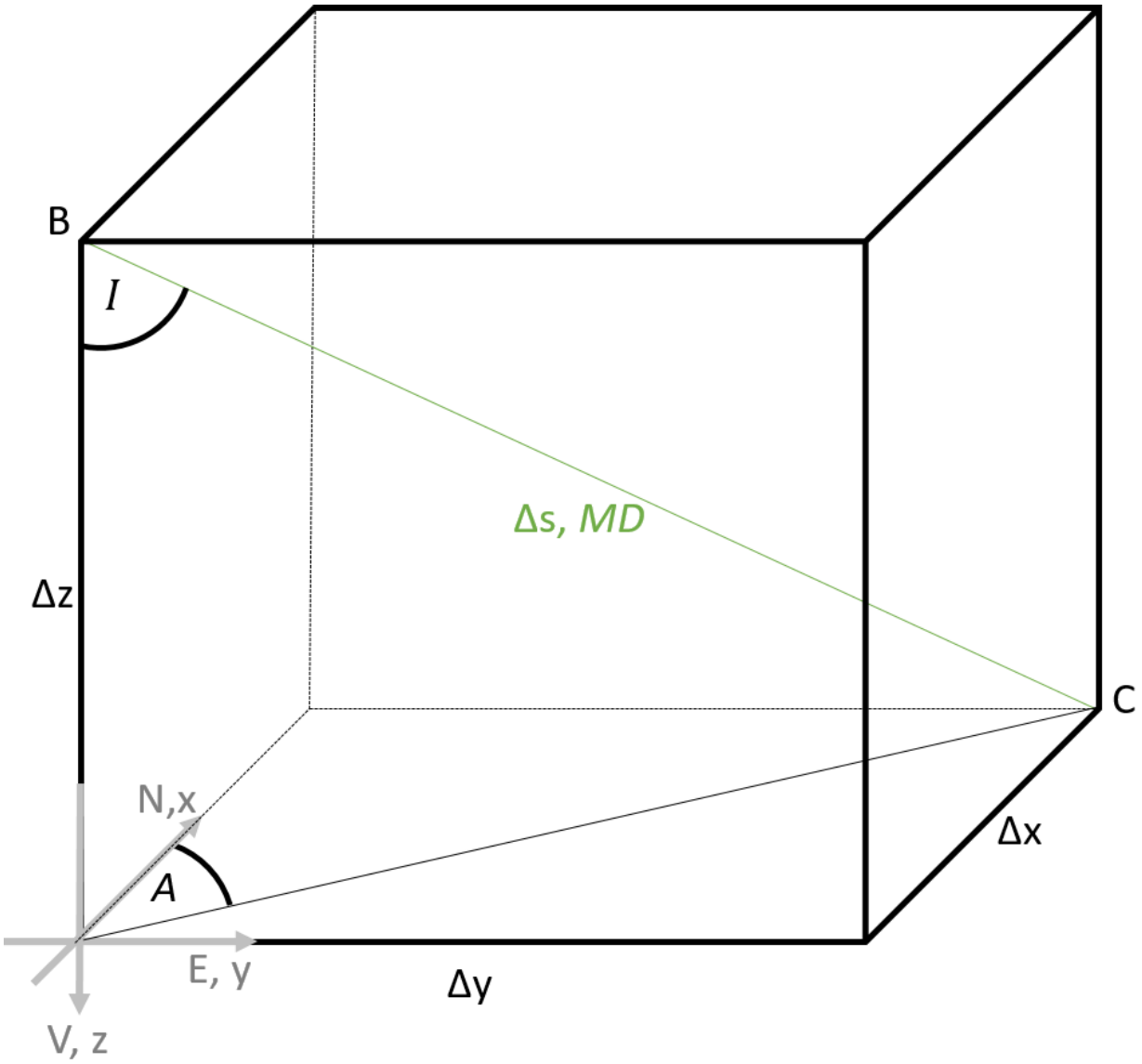

Figure 1: Segment of a wellbore. Typically, survey stations (B&C) measure the inclination angle (I) and azimuth angle (A) while drilling. The measured depth is a manual measurement at surface. With the three parameters, it is possible to define every survey station in the appropriate coordinate system (most likely a NEV-system).

2.1.1. Surveying

A well is typically surveyed by a discrete number of survey stations. Figure 1 shows two survey stations, B and C. The measurement made at each point consists of the inclination angle I (angle between vertical and wellbore) and the direction angle A (azimuth between Geographic North and the projection of the wellbore onto a horizontal plane). Combined

with the record of MD at the surface, the wellpath can be explicitly defined (the resolution depends on the survey station interval).

The two angles can be derived from special tools such as magnetometers and accelerometers using the following equations:

$$I = cos^{-1}\left(\frac{G_z}{\sqrt{G_x^2 + G_y^2 + G_z^2}}\right) \quad (1)$$

$$A = tan^{-1}\left(\frac{\left(G_x B_y - G_y B_x\right)\sqrt{G_x^2 + G_y^2 + G_z^2}}{B_z(G_x^2 + G_y^2) - G_z(G_x B_x + G_y B_y)}\right) \quad (2)$$

with $G_x, G_y, G_z, B_x, B_y \; and \; B_z$ being the measurements of the Earth's gravity and magnetic field, respectively.

2.1.2. Survey Calculation Methods

The industry standard for the calculation of 3D directional surveys is the minimum curvature method (MCM). Sawaryn & Thorogood (2005) generated *A Compendium of Directional Calculations Based on the Minimum Curvature Method,* that summarized the mathematical background and presented a consistent methodology to use it. As the calculations in this thesis solely use the MCM, other simpler methods (Tangential, Balanced Tangential, Average Angle and Radius of Curvature) will not be highlighted.

The MCM assumes that the wellbore is a curved path between two survey points. This statement is a simplification, necessary to build the mathematical framework. In reality, the wellbore has a geometric complexity, that is difficult to record and describe. The tortuosity is therefore characterized by the survey stations and minor scale tortuosity is neglected.

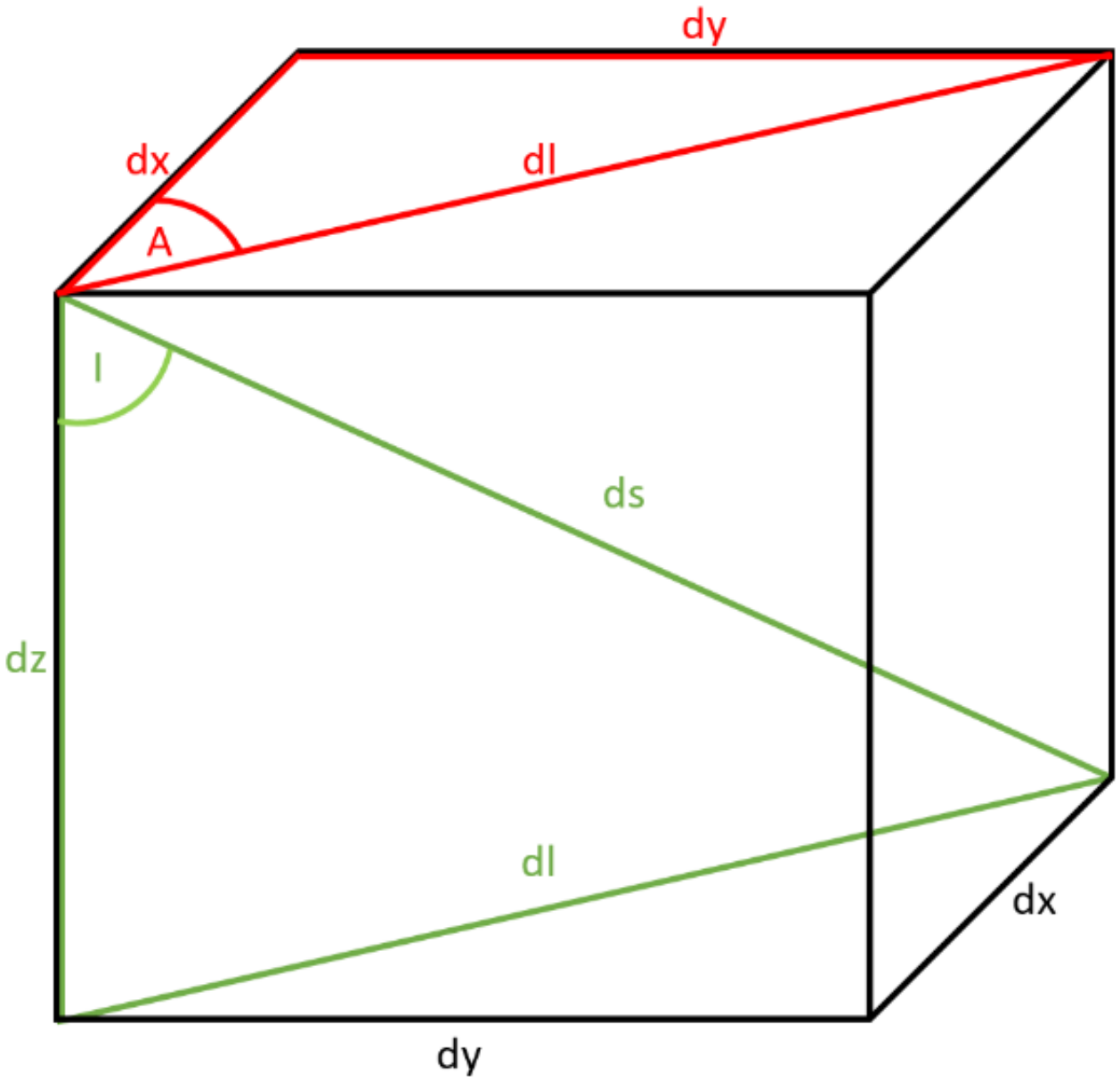

Figure 2: The Wellbore Element with the basic trigonometric relationships highlighted. Equations (3-10) can easily be derived from the trigonometric relationships between the variables.

Figure 2 shows again the element ds of the wellbore, which in this case is assumed to be very small and thus straight. The figure highlights two right-angled triangles. Straightforward, the fundamental equations for directional drilling practices (Equation 3-11) can be formulated (Mitchell & Miska 2011).

$$\mathrm{B}(s) = \frac{dI(s)}{ds} \tag{3}$$

$$\mathrm{T}(s) = \frac{dA(s)}{ds} \tag{4}$$

$$\sin(A) = \frac{dy}{dl} \tag{5}$$

$$\cos(A) = \frac{dx}{dl} \tag{6}$$

$$\sin(\mathrm{I}) = \frac{dl}{ds} \tag{7}$$

$$\cos(I) = \frac{dz}{ds} \tag{8}$$

$$\frac{dx}{ds} = \frac{dx}{dl}\frac{dl}{ds} = \cos(\mathrm{A})\sin(\mathrm{I}) \tag{9}$$

$$\frac{dy}{ds} = \frac{dy}{dl}\frac{dl}{ds} = \sin(\mathrm{A})\sin(\mathrm{I}) \tag{10}$$

The first two equations (Equation 3 and 4) describe turn rates. $\mathrm{B}(s)$ is the rate of change of the hole inclination along the wellpath (build rate). $\mathrm{T}(s)$ determines the rate of change of the azimuth along the wellbore (turn rate).

The two triangles can be used to derive Equations 5-8. It is then possible to extend the formulas and define Equation 9 and 10, which are essential for the characterization of movements in three dimensions. They are used to describe a certain change in the respective direction that solely consists of azimuth and inclination readings.

The traditional reference frame for wellbore locations uses north [N], east [E] and vertical [V] coordinates, comprising a right-handed coordinate system. For the sake of simplicity this denotation will be used. It is now possible to follow Sawaryn & Thorogoods procedure by introducing a unit direction vector $\underline{t}$.

$$\underline{t} = \begin{bmatrix} \Delta N \\ \Delta E \\ \Delta V \end{bmatrix} = \begin{bmatrix} \cos(\mathrm{A})\sin(\mathrm{I}) \\ \sin(A)\sin(I) \\ \cos(I) \end{bmatrix} \tag{11}$$

The standard nomenclature for wellbore curvature is frequently called dogleg severity (DLS), usually expressed in degrees per 100 [ft] or degrees per 30 [m]. Figure 3 depicts the DLS along two direction vectors. The following expression for the dogleg severity (Equation 12) was found (Sawaryn & Thorogood 2005):

$$DLS = 2\sin^{-1}\left\{\sqrt{\left[\sin^2\left(\frac{I_2 - I_1}{2}\right) + \sin(I_2)\sin(I_1) * \sin^2\left(\frac{A_2 - A_1}{2}\right)\right]}\right\} \qquad (12)$$

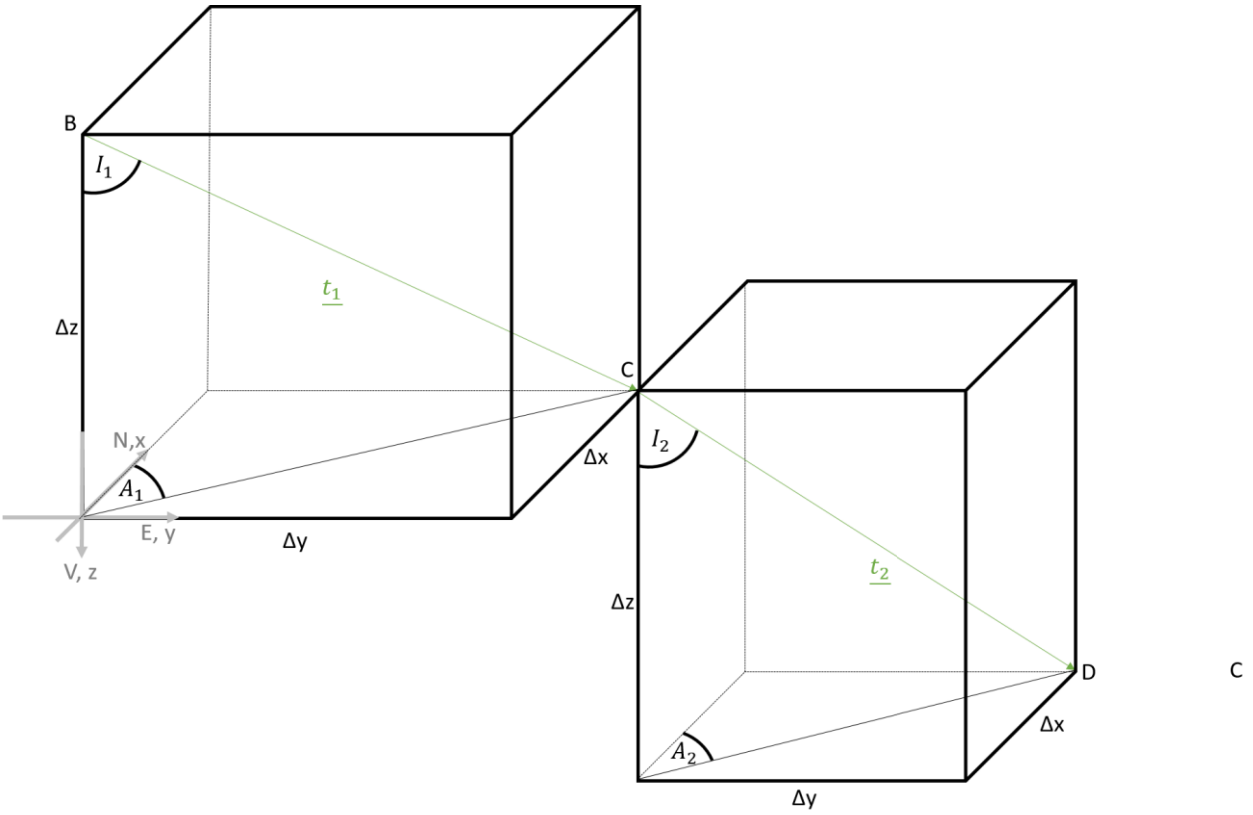

Figure 3: Dogleg Severity (DLS). B, C and D are survey stations where measurements while drilling are made. $\underline{t_1}$ *and* $\underline{t_2}$ *are direction vectors.*

The DLS is related to the radius of curvature R, the course length S_{12} and the curvature of the arc κ.

$$\kappa = \frac{1}{\mathrm{R}} = \frac{\mathrm{DLS}}{S_{12}} \qquad (13)$$

The position of a survey point can now be calculated (if $\underline{p_1}$ is known):

$$\underline{p_2} = +\frac{S_{12} f(\alpha)}{2} * \begin{bmatrix} \sin(I_1)\cos(A_1) + \sin(I_2)\cos(A_2) \\ \sin(I_1)\sin(A_1) + \sin(I_2)\sin(A_2) \\ \cos(I_1) + \cos(I_2) \end{bmatrix} \qquad (14)$$

with the shape factor $f(\alpha) = \frac{\tan(\frac{\alpha}{2})}{\alpha/2}$. The advancements are summarized in the following equations. Transformation into a NEV coordinate system makes this method easily usable if computing power is available.

$$\Delta V = \left(\frac{\Delta MD}{2}\right) * (cos(I_1) + \cos(I_2)) * f(\alpha) \qquad (15)$$

$$\Delta N = \left(\frac{\Delta MD}{2}\right) * [(sin(I_1) * \cos(A_1)) + (sin(I_2) * \cos(A_2))] * f(\alpha) \qquad (16)$$

$$\Delta E = \left(\frac{\Delta MD}{2}\right) * [(sin(I_1)\sin(A_1)) + (sin(I_2)\sin(A_2))] * f(\alpha) \qquad (17)$$

2.2. ISCWSA Error Model

Now that the mathematical basis is known, it is important to evaluate how measurement errors influence the knowledge on the exact position of the wellbore. It is crucial to recognize that systematic and random errors may deflect the wells trajectory, and that this deviation may have severe consequences (risk of human life, equipment, environment and reputation).

The collision-avoidance calculations were performed with the ISCWSA error model (Revision 4). Williamson (2000) and Torkildsen et al. provided (2004) the keystones to the development of all models in usage today.

Historically four error models can be identified, all of the models share the basic thought to investigate how various error sources affect the positional accuracy of MWD. The main criteria for a successful model is the ability to choose the correct values for various tools and use reliable data to apply corrections such as sag, IFR (In-Field Referencing), stretch and interference.

2.2.1. Normal distribution

It was stated in the previous sections that uncertainty in sensor measurements can be quantified. This procedure is based on the assumption that most of the independent error sources follow Gaussian distributions (Figure 4). The curve is defined by the standard deviation σ and the mean value μ. The confidence intervals (black lines) represent the respective percentage of values lying in that range. To put it simply, if we calculate the one sigma standard deviation of an error source, we have approximately 68% certainty that a specific value lies within that range. If we apply this concept to the wellbore, and we have several normal distributed influencing factors, we can say with 68% certainty (or with 95% or with 99.7%) that the wellbore is in a specific interval.

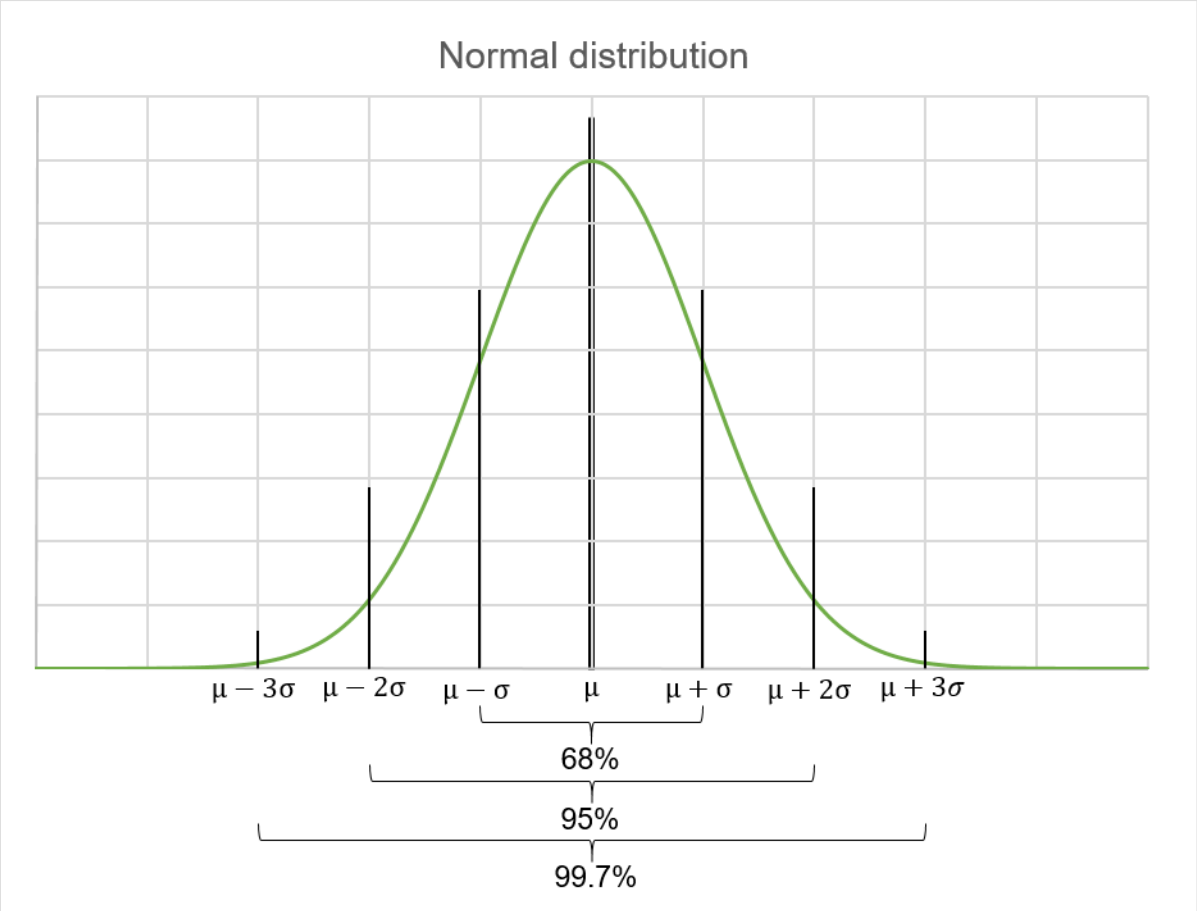

Figure 4: Normal distribution. The Gaussian distribution is an important concept for anti-collision calculations. The various sensor errors are said to follow this distribution, thereby the standard deviations and means can be used to describe the influencing factors (error sources)

Table 1: Probability of standard deviations. The influence of dimension and standard deviation on the probability (ISCWSA 2013b).

Probability	standard deviation				
dimensions	± 1	± 2	± 2.58	± 2.79	± 3
1	68.27%	95.45%	99.01%	99.47%	99.73%
2	39.35%	86.47%	96.41%	97.96%	98.89%
3	19.87%	73.85%	91.63%	94.94%	97.07%

Table 2: Confidence levels and their respective standard deviations in three dimensions (ISCWSA 2013b).

Probability	confidence level				
dimensions	68.3%	90%	95%	99%	99.7%
1	0.9999	1.6448	1.9599	2.5758	2.9677
2	1.5151	2.1459	2.4477	3.0348	3.4086
3	1.8779	2.5002	2.7954	3.3682	3.7325

Table 1 and 2 show the probability values for a variable to be in a certain interval. The tables also depict the influence of dimensions on the probability. Table 2 is of special importance for this thesis, as the collision-avoidance rules often follow preset probability values, requiring the confidence to be above 95% for example.

It is crucial to recognize the importance of the normal distribution and the consequences, as a mistake in the standard deviation can change the results dramatically.

The idea that all sensor errors follow the normal distribution has been partly disproved by Gjerde (2008) but until now, the normal model remains standard for the industry and will be used in this thesis. Gjerde pointed out that magnetic declination follows a Normal Inverse Gaussian distribution, but the results were not clear without ambiguity and differed significantly.

2.2.2. Definitions and Assumptions

The error model requires a rigorous mathematical framework, with assumptions and limitations being clearly defined.

The survey measurements have to be recorded under standard procedures. This includes rigorous and regular tool calibration, a maximum length of 100 [ft] survey intervals, quality checks according to Ekseth et al. (2006 and 2007), sufficient non-magnetic spacing for MWD surveys (according to standard charts) and attention given during MWD for a clean magnetic environment (Williamson 2000).

The model consists of error sources, which are physical effects changing a survey measurement. An error source can impact the measured depth, inclination and azimuth in different ways, so weighting functions are used to describe the influences. Typical error sources are bias and scale factors, misalignment of the tool, declination of the magnetic field, depth issues and sag.

The attributes related to an error source can be summarized in an error term. This term contains a name, a weighting function, a mean value μ and a magnitude σ (usually quoted as a 1 standard deviation value). The values for σ have to be carefully picked and are dependent on each particular tool. Different techniques require different magnitudes, for example if In-Field Referencing is applied, the error related to magnetic measurements can be reduced. The process can be imagined as if the crew would run 100 survey runs before the actual survey takes place. The result would be a distribution with a specific mean value and a standard deviation. It is common practice to use a one-sigma standard deviation for error magnitudes defined in the ISCWSA model.

Another essential part of the error term is the weighting function. With the source and the magnitude already defined, the missing part is the direction of the effect. The weighting function declares with an equation whether the azimuth, inclination or measured depth have to be revised. To find a weighting function, the partial derivatives of Equation 1 and 2 have to be taken with respect to the error source. The complete list that was used in this thesis can be found in the appendices.

Brooks & Wilson summarized in 1996 the basic strategy for computing positional uncertainty. Williamson used this approach in his *Accuracy Prediction for Directional Measurement While Drilling* work. It is stated that a measurement error will lead to an error (vector) in the calculated well position:

$$e_i = \sigma_i \frac{dr}{dp} \frac{\partial p}{\partial \epsilon_i} \qquad (18)$$

where e_i is the vector error, σ_i is the magnitude of the ith error source, $\frac{\partial p}{\partial \epsilon_i}$ is the related weighting function and $\frac{dr}{dp}$ denotes how the wellbore position vector r changes with the measurement vector.

In addition to that it is necessary to define correlation coefficients, explaining the propagation mode of error values. To ensure that the coefficients are well defined, the correlation between error values in the same survey leg (but different stations), in different survey legs (but the same well) and between different wells (but in the same field) is noted in the error term by R (random), S (systematic), W (well by well) and G (global) (Williamson 2000).

The propagation mode depends on the question whether an error is correlated to another one. If an error is independent, the contributions must be root sum squared. If the contributions are linked to each other, they have to be summed up.

The final outcome of the model is a covariance matrix $[C]$ that describes the error ellipse or ellipsoid at a particular measurement station. The diagonal variables $\sigma_N^2, \sigma_E^2, \sigma_V^2$ are the variances of the respective direction and $\sigma_N\sigma_E$, $\sigma_N\sigma_V$, $\sigma_E\sigma_V$ are the covariances describing the correlation between the respective directions. In the NEV-axes it can be defined as:

$$[C] = \begin{bmatrix} \sigma_N^2 & \sigma_E\sigma_N & \sigma_N\sigma_V \\ \sigma_N\sigma_E & \sigma_E^2 & \sigma_E\sigma_V \\ \sigma_V\sigma_N & \sigma_V\sigma_E & \sigma_V^2 \end{bmatrix} \qquad (19)$$

This matrix is the essential result of all calculations, procedures and practices explained before. It is crucial to perform all the different steps with caution, as a mistake can sum up significantly.

According to the mathematical definition, a covariance matrix is always symmetric and positive definite. It can be expressed as ellipse parameters (2D) and TVD uncertainty (1D) through the eigenvalues of the covariance matrix (Haarstad et al. 2002):

$$\lambda_{1,2} = \frac{\sigma_N^2 + \sigma_E^2}{2} \pm \sqrt{\frac{(\sigma_N^2 + \sigma_E^2)^2}{4} + \sigma_E \sigma_N \sigma_N \sigma_E - \sigma_N^2 \sigma_E^2} \qquad (20)$$

$$Major\ semi - axes = \sqrt{\lambda_1} * k \qquad (21)$$

$$Minor\ semi - axes = \sqrt{\lambda_2} * k \qquad (22)$$

$$TVD - Uncertainty = \sigma_V^2 * k \qquad (23)$$

where k is dependent on the confidence levels.

It is furthermore very important to recognize the base of the model. Statistical methods were used to describe the magnitudes of various error sources. This means that the model cannot cover all eventualities and is unable to characterize specific attributes about a single survey (Jamieson 2012). The results could be pictured as the distribution that would arise from a survey that was recorded several times. Another limitation is that the model does not cover gross blunders (errors resulting from referencing mistakes, typos or other unpredictable processes).

All the introduced restrictions do not allow for compensation if the assumptions are not met. Meaning that if non-magnetic spacing was neglected, or if the survey interval was above 100 [ft], the model is simply invalid. Beside this, the reader has to be aware that all probabilities are restricted to the simple condition that a collision occurs or does not occur. The probability is not expanded to a risk term as an interpretation of consequences would not fit into the scope of this thesis.

2.3. Anti-Collision

A standard for collision avoidance calculations has not been set yet. Different companies apply different procedures and policies to define a safety factor that represents a distance between the reference and the offset well. There are several ways to describe and report the true distance between two wells.

2.3.1. Separation Factor

The literature presents several methods to estimate the risk of two wells (with the according ellipsoids of uncertainty) colliding.

The simplest form is to calculate the straight separation space between the two wells. The wells are represented by coordinates like [N, E, V], so straightforward the length can be determined. Ellipses of uncertainty are not considered here, so caution should be taken when using this method. It might be used in shallow wells in combination with other methods, since uncertainty is low and might lead to unreliable results.

The second method evaluates uncertainties related to survey errors (usually covariance matrices). The error model was already explained and the output was said to be covariance matrices describing the magnitude of the survey errors in the chosen coordinate frame (Jamieson 2012). The two standard ways to estimate the separation factor are shown in Equation 24 and 25. The difference between the two ways can be seen easily, but to evaluate the consequences, several cases have to be considered and investigated. The main part of this study will focus on this problem and demonstrate the limitations of each method.

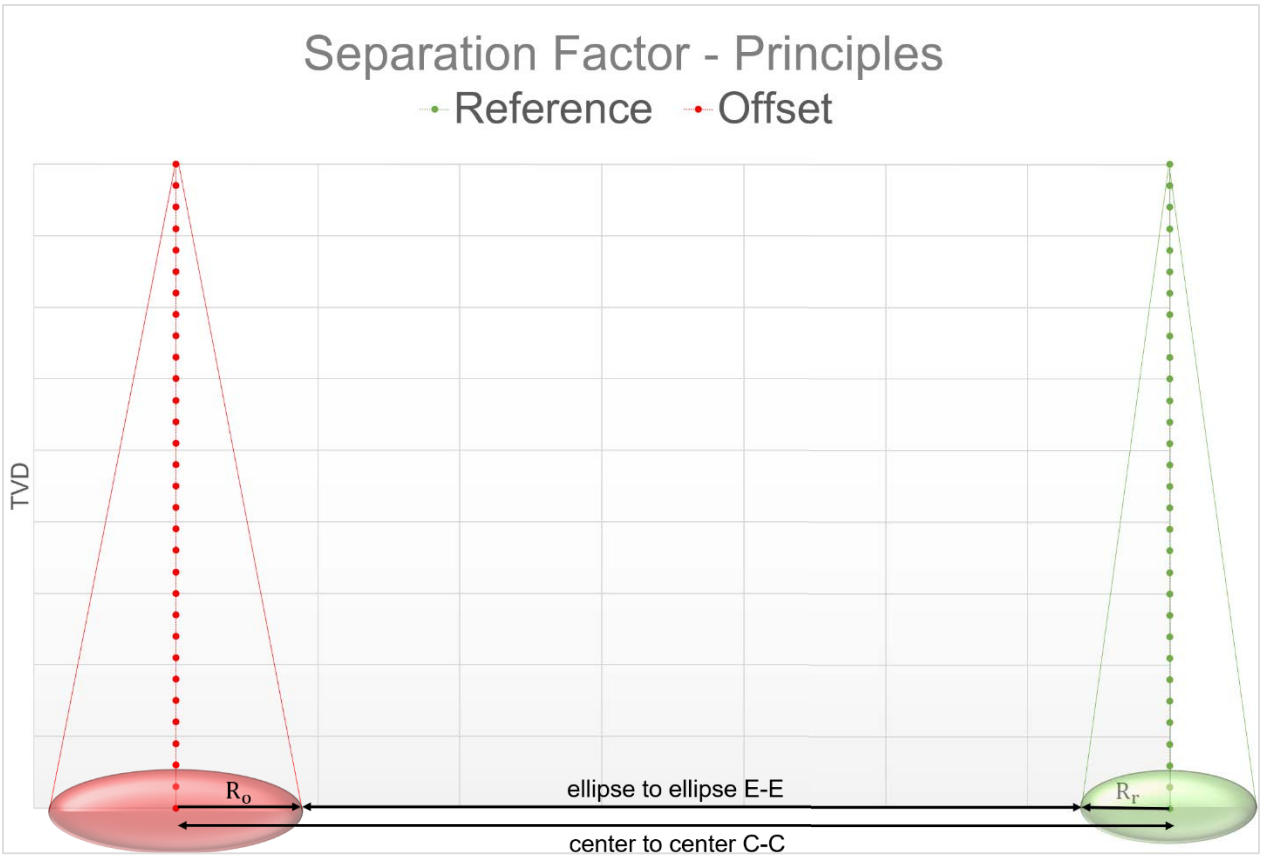

Figure 5: Separation Factor Estimate Methods. The straightforward approach does not consider uncertainty and simply returns the center-to-center distance. This does not represent the truth and should be strictly avoided. The only valid situation is in shallow depths under the assumption that more sophisticated methods are also incorporated. The major part of collision-avoidance politics involves a separation factor that takes the ellipsoid of uncertainty into consideration and their specific geometry.

$$SF = \frac{Center\ to\ Center\ Distance}{Center\ to\ Center\ Distance - Distance\ between\ Ellipsoids} \quad (24)$$

$$SF = \frac{Center\ to\ Center\ Distance}{Sum\ of\ the\ Major\ Half - Axis} \quad (25)$$

2.3.2. Collision Probability

The basis of the ellipsoid of uncertainty is a normal distribution, meaning it is associated to probability already. This key feature allowed the quick development of probability-based equations that would predict the collision likelihood.

The first mathematical analysis of probability is shown in Equation 23 (Thorogood et al. 1990). This simple expression is made for two parallel wells with a diameter d, standard deviations of survey uncertainty σ_A and $\sigma_B$and a distance D between their centers. The collision probability *P* is defined as:

$$P = \frac{d^2}{2 * (\sigma_A^2 + \sigma_B^2)} * \exp^{-\frac{D^2}{2*(\sigma_A^2+\sigma_B^2)}} \quad (26)$$

Equation 23 was initially more complicated but due to difficulties when applying too complex methods, this simple version was advised to be used.

The next formula (Equation 24) is widely accepted and will be used by this thesis, therefore it will be explained in detail. Two wells are considered in the derivation, which are straight and cross at a high angle (Figure 6). S is denoted as the center to center distance, and σ is the uncertainty (in the direction of closest approach – normal to the subject well). Keeping in mind the measurement errors are normal distributed, the probability density function can be generated. If this function is integrated over the sum of the individual radii (as shown in Figure), we get the probability of the two wells colliding (Williamson 1998). A further remark is that the rectangular shown in Figure 6 is calculated, thereby overestimated.

$$P = \frac{d_s + d_o}{\sigma * \sqrt{2\pi}} * \exp^{-\frac{[S-\frac{d_s+d_o}{2}]^2}{2\sigma^2}} \quad (27)$$

Where d_s and d_o are the diameters of the subject and object well and σ is the combined standard deviation:

$$\sigma = \sqrt{\sigma_s^2 + \sigma_o^2} \quad (28)$$

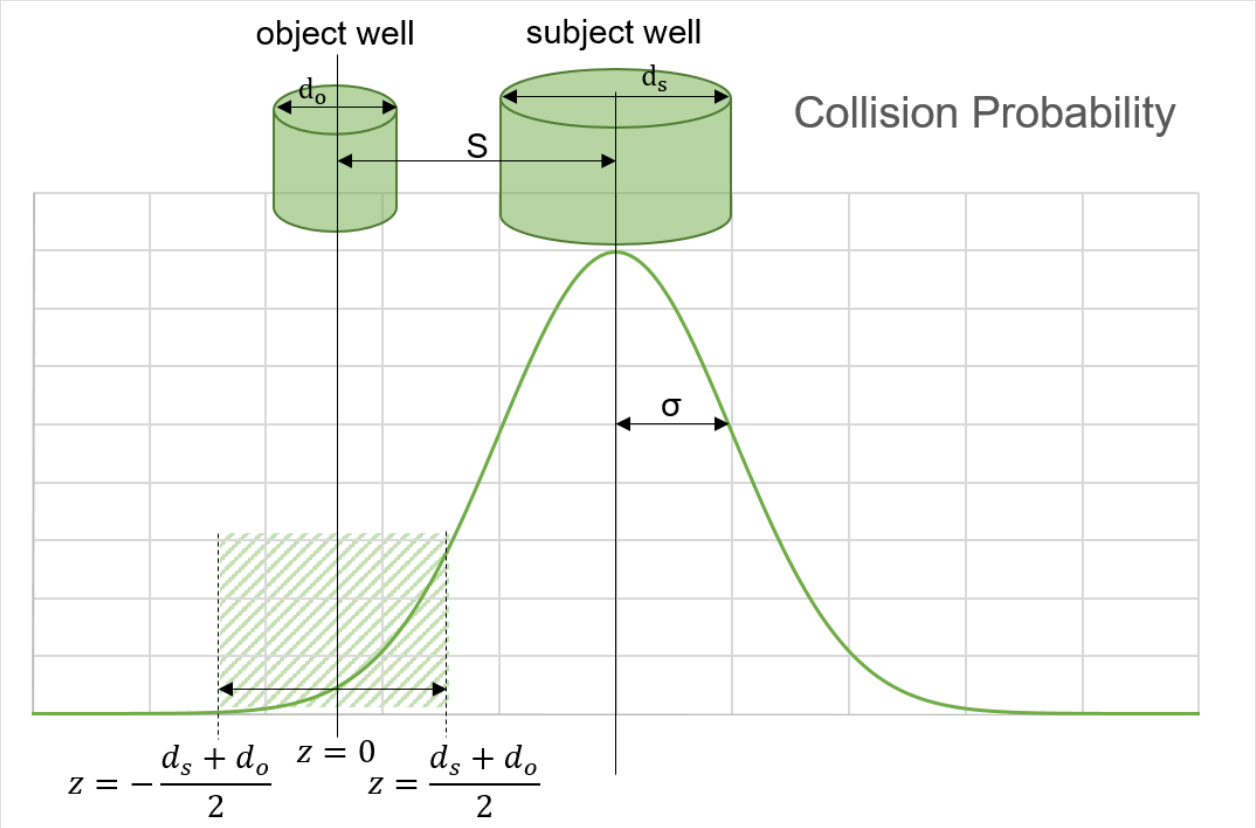

Figure 6: Collision Probability Calculation. The probability density function is created with Equation 24, using the combined standard deviation (uncertainty of both wells), the mean value (minimum separation distance) and the respective diameters. This can be integrated to determine the probability of collision.

2.3.3. Scanning Method

Several scanning options are available in most collision-avoidance systems. The working principle is shown in detail in the methodology chapter. However, the simple question of how close a point of interest is towards a reference point or interval, is answered by complex geometrical calculations. The travelling cylinder (TC) plane, introduced to the oil and gas industry for a long time (Thorogood & Sawaryn 1990), is widely used by drillers, where a perpendicular plane is created and checked for wells intersecting it. It is a great tool to visualize the specific condition during drilling, as it can be compared to a radar and intuitively operated. However, the weaknesses can be seen straightforward in Figure 7. Due to the limitations and deviations in all scenarios, this method was not considered in

this thesis. The same applies to the horizontal method, which simply creates a horizontal plane and checks for wells in this plane.

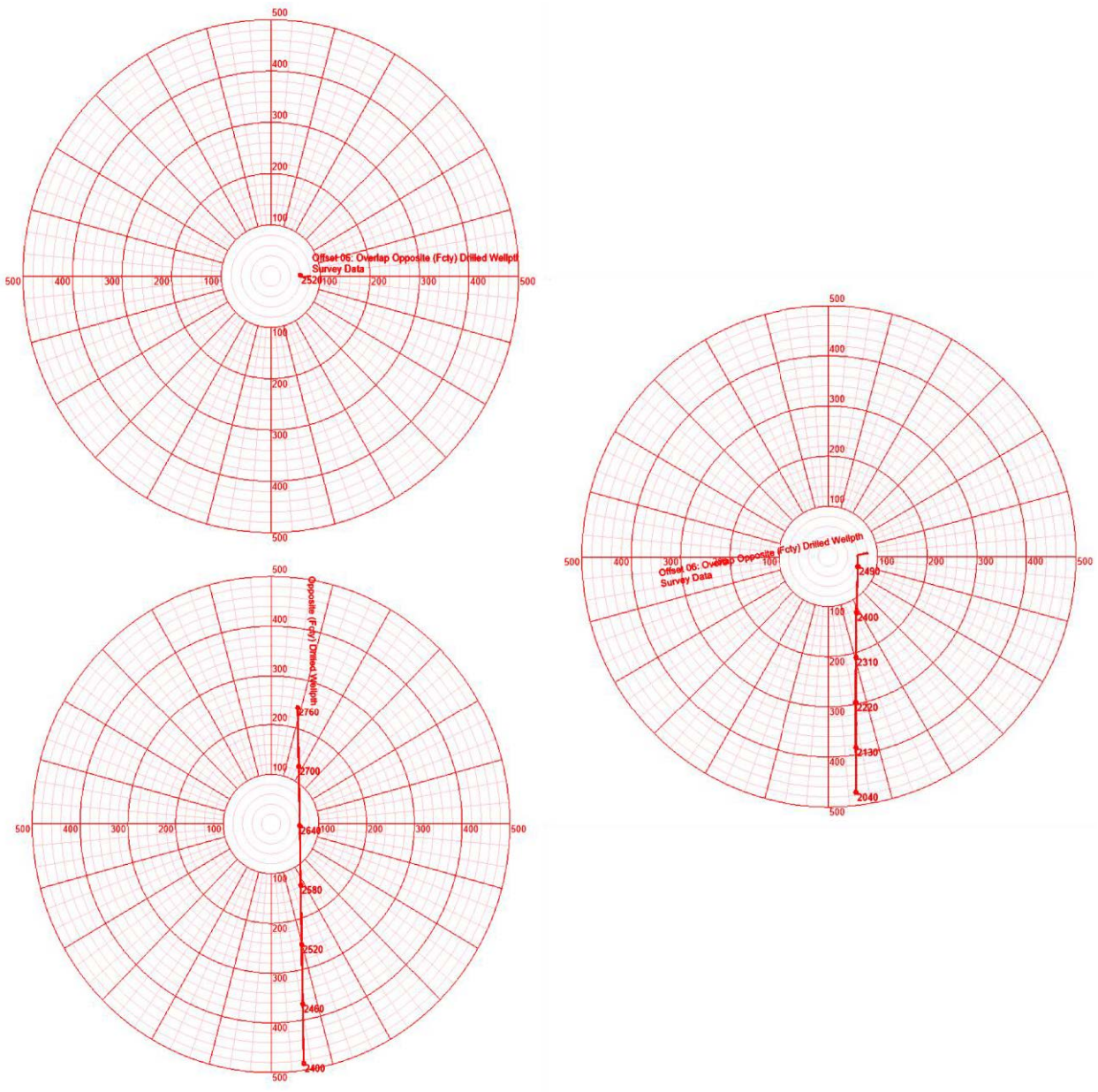

Figure 7: Travelling Cylinder Plot for Short Opposite (red) and Reference well. The upper-left TC is based on the horizontal plane, the lower-left is based on the TC-method and the right one on the minimum distance method (MDM). The right one is the only procedure that delivers acceptable results, for this reason all calculations were based on minimum distance. The well is supposed to stop shortly before the Reference well. While the first one delivers no results at all, the lower-left one overestimates the distance of the Offset well. The right one shows the scenario as it is.

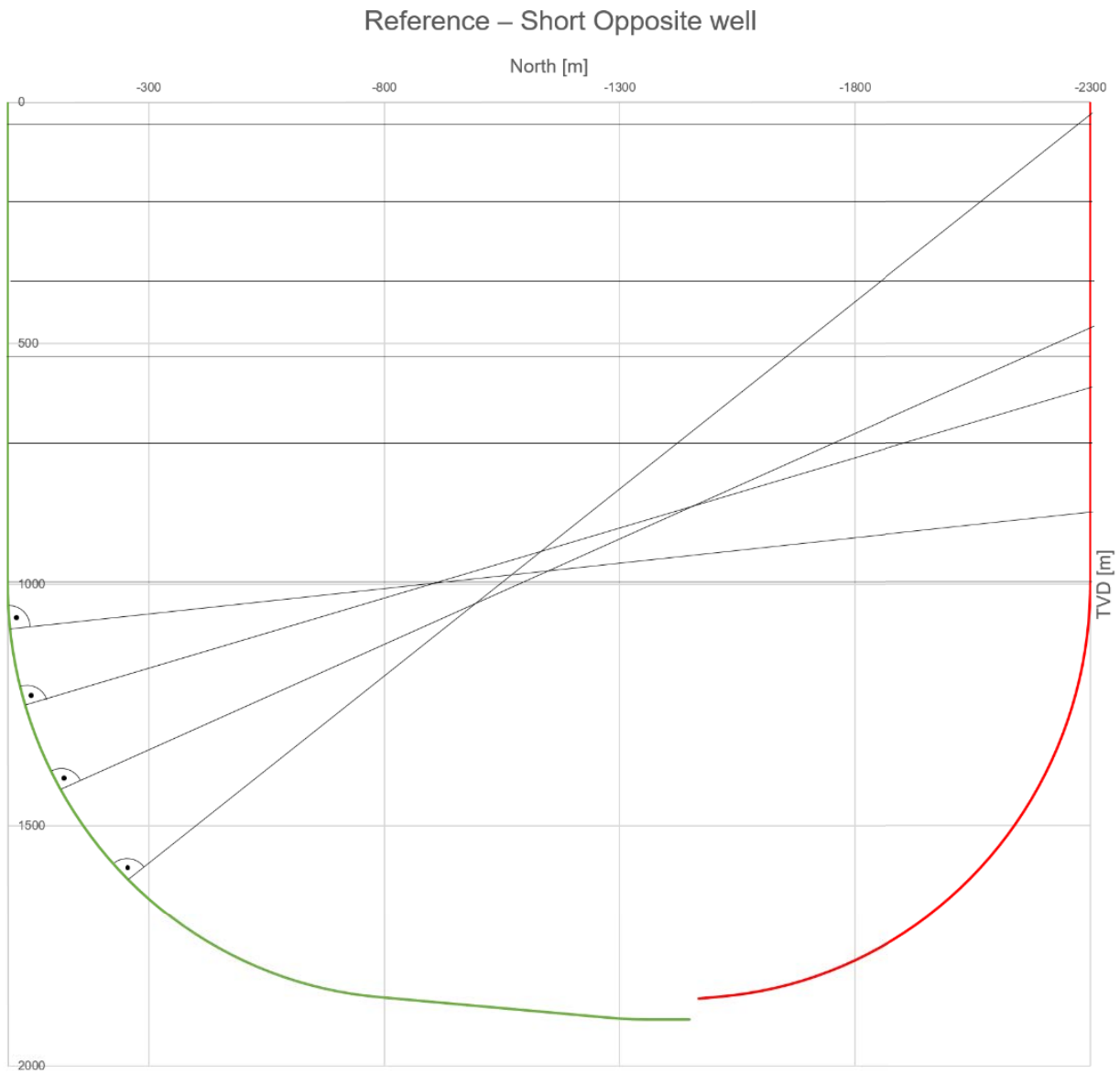

Figure 8: Travelling Cylinder Principle. The drawbacks of this method are clearly visible. The Reference well (green – the well which is drilled) is scanned for adjacent wells and the relative distances, but since it is deviated, the closest distance is never correct.

2.3.4. Closest Distance

The last section (Scanning Method) already introduced the concept of determining the closest distance of a well to a point of interest. Generally, three methods to determine the separation distance can be distinguished (Figure). If the separation factor (k_s) is calculated by the center-to-center distance (δ) divided by the sum of the radii (s_1+s_2) the

shortcomings can be identified. In Figure 9 the Pedal-curve method (PCM) produces reasonable estimates, where the Center-vector method (CVM) is too optimistic. The disadvantage of the Pedal-curve method was highlighted in a presentation by Bang & Nyrnes (2015) and can be seen in Figure 10. Sawaryn et al. (2013) created a separation distance calculation, which incorporates the expansion factor of the ellipses. With that, it is impossible to over- or underestimate the distance. The advantages of this method will have a huge impact on the results of this thesis.

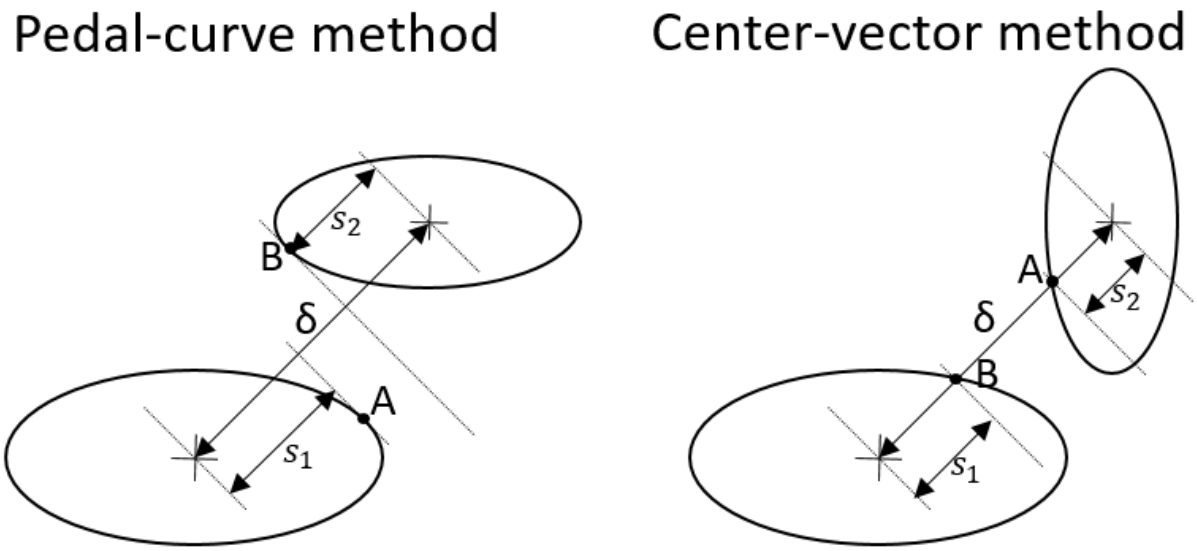

$$k_s = \frac{\delta}{s_1 + s_2}$$

Figure 9: Principles of the Pedal-curve and Center-vector method. While the Pedal-curve is too conservative, the Center vector method can be too optimistic. A conservative behavior is acceptable, but an underestimated separation factor can endanger HSE aspects and should therefore be avoided.

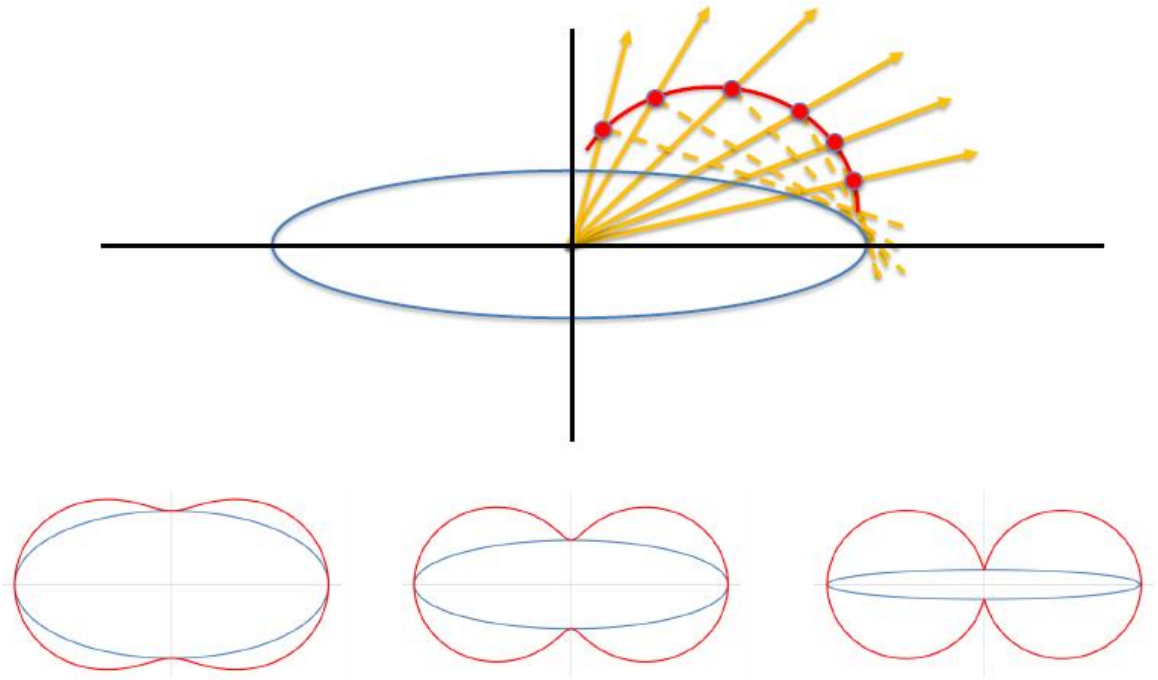

Figure 10: The Pedal-curve Method (Bang & Nyrnes 2015). The disadvantage of the resulting shape is that the pedal curve radius is always larger or equal to the ellipse radius. This leads to conservative estimations of the distance.

The Pedal-curve Method and Expanding Ellipses Method are both used in various software applications. The ISCWSA Collision-Avoidance Work Group compared both methods, and it was voted that the PCM should be improved and then set as a standard. However, both methods were said to produce reliable results.

3. Methodology

This chapter will provide the workflow of all calculations, estimations and implementations performed in the thesis. The calculation software is described in detail to ensure a transparent overview.

3.1. ISCWSA Test Data

The quantification of the separation distance is of paramount importance for every company that drills wells. If the weaknesses of survey tools are not recognized and the wellbore position is not adequately represented, HSE aspects can be violated and in the worst case a loss of life can occur. The variety of tools, software and error models available on the market is tremendous and was discussed by Okewunmi & Brooks (2011). It was concluded that substantial variation among the results was obtained, even though the service companies to be tested were given the same input data.

A model is therefore created that can be used to test collision-avoidance software. The created wells were published by the ISCWSA (ISCWSA 2013c), and are summarized in Table 1 with the respective relationship to a reference well. With this model it is possible to examine a certain situation and check the results for variation. Since Kellydown™ (the calculation software used in this work) is updated regularly, the computed error ellipses and clearance factors are state of the art and can be used to compare outcomes.

Table 3: ISCWSA Well Test Data. One reference well with eleven offset wells. The different scenarios will cover most real-world situations.

Name Well	Relationship to Reference Well
Reference (RW)	Reference Well
East100	Parallel to reference Offset 100m to East
North100	Parallel to reference Offset 100m to North

East10	Close top hole, then crossing RW at shallow incident angle
East20	Drilled double dip wellpath
Angular (AW)	Approaching at depth at an acute angle
Overlap Opposite (OOW)	Approaching at 180° relative azimuth and overlapping
Short Opposite (SOW)	Approaching at 180° relative azimuth and stopping short
Perpendicular (PW)	Approaching at 90° relative azimuth
Vertical (VW)	Vertical well intersecting 85° inc. tangent
Sidetrack (SW)	Sidetrack from 900m MD, Sidetrack that diverges from, then approaches the reference well
Horizontal (HW)	Approaching the horizontal plane at 90° relative azimuth

For the sake of continuity and simplicity, it was decided that the setup for all wells should be equal in terms of magnetic declination, dip angle and field strength. The set parameters are listed in Table 4.

Table 4: Field Parameters of the ISCWSA Test Well Scenario.

Field Parameter	Value	Unit
Declination	0	°
Magnetic Dip Angle	70	°
Magnetic Field Strength	50	µT
Gravity Constant	9.80665	m/s²

3.2. KellyDown™ – Principles

All calculations were performed with Kellydown™, a software package for directional drillers. It is capable of executing all methods that were discussed in this thesis. In order to construct a model, which can be used as a reference, it was mandatory to use up-to-date software. This means the error ellipses had to be calculated using the newest revision (ISCWSA MWD Error Model Rev. 4 from 05-Jun-2015). An additional requirement was the availability of the Scalar Method (expanding ellipsoid) introduced by Sawaryn et al. (2013).

The instrument performance model (IPM) for all wells was MWD. This is very important, since a different set of magnitudes would lead to changes in the results. The IPM was therefore controlled and compared to the newest published version of the ISCWSA error model. As Table 5 shows, the ellipsoid of uncertainty was calculated with the latest revision of the ISCWSA model. The distance between wells was estimated by the minimum distance method (in the industry it is commonly referred to as the closest approach). This feature always detects the adjacent well, as it scans the comparison well down its entire length for the closest distance. In order to support this claim, Figure 11 and Table 6 were created to demonstrate the operating principle of the minimum distance method. The other distance-evaluation methods were not considered, as the quality of the results was poor.

Table 5: Overview of the Calculation Methods performed by Kellydown.

Calculation Type	**Source/Equation**
Ellipse of Uncertainty	ISCWSA Error Model Rev. 4
Distance between Wells	Minimum Distance Method
Separation Factor	Equation 22&23

Table 6: Comparison of Reference and Horizontal well. The jump that is shown in Figure 6 is highlighted. It should be noted that the center to center and ellipsoid to ellipsoid distance does not jump, but steadily and in accordance to the previous values, shrinks. This implies that the calculation is correct, since the center to center distance should continuously decrease

Reference well					**Horizontal well**							
MD [m]	**TVD** [m]	**North** [m]	**East** [m]	**Major half-axis** [m]	**MD** [m]	**TVD** [m]	**North** [m]	**East** [m]	**Major half-axis** [m]	**Cr-Cr** center to center [m]	**Ell-Ell** ellipsoid to ellipsoid [m]	**Separation Factor**
840	840	0 N	0.00 E	3.71	840	840	1400 S	1000 W	3.71	1720	1712	>100.00
870	870	0 N	0.00 E	3.81	870	870	1400 S	1000 W	3.81	1720	1712	>100.00
900	900	0 N	0.00 E	3.92	900	900	1400 S	1000 W	3.92	1720	1712	>100.00
930	930	0 N	0.00 E	4.03	2.531	1900	1400 S	0 E	29.94	1703	1673	56.85
960	960	0 N	0.00 E	4.14	2.531	1900	1400 S	0 E	29.94	1686	1656	55.81
990	990	0 N	0.00 E	4.24	2.531	1900	1400 S	0 E	29.94	1669	1638	53.42
1020	1020	0.35 S	0.00 E	4.24	2.531	1900	1400 S	0 E	29.94	1653	1622	53.71

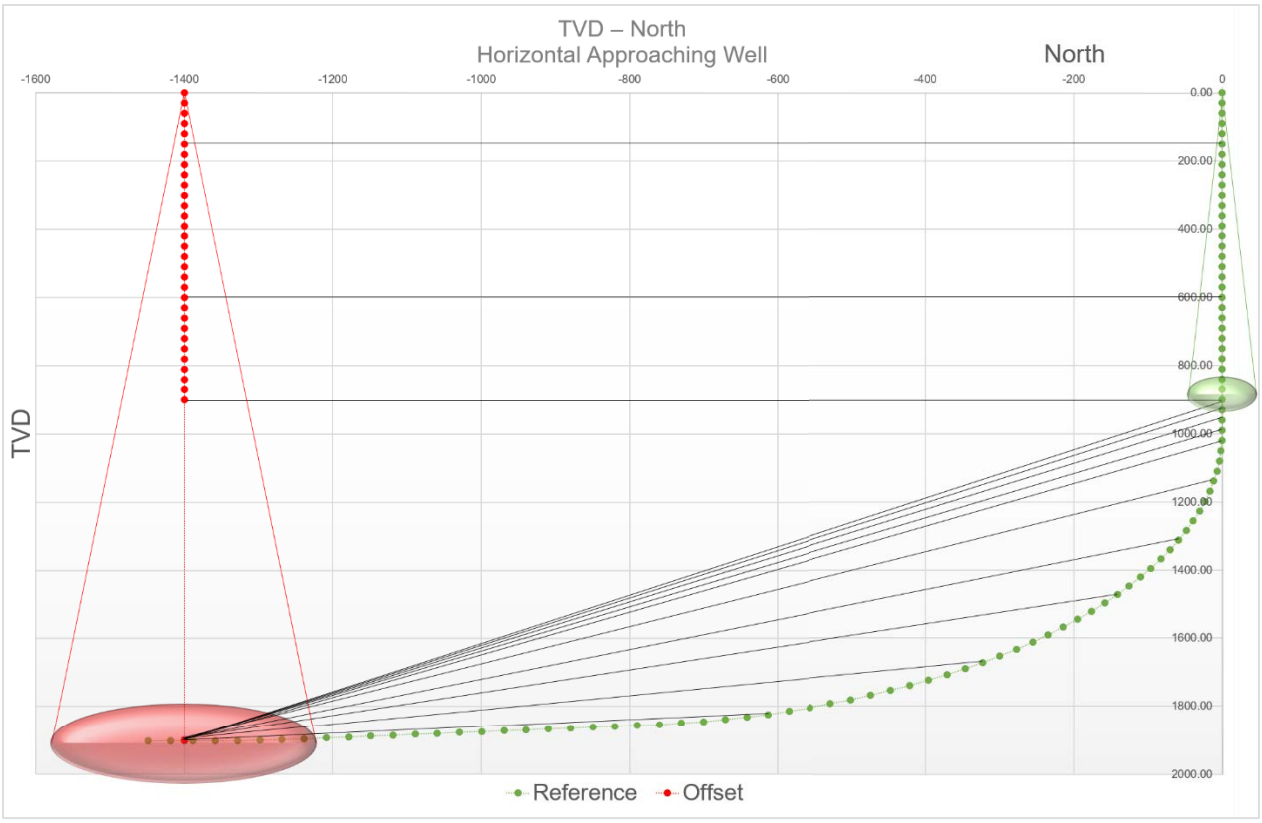

Figure 11: The Minimum Distance Method shown in the Horizontal well. It can be seen in the vertical section that the closest distance switches to the endpoint of the offset well. This can be explained by the procedure of the method, which scans down the entire comparison well at each scan interval. The figure is plotted in two dimensions to visualize the working principle. The MDM calculates the distance in three dimensions, so the graph is true, even though the diagonal line seems to be bigger than the horizontal line

The Directional Difficulty Index (DDI) is another useful tool, which will allow better classification of the scenarios. A well profile with high tortuosity will lead to larger uncertainty magnitudes. Equation 29 shows the calculation principle with MD, Along Hole Distance (horizontal offset), Tortuosity [°] and Vertical Depth (Oag & Williams 2000a). For straight sections, a dogleg rate of 0.5°/30m is used to simulate irregularities in the drilled well.

$$DDI = Log_{10}\left(\frac{Measured\ Depth * Along\ Hole\ Distance * Tortuosity}{Vertical\ Depth}\right) \qquad (29)$$

The DDI is used to determine the difficulty associated to a well. A more complex well will take longer to be drilled. Kellydown™ (Agilis Software Solutions 2016) recommends the classification system described by Oag & Williams.

Table 7: Directional Difficulty Index.

DDI	Interpretation
<6	Simple profile with low tortuosity
6 – 6.4	Regular well with normal tortuosity
6.4 – 6.8	Longer well with relatively tortuous path
>6.8	Long tortuous well profile wit high degree of difficultly

3.3. Establishment of the Well Testing Model

The following steps were taken to build the test model:

1. **Implementation of data into collision-avoidance software**

The data of the offset wells is freely available on the ISCWSA website (www.iscwsa.net). Firstly, the measurements (MD, TVD, A and I) were inserted into Kellydown™. The next step was the correct assignment of preset values (Table 4). All data was checked for gross blunders and discrepancies.

2. **Calculation of ellipsoids of uncertainty (ISCWSA MWD Rev. 4) with different standard deviations (1, 2, 2.58, 3)**

Figure 12 is the product of the second step for the Angular well. The big impact of the confidence level is clearly visible. The ISCWSA added to the wellpaths the dimensions of the uncertainty ellipsoid (calculated with ISCWSA MWD no bias Rev. 2 model). So the EOUs were compared and a slight deviation was recognized (the new model had bigger EOUs). This can be explained with the usage of a different revision and thereby a different model. The trends and ratios were in absolute agreement to each other.

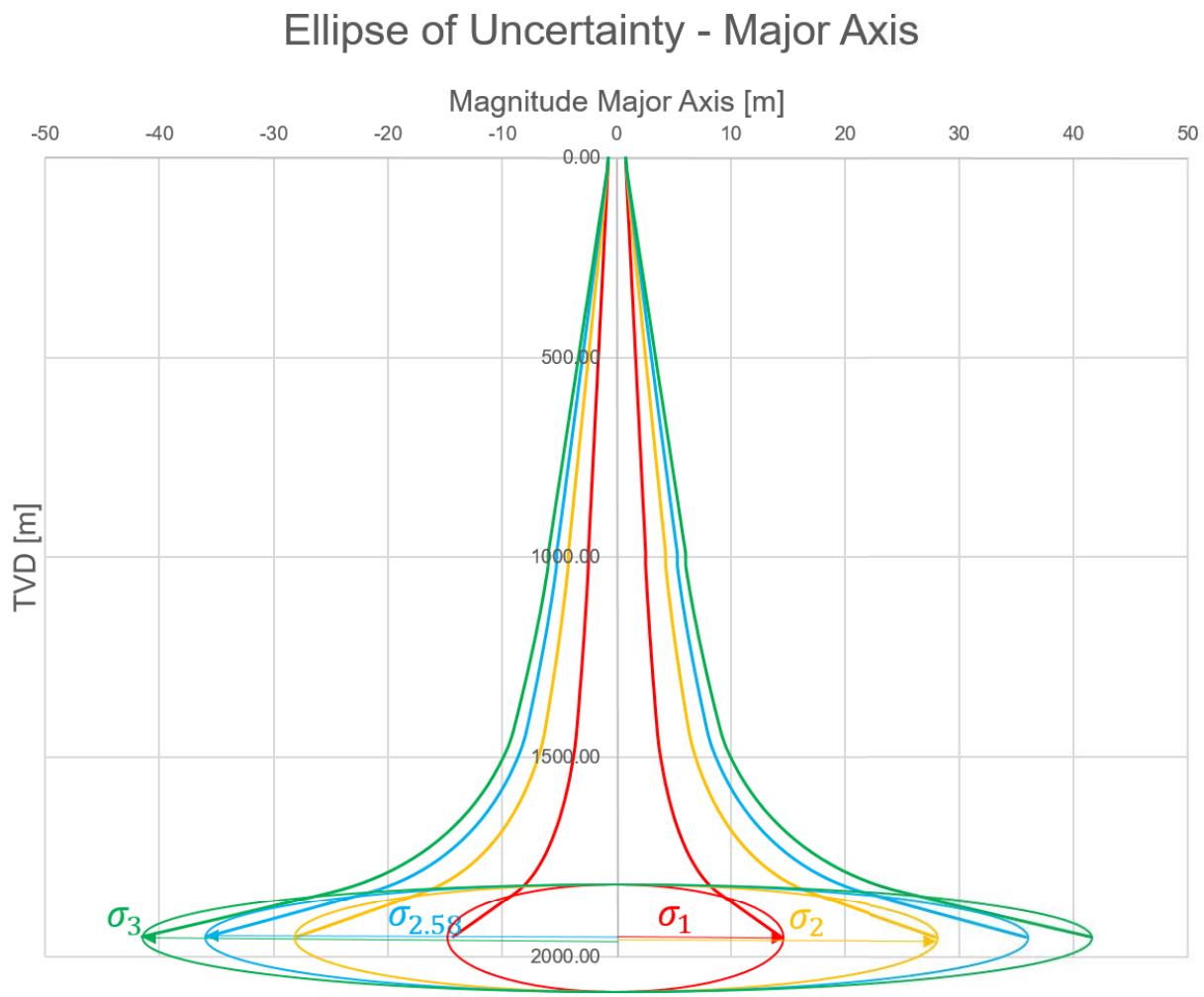

Figure 12: Ellipse of Uncertainty for the Angular well. The major axes of the ellipsoid are drawn versus TVD. The minor axes are not to scale and are just used to visualize the ellipse. The probability distribution for the different standard deviations is summarized in Table 8. The choice of the confidence interval has a big impact on all further calculations.

3. Calculation of distances between reference and offset wells (center to center, ellipsoid to ellipsoid)

The method of choice for this calculation is the minimum distance (also known as closest approach in popular software applications such as Compass™). The advantages were already explained and proven in the previous sections.

Table 8: Probability Related to a Specific Standard Deviation. For this thesis, all uncertainty ellipsoids and thereby separation factors and probabilities were calculated in the four variations

Standard deviation	Probability
1	68%
2	95%
2.58	99%
3	99.7%

4. **Calculation of separation factors with four different standard deviations and two different separation factor calculation methods**

The comparison of Okewunmi & Brooks in 2011 showed that several standard deviations were used by the selected companies. In order to cope with this, a wide range of σ was thought to be necessary. In addition to that, the results will give a clearer picture of the influence of standard deviations on SFs.

5. **Calculation of collision probability (Equation 24)**

This procedure was performed for every offset well. It should be noted that the recommendation of the ISCWSA was followed and a diameter of 36 [inch] for the reference well and 24 [inch] for the offset wells was chosen, from zero to target depth (TD).

6. **Calculation of separation factors with four different standards (four different companies)**

In order to check the results with real-world standards, the collision-avoidance standards of four companies were compared (Bang & Nyrnes 2015, ISCWSA 2007).

Company 1-4:

C1 $$SF = \frac{D - (r_r + r_o)}{3 * (R_r + R_o)} \quad (30)$$

C2 $$SF = \frac{D}{2 * (R_r + R_o)} \quad (31)$$

C3 $$SF = \frac{D - (r_r + r_o)}{2.79 * \sqrt{2} * (R_r + R_o)} \quad (32)$$

C4 $$SF = \frac{D - (r_r + r_o)}{2.878 * (R_r + R_o)} \quad (33)$$

with D (center to center distance), $r_r \& r_o$(casing radius of reference and offset well, respectively) and $R_r \& R_o$ (ellipsoid radius of reference and offset well, respectively). In addition to that, the four companies have varying reaction standards if a certain SF is reached.

In order to derive meaningful outcomes, the equations were performed in three dimensions, using the expanding ellipsoid method in combination with the closest approach. The calculation method might vary in reality within the four companies, which does not affect the validity of the outcomes in this thesis.

3.4. Description of Offset wells

The objective of this chapter is to give the reader an understanding for the scenarios and difficulties of each individual case. In several meeting minutes of the ISCWSA (ISCWSA 2011 & ISCWSA 2015) confirmed the need for a model to evaluate separation factor calculations, which has not been published in the literature so far. The following work will attempt to deliver such a model. The main focus will be drawn to the development of a transparent approach of the separation factors, explaining all steps and showing the results. It should then be possible to follow each step and check software for misalignments.

The following table lists key trajectory parameters of the offset wells. The wells are not categorized as designer wells or extended-reach wells with complex trajectories. This is absolutely necessary to develop a model that can be used for comparison applications.

Table 9: Directional Parameters of Offset Wells. East20 has the highest directional complexity, whereas the Short Opposite maintains the simplest trajectory. Large inclination angles can be

found in every offset well, representing nowadays situation where directional drilling is of great importance. The MD is in a range of 2200-3090 [m] with a horizontal offset range of 0-1541 [m].

Well	MD [m]	TVD [m]	Horizontal Offset [m]	Total Dogleg [°]	Total Tortuosity [°]	DDI
Angular	2655	1950	1153	70	102	5.2
East10	2820	1915	1316	87	112	5.3
East100	2940	1904	1448	90	116	5.4
East20	2850	1864	1341	118	138	5.5
Horizontal	2590	1900	1059	90	110	5.2
North100	3090	2003	1541	90	116	5.4
Overlap Opposite	2775	1900	1283	85	110	5.3
Perpendicular	2450	1795	1082	70	99	5.2
Short Opposite	2325	1861	834	85	103	5.0
Sidetrack	2430	1900	931	100	123	5.2
Vertical	2200	2200	0	0	0	0

3.4.1. Ellipsoid of Uncertainty – Major Axis

The concept of ellipsoids of uncertainty were discussed in several parts of this thesis. Figure 13, 14, 15 and 16 show the resulting dimensions. The largest major-half axes are created by the Horizontal and Perpendicular wellbores (Figure 14). It is crucial to recognize that a 1 Sigma s.d. (standard deviation) is only half of a 2 Sigma s.d. (Figure 13). Furthermore, the diagram looks similar to the actual trajectory, giving straightforward indication that deviation is proportional to the major uncertainty axis.

Table 10: EOU – Major Axis Magnitude divided by MD. This number gives an overview on the magnitude of the biggest uncertainty normalized to the measured depth. The perpendicular and

horizontal well create the biggest uncertainty due to the fact that the azimuth is 90° and the inclination as well. The MWD model is sensitive to horizontal drilling in East-West directions.

Well	$\frac{\sigma_1}{MD}$	$\frac{\sigma_2}{MD}$	$\frac{\sigma_{2.58}}{MD}$	$\frac{\sigma_3}{MD}$
Angular	0.0054	0.0105	0.0134	0.0156
East10	0.0050	0.0096	0.0124	0.0143
East100	0.0051	0.0100	0.0129	0.0149
East20	0.0050	0.0097	0.0124	0.0143
Horizontal	0.0062	0.0122	0.0156	0.0181
North100	0.0052	0.0101	0.0130	0.0151
Overlap Opposite	0.0048	0.0093	0.0120	0.0139
Perpendicular	0.0069	0.0134	0.0172	0.0199
Short Opposite	0.0040	0.0077	0.0098	0.0113
Sidetrack	0.0042	0.0082	0.0105	0.0121
Vertical	0.0021	0.0039	0.0049	0.0056

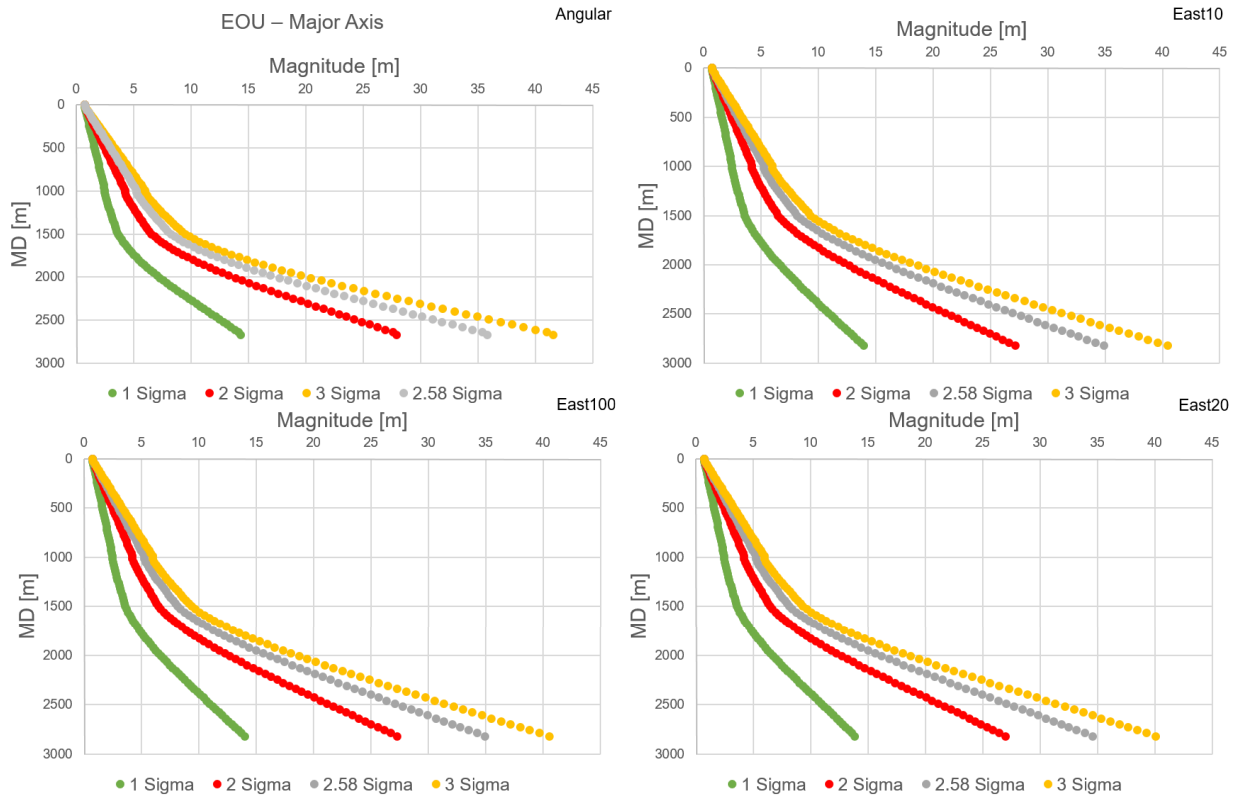

Figure 13: EOU Major Axis Magnitude for AW, East10, East100 and East20 well. The MD and magnitudes of uncertainty are quite similar. The diagrams demonstrate the importance to assign the correct standard deviation to collision-avoidance calculations

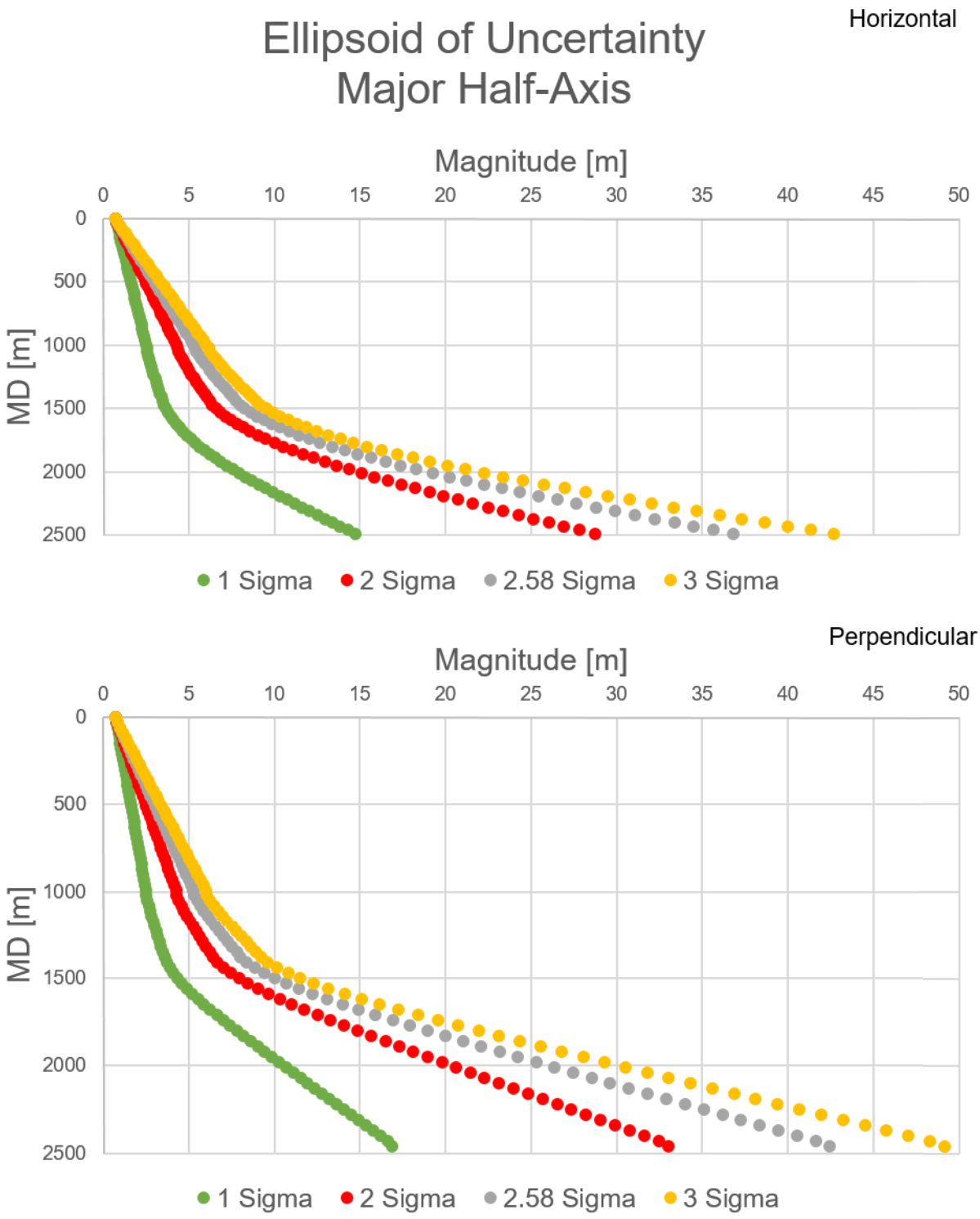

Figure 14: EOU Major Axis Magnitude for HW and PW. The two wells produce the highest uncertainty (Table 8). The drilling direction and inclination angle are two significant attributes in the equations, changing the magnitude of uncertainty.

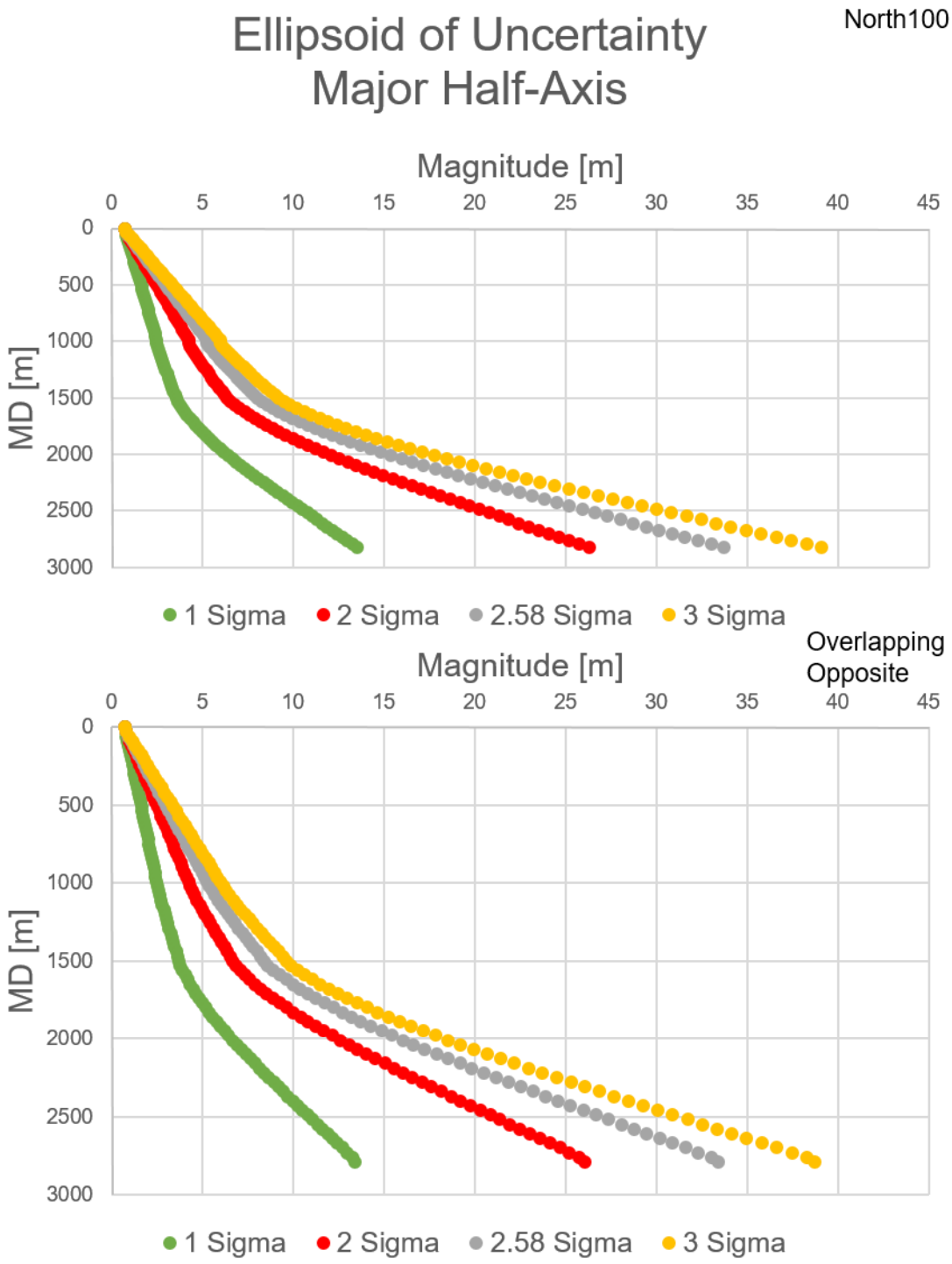

Figure 15: EOU Major Axis Magnitude for North100 and Overlapping Opposite well.

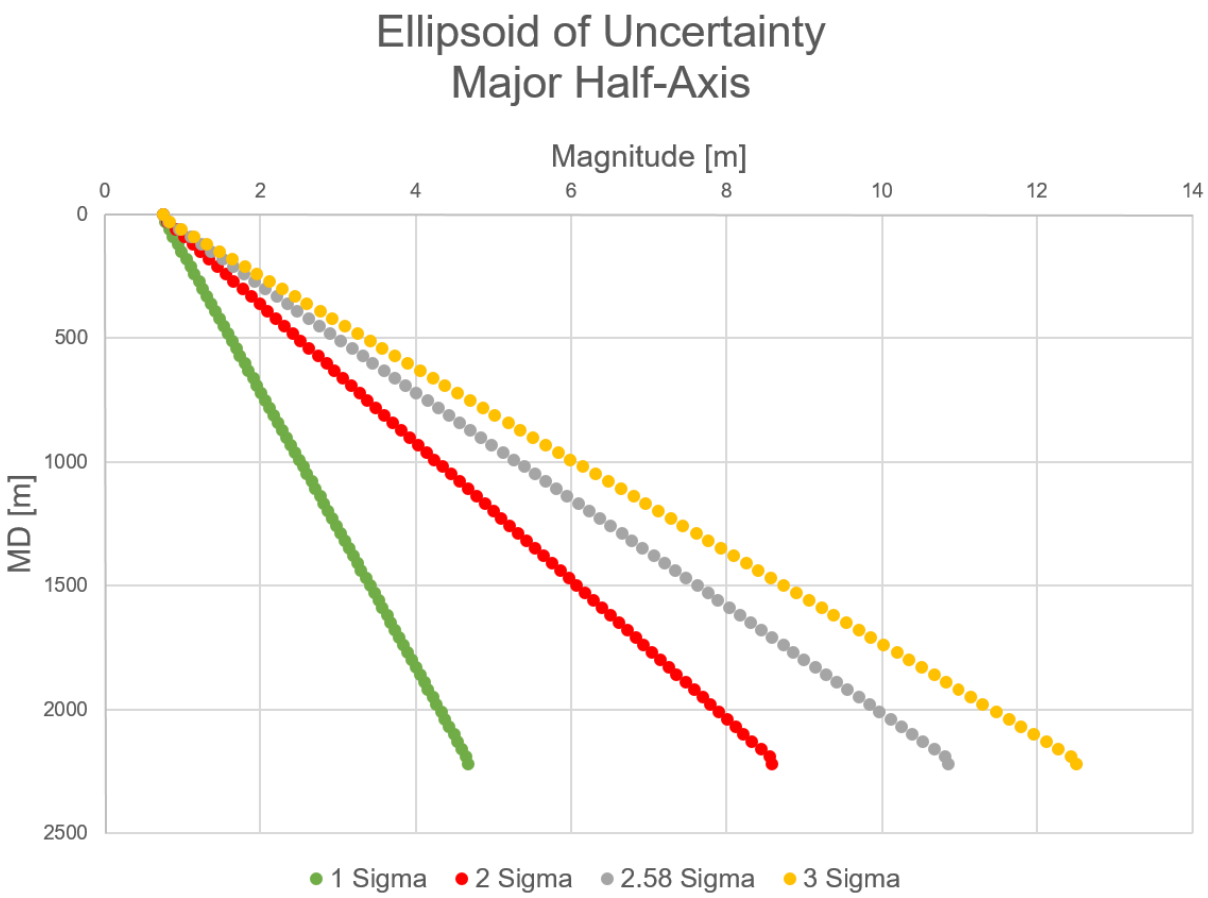

Figure 16: EOU Major Axis Magnitude for Vertical well The Ellipsoid of Uncertainty has the lowest dimensions for the Vertical well. In contrast to the other wells, the increase of uncertainty is linear. The weighting functions of the MWD model are highly sensitive to inclination and azimuth readings. With no deviation present in a well, the function rises steadily.

3.4.2. Effective Distances Between the Wells

The analysis of separation factors can only give conclusions if effective distances are considered. The closest points are listed in Table 11, ranging from 100 [m] to 1.23 [m].

Table 11: Effective Distance Between Reference and Offset Wells.

Well	Closest Point [m] – Center to Center
Angular	29.8
East10	11.48
East100	100
East20	9.91
Horizontal	12.73

North100	99.64
Overlapping Opposite	58.69
Perpendicular	45.18
Short Opposite	51.68
Sidetrack	12.48
Vertical	1.23

3.5. Test Wells

The wells will be described with three graphs, showing the plan view and vertical sections (towards East and North).

3.5.1. Angular

The Angular well simulates a situation where the RW is crossed at an acute angle. The key parameters are summarized in Table 7, 8 and 9. Figure17 explains the geometries of the two wells and the type of collision. The Reference well passes the Angular well slightly above it, in an azimuthal difference of 35° (Ref. well: 180°; Ang. well: 145° azimuth). The inclination of both wells is approximately the same when the wellpaths intersect.

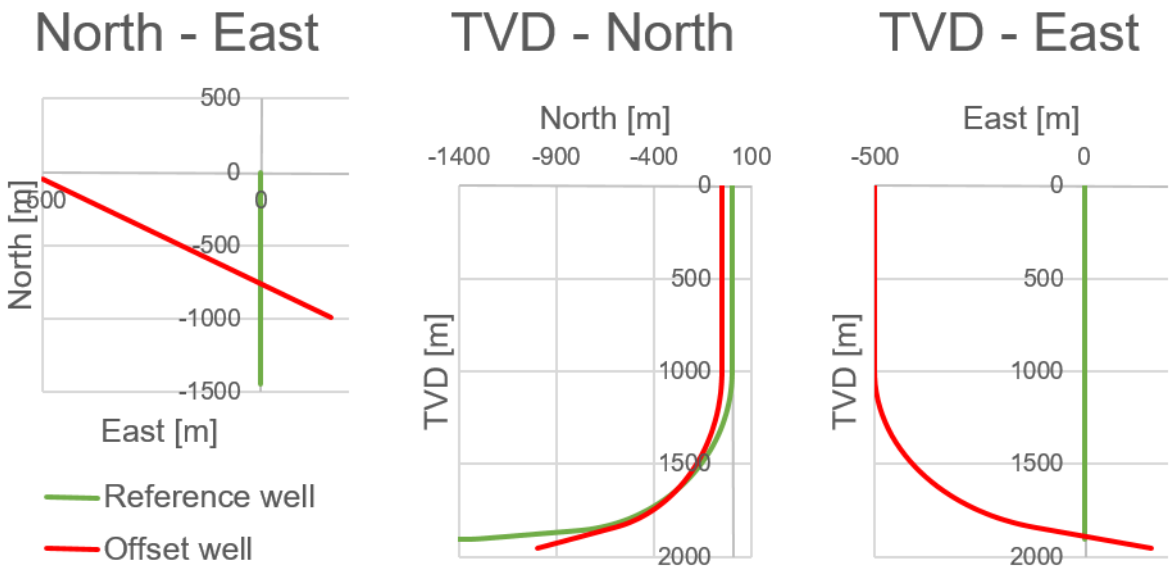

Figure 17: Plan view and vertical section of Angular and Reference well . The two wells collide deep with an azimuth difference of 35° and equal inclination.

3.5.2. East10

The East10 well is very close to the Reference well and crosses the wellpath in the deeper section. The Reference well is again above East10, thereby the calculations should match.

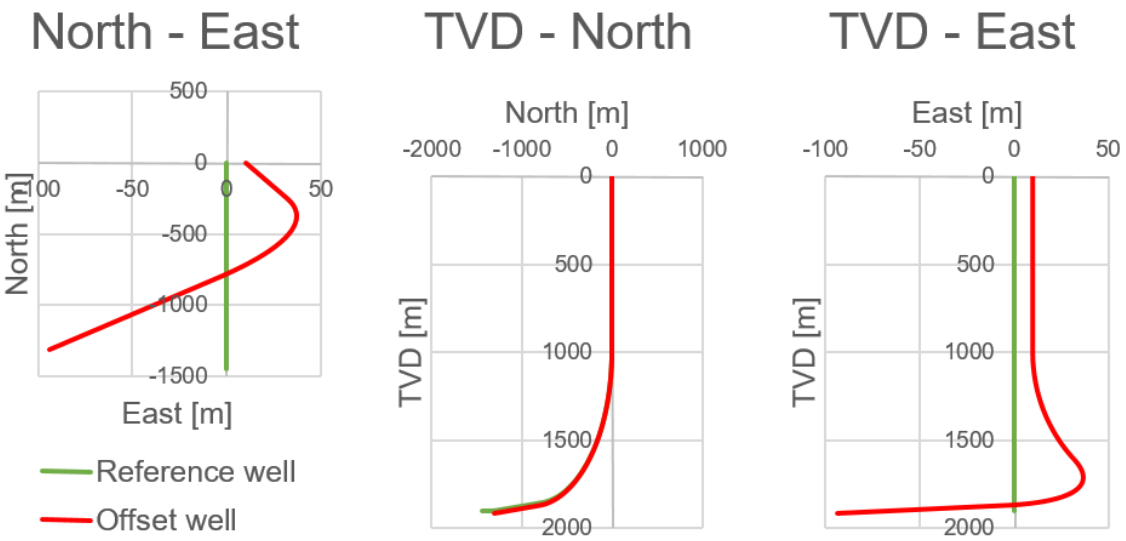

Figure 18: Plan view and vertical section of East10 and Reference well.

3.5.3. East100

The trajectory of the East100 is equal to the Reference well. The starting location is 100 [m] east and completely parallel.

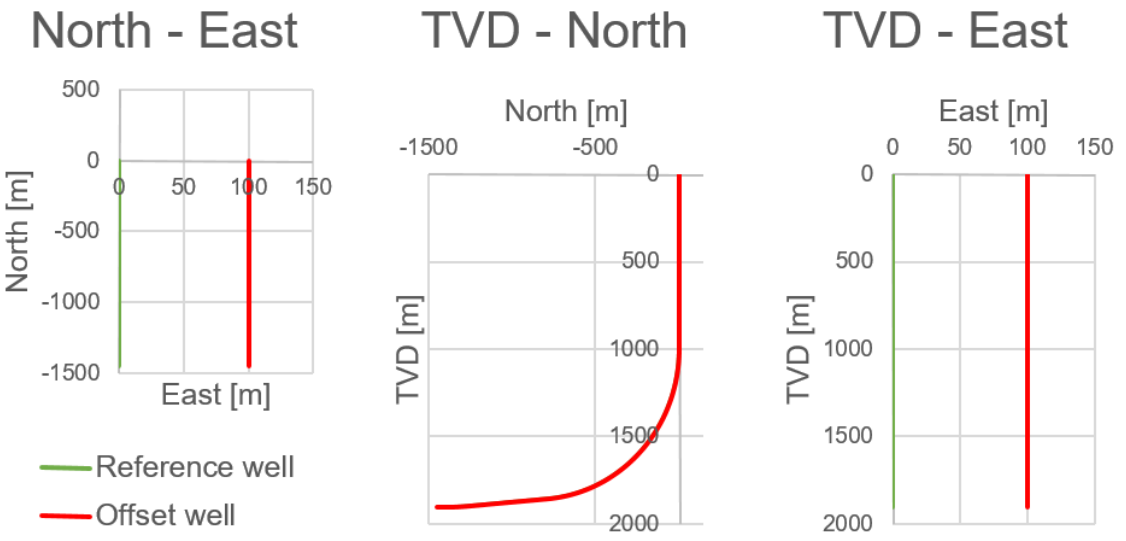

Figure 19: Plan view and vertical section of E and Reference well.

3.5.4. East20

East 20 has the highest value for DDI, which can be seen in Figure 20. The well is drilled close to the Reference well and intersects at nearly 90° in the deeper section.

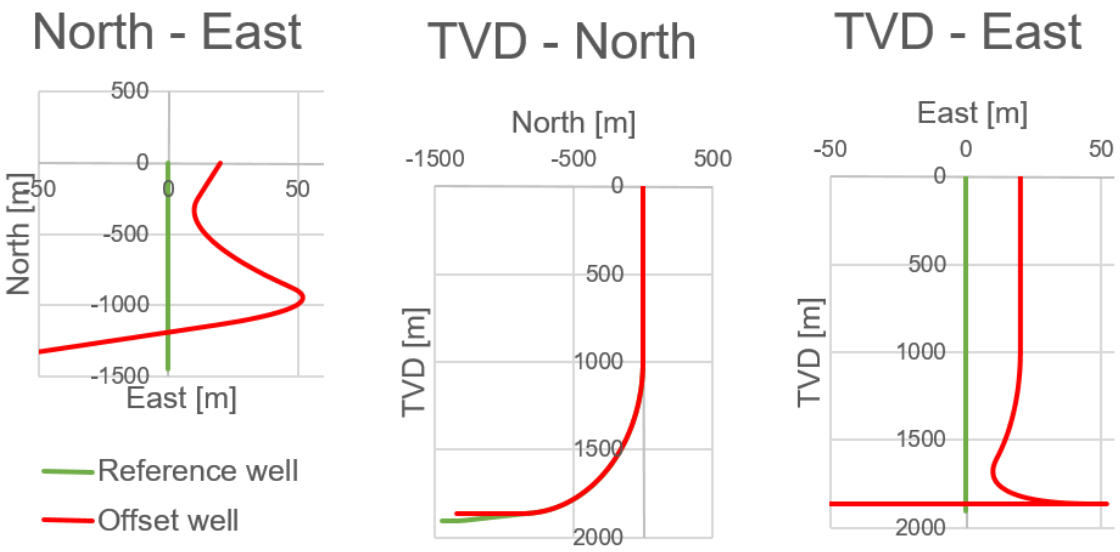

Figure 20: Plan view and vertical section of East20 and Reference well.

3.5.5. Horizontal

The horizontal well approaches RF from the west and hits it directly. The inclinations of both wells are equal and the collision angle is 90°.

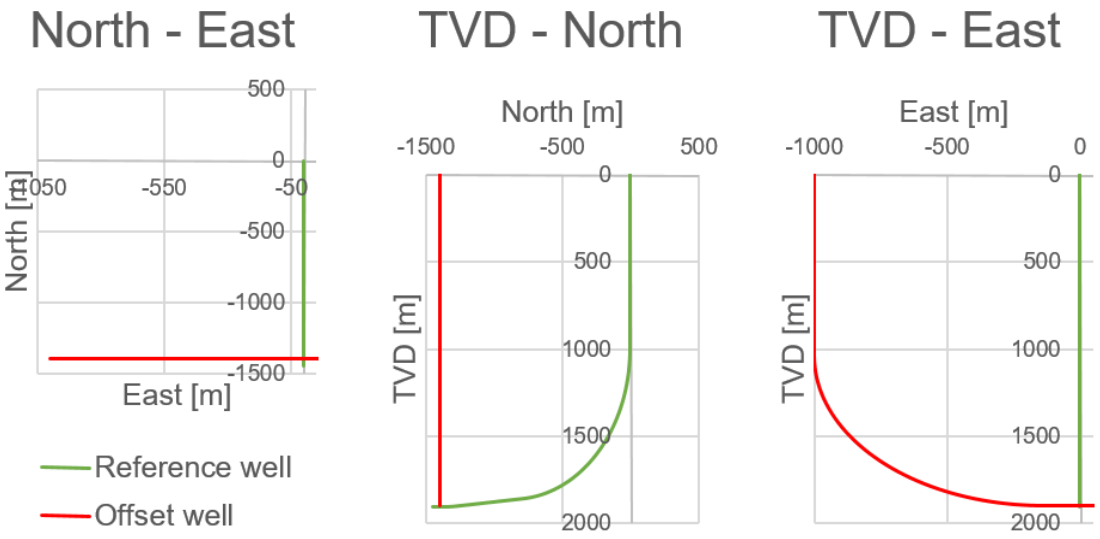

Figure 21: Plan view and vertical section of Horizontal and Reference well.

3.5.6. North100

North100 simulates a scenario where the Reference well is drilled right above an adjacent well. Just like the East100, it is completely parallel.

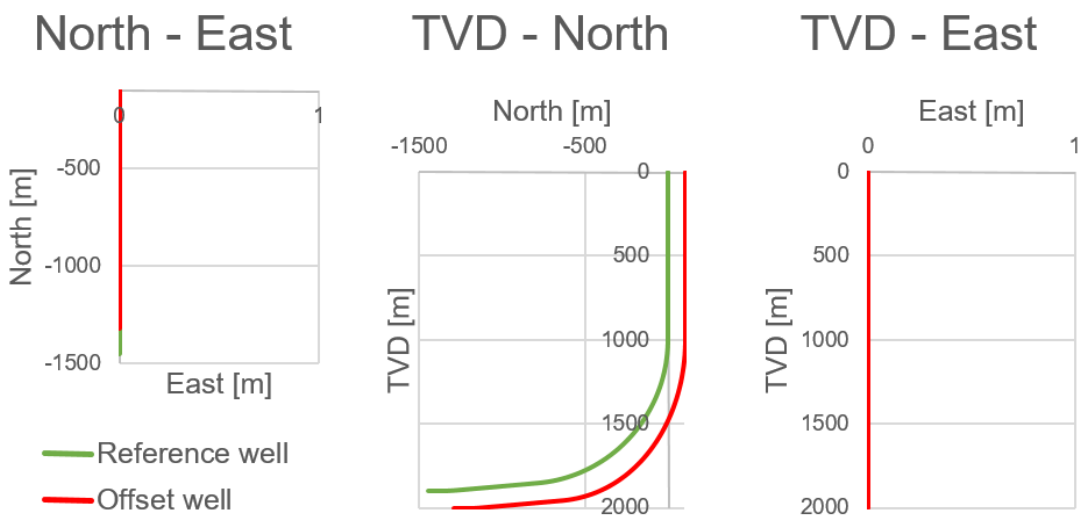

Figure 22: Plan view and vertical section of North100 and Reference well.

3.5.7. Overlap Opposite

The Overlapping Opposite well approaches the RW from the opposite direction. This scenario incorporates a dangerous situation, as the distance between the wellbores will decrease fast. In contrast to the SOW, the two wells overlap, which is a complex scenario if the problem is not treated in three dimensions.

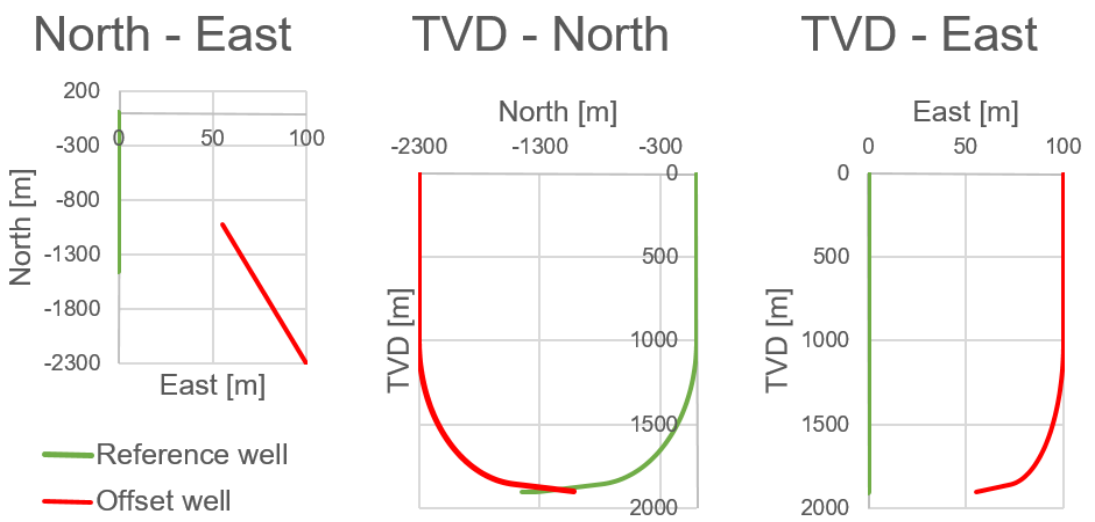

Figure 23: Plan view and vertical section of Overlap Opposite and Reference well.

3.5.8. Perpendicular

The Perpendicular situation is similar to the Horizontal well scenario, besides that the well hits the RW at the end of the build section. The inclination of both colliding wells is equal.

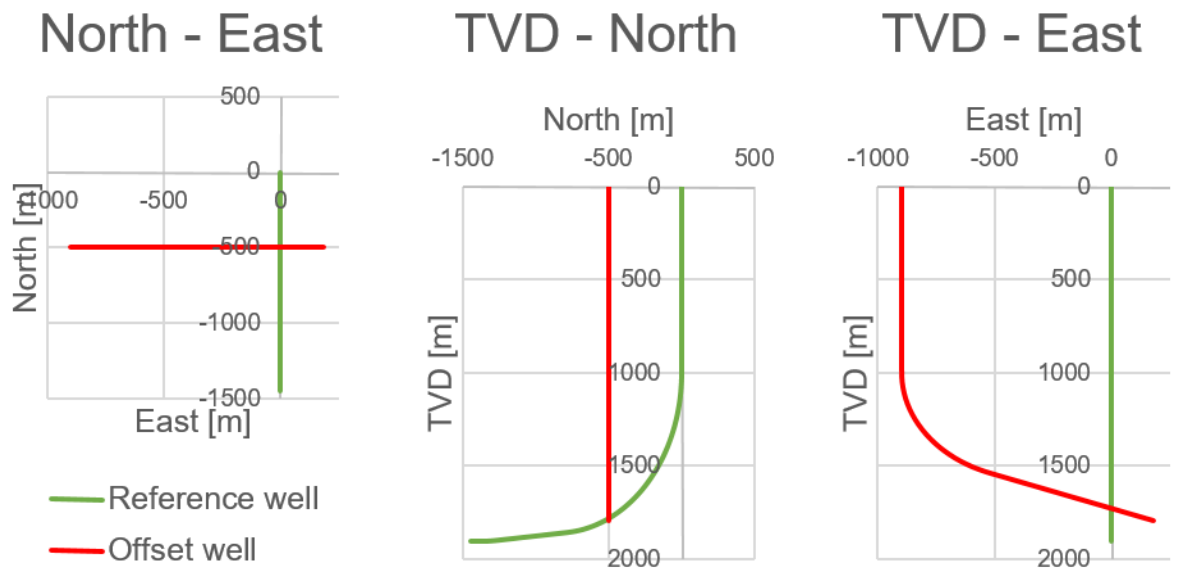

Figure 24: Plan view and vertical section of Perpendicular and Reference well.

3.5.9. Short Opposite

The Short Opposite well approaches the RW from the opposite direction. The trajectory specifications can be seen in Table 7. This situation is dangerous as the SF will change rapidly, and it might be impossible to take appropriate collision-avoidance measures. If a well has to be planned in a similar way, special attention should be given to along-depth errors, such as stretch and thermal expansion. In addition to that, the procedure to record MD (pipe tally or sensors) should be observed.

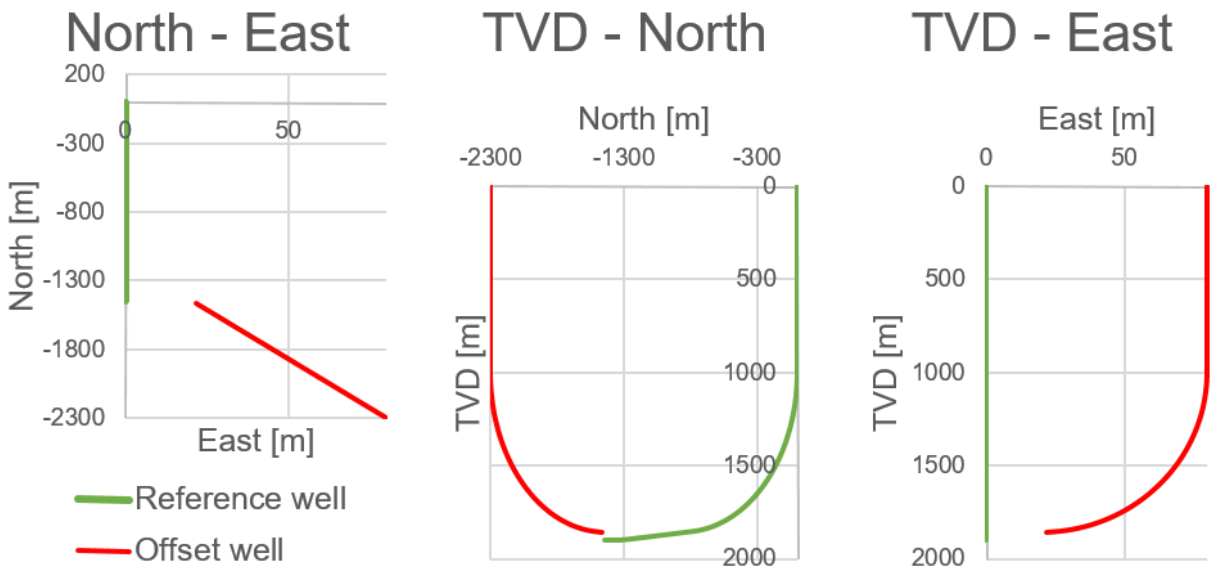

Figure 25: Plan view and vertical section of Short Opposite and Reference well.

3.5.10. Sidetrack

A sidetrack has to be drilled if the wellpath is blocked. This situation is often encountered and points out how collision-avoidance software deals with high uncertainties in combination with very low separation distances (when the sidetrack is started).

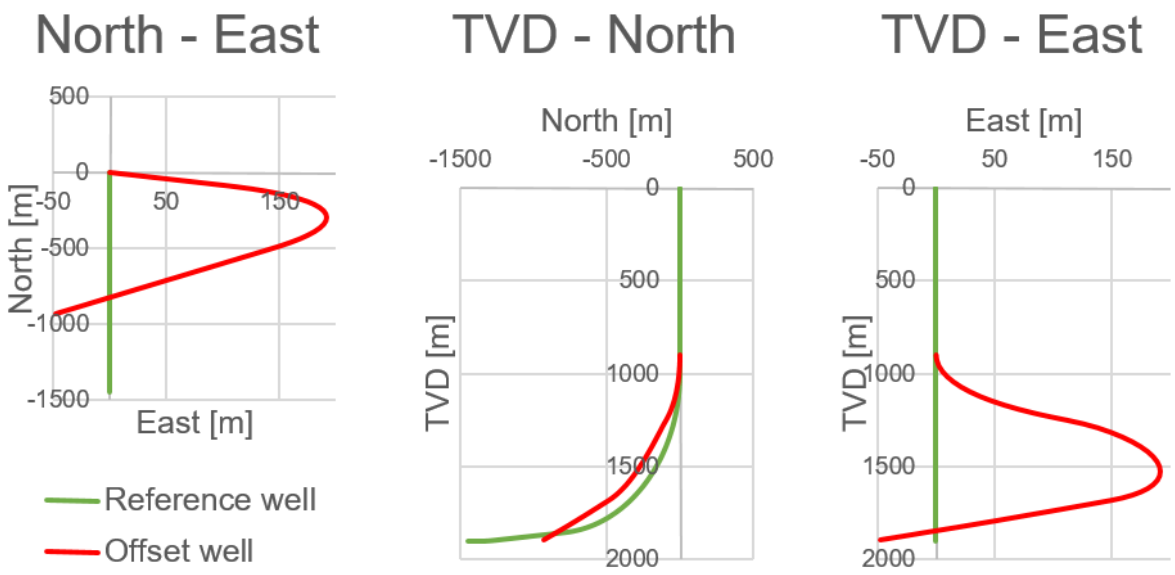

Figure 26: Plan view and vertical section of Sidetrack and Reference well.

3.5.11. Vertical

The vertical well has the closest center-to-center distance of all offset wells.

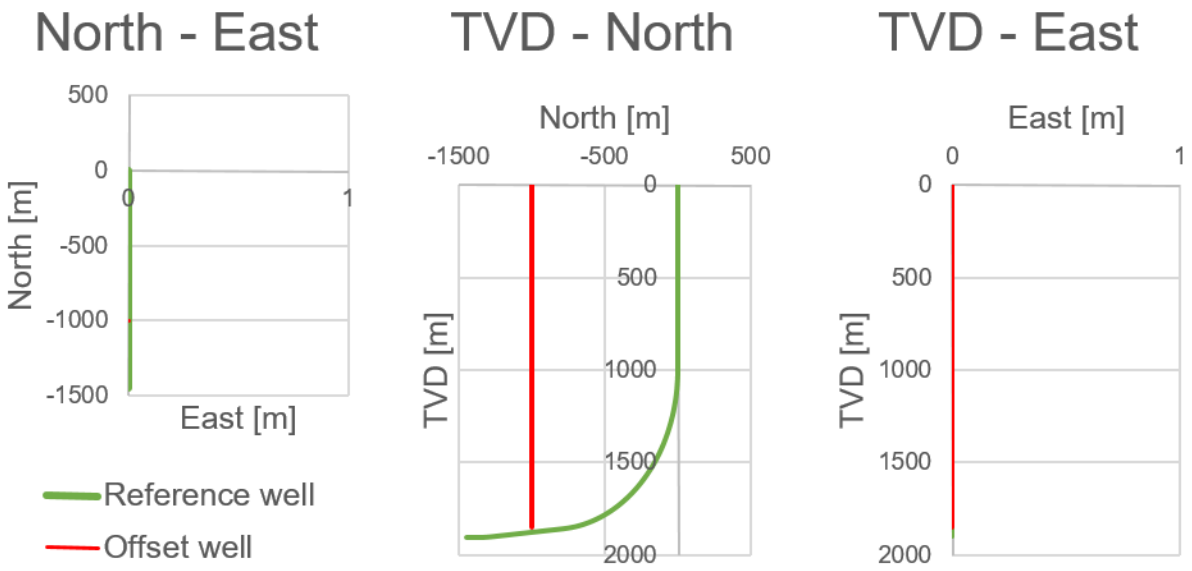

Figure 27: Plan view and vertical section of Vertical and Reference well.

4. Results

This chapter provides the results of separation factor and probability calculations. As the previous sections explained, the separation factor can be established, if the uncertainty is assessed by ellipsoids. The two methods which are currently in use are compared and limitations addressed. In order to fully evaluate the functionality of a method it is mandatory to simulate different scenarios. To give the reader a better overview, wells showing a strong analogy will be summarized in this section.

4.1. Separation Factor and Probability Comparison

The following part will present the results for separation factor calculations. The figures and interpretations will focus on SFs below 10. It should be memorized that a separation factor is not a safety factor. If the SF is doubled, it does not mean a doubled safety. To see the outcomes for differing collision-avoidance standards between companies in the oil and gas industry, the separation factors of several companies were calculated for the specific well.

4.1.1. Angular

The Angular well was described in the methodology chapter and the resulting separation factors are shown in Figure 28. One issue for this well is the azimuthal difference between the wells, leading to differences in the ellipsoids major axis direction. The second problem is a vertical separation at the cross point. The results can be seen in Figure 28. With a large center-to-center distance the separation factors have a slight mismatch (if the SF of equal standard deviation are considered). This changes at SFs below 2.0, as the radii of the ellipsoidal major axes are becoming the dominant part in equation 22. The result is a huge variation between SFs of the same standard deviation. The combination of large measured depth and very close crossing leads to high collision probabilities and very low separation factors. It is interesting to see the gap between 1 sigma and the other standard deviations. If the well was monitored with 1 standard deviation, the drilling could have

continued (most companies react when the SF gets below 2), even though this is an extremely dangerous incident.

Dependent on the method, the SFs vary between 3.5 and approximately 0.5 for the same MD (RW). So the question, what SF calculation method produces the best outcome, has to be answered. SFs calculated based on ellipse summation are between 1.5 and 0.5. This means that the wells should have very high collision probabilities, which is not the case. If the geometry of the colliding situation is remembered, it is reasonable to say that the SFs based on ellipse separation deliver better results.

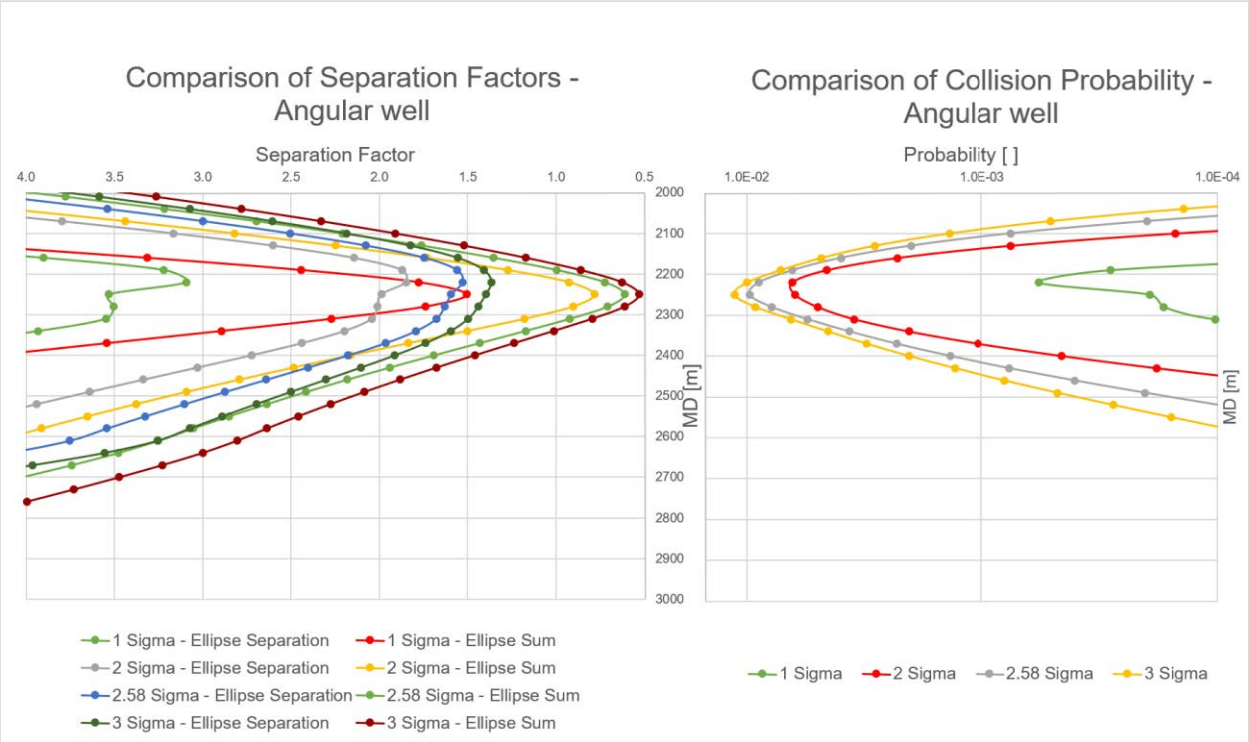

Figure 28: Results for Angular well. The left diagram compares the two separation factor calculation methods. Four different standard deviations (for the calculation of the EUOs) are used to illustrate the effects of the EOUs magnitude. The right diagram shows the probability at the respective depth.

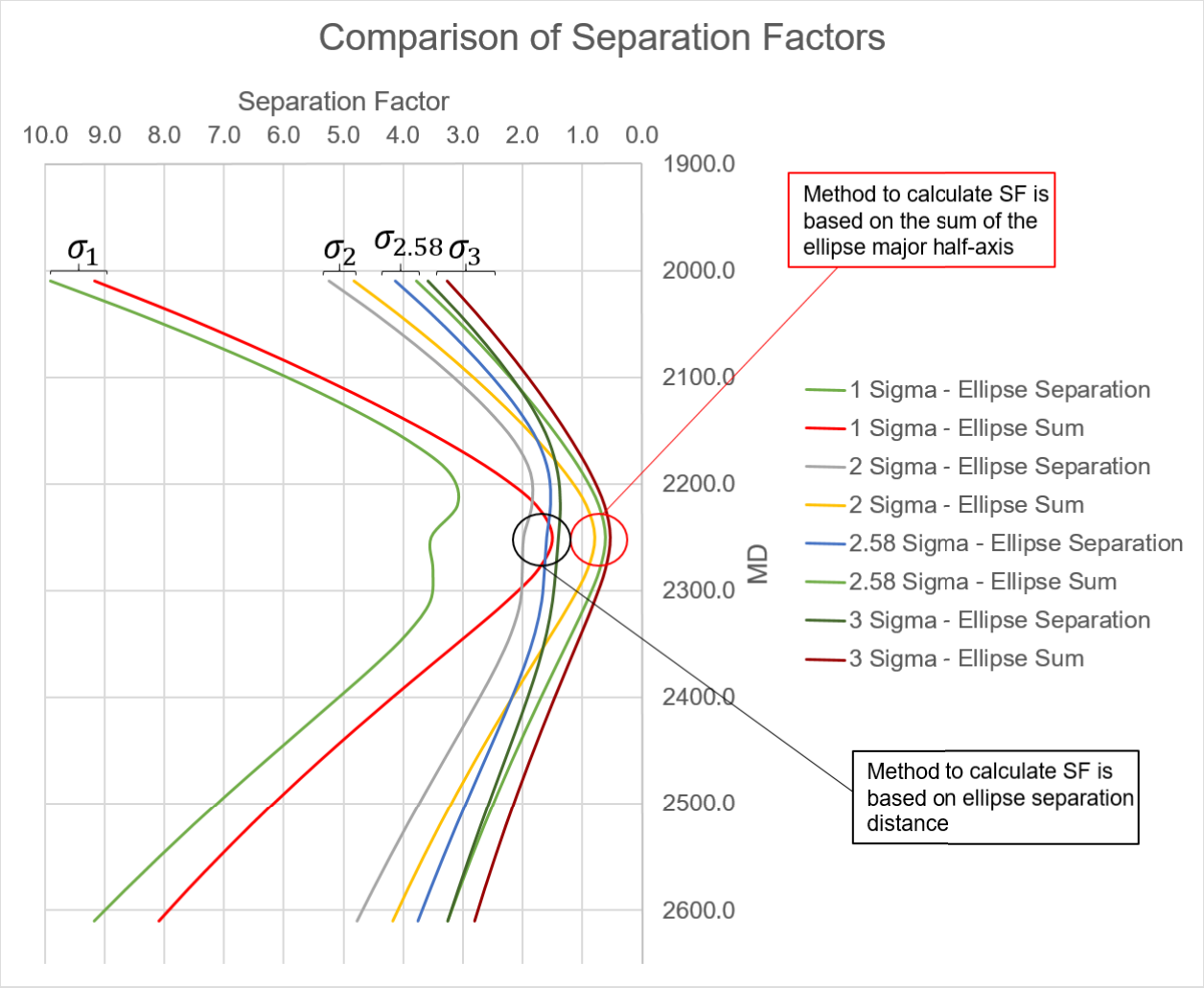

Figure 29: Comparison of Separation Factors (Angular well) . The difference between the two methods is illustrated and special attention should be given to the gap between σ_1 and σ_2, $\sigma_{2.58}$ and σ_3. In one situation (approximately 2250 [m] MD) the SF is reversing the trend of the others. This could give a false impression of safety.

In Figure 30 four different companies were compared to emphasize the demand for a standard procedure. The companies consist of three service providers and one operator. The reactions range from a complete drilling stop combined with a major-risk alert, shut in of the well and monitoring of offset wells to no reaction at all. If a software was to be tested, Figure 30 should be created and compared to the results of the software.

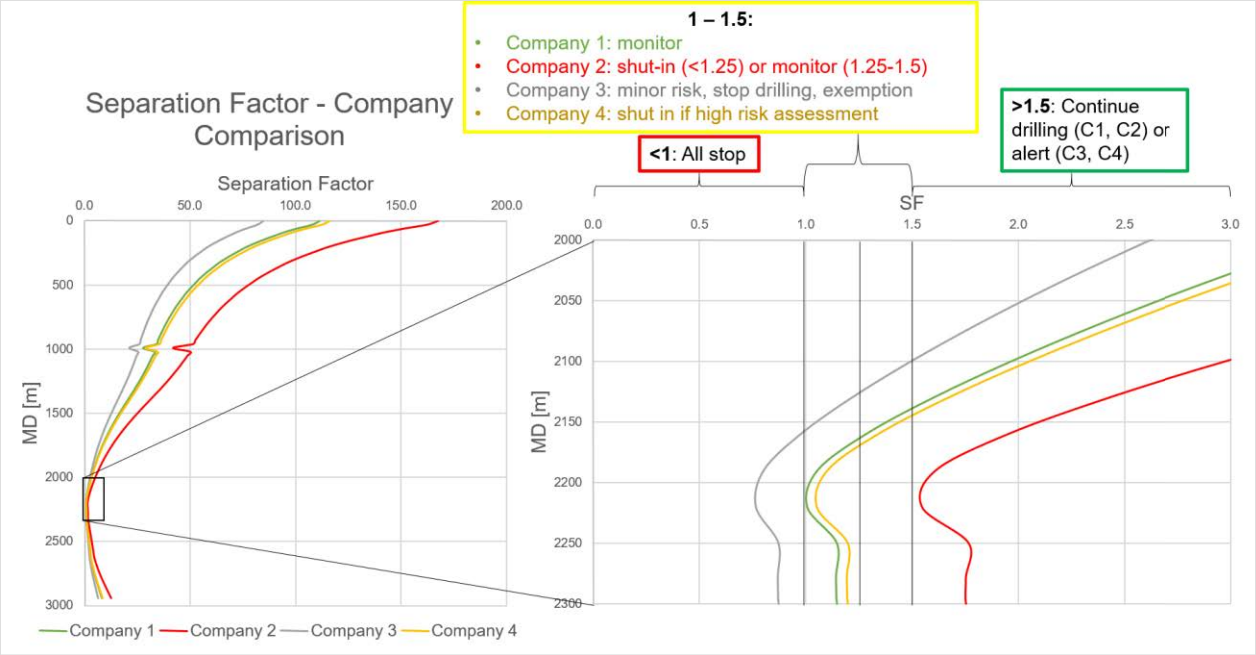

Figure 30: Separation Factor Comparison between Companies for Angular well. The left diagram shows the entire RW and the respective SF towards the Angular well. The magnified section of interest can be seen in the right diagram. The different policies will lead to big differences in the actions taken to mitigate well collision risks. While C3 would stop drilling at 2100 [m] MD, C2 would not react at all.

4.1.2. East10

The East10 well starts, as the name indicates 10 [m] East to the RW. Both equations work accurately, as the major axes point into the same direction. Figure 31 confirms the excellent matching, where only slight differences can be noticed between each type of SF. The probabilities of the standard deviations above 1 are equal. This can be explained by the low separation distance between the wells. The σ value in equation 24 is large for each standard deviation, which will result in nearly equal values if the separation distance is small.

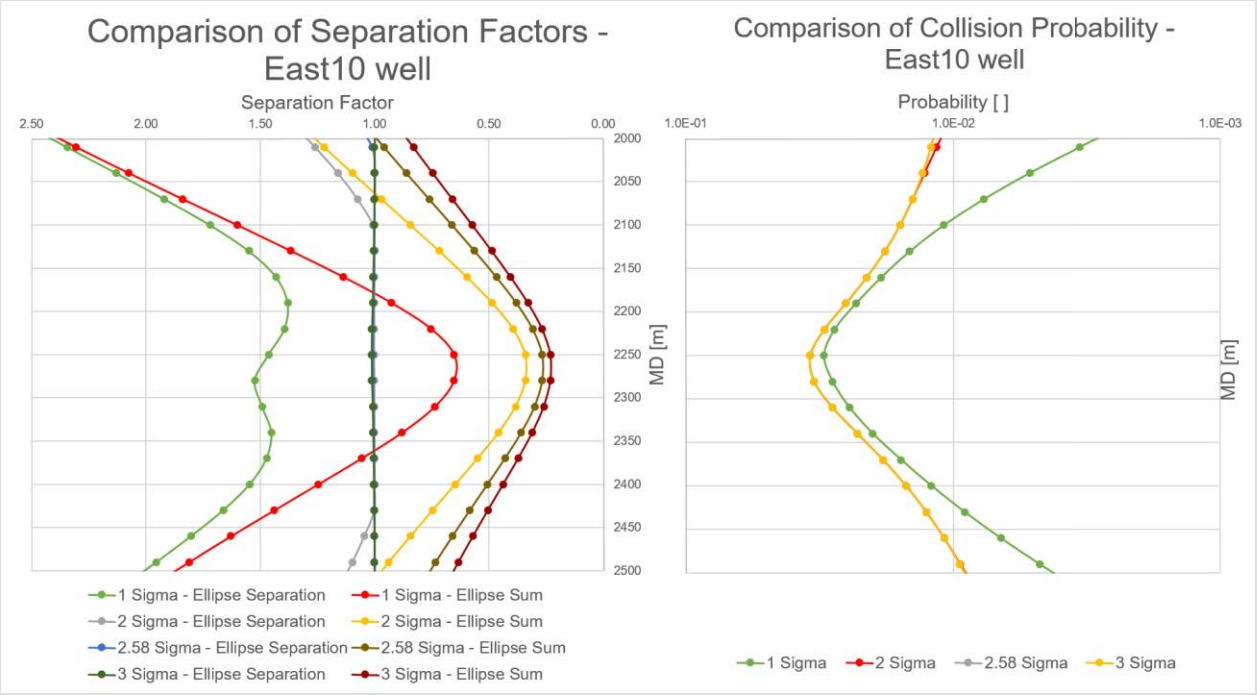

Figure 31: Results for East10 well . The SFs based on ellipse-summation are grouped below a SF of 1. The two methods differ by a factor of two when calculated with 1 standard deviation. The right diagram shows the probability distribution in the collision zone. In theory, the two wells do not collide by a 100%, so the probability should be below 1. It is interesting to see that the deviations above 1 are completed aligned (probability figure). This can be explained by the normal distribution that the probability equation (Equation 27) is based on (Figure 6).

Figure 32 depicts the results for the company comparison of the East10 well. The complete well will be tagged as major-risk well in all standard procedures. The difference in collision-avoidance politics can be recognized, as Company 3 would not drill one meter, while company 2 would start monitoring at 500 [m] and shut-in at 1000 [m].

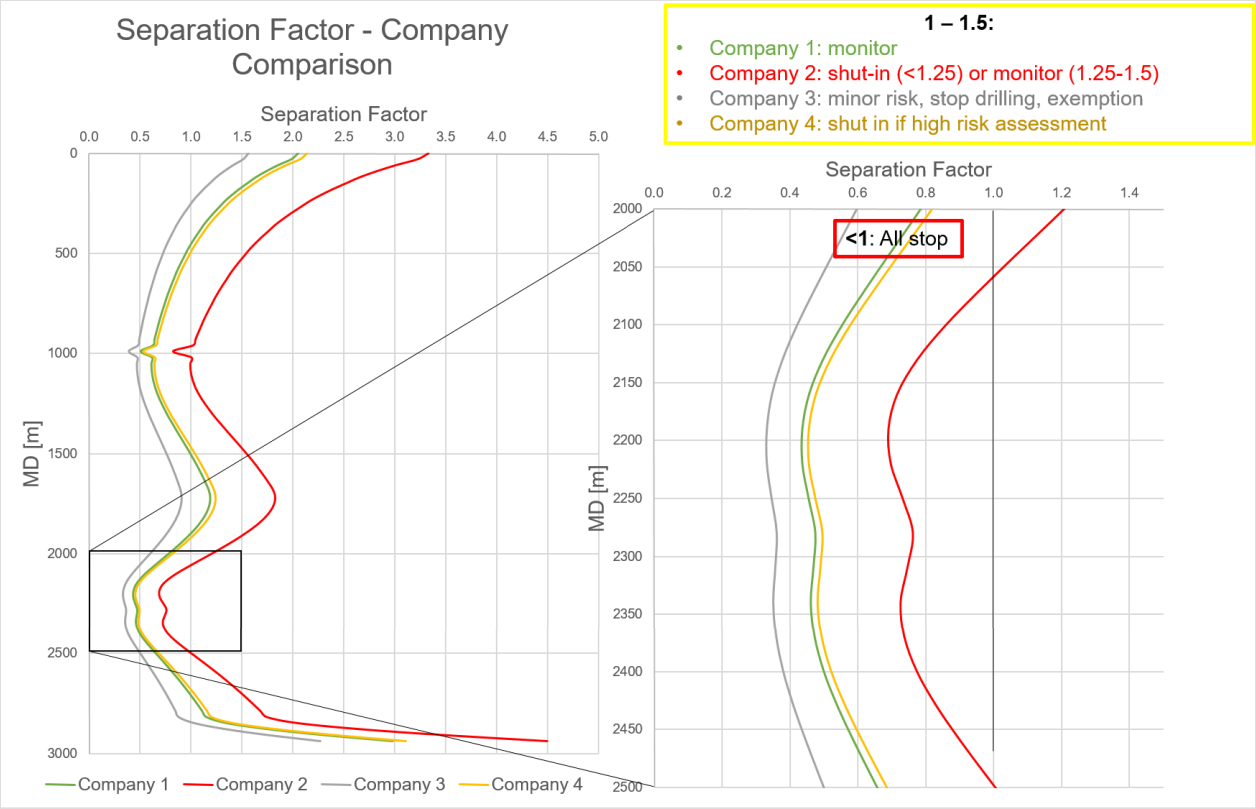

Figure 32: Separation Factor Comparison between Companies for East10 well. For all companies this well would be a major risk well. The SF remains below 1.5 for most companies. The deviation between Company 2 and 3 is tremendous.

4.1.3. East100&North100

A parallel well, like the East100 or North100, will steadily increase its positional uncertainty. It is therefore obvious that the SF and probability are following a nearly linear trend. The only difference is the distribution within two standard deviations. While in East100 (EOU parallel) the ellipsoids axes show into the same direction, North100 is below RW. It is reasonable to say that the depth uncertainty should be decisive on the separation distance. Ellipse separation takes this into account and delivers the correct separation factor.

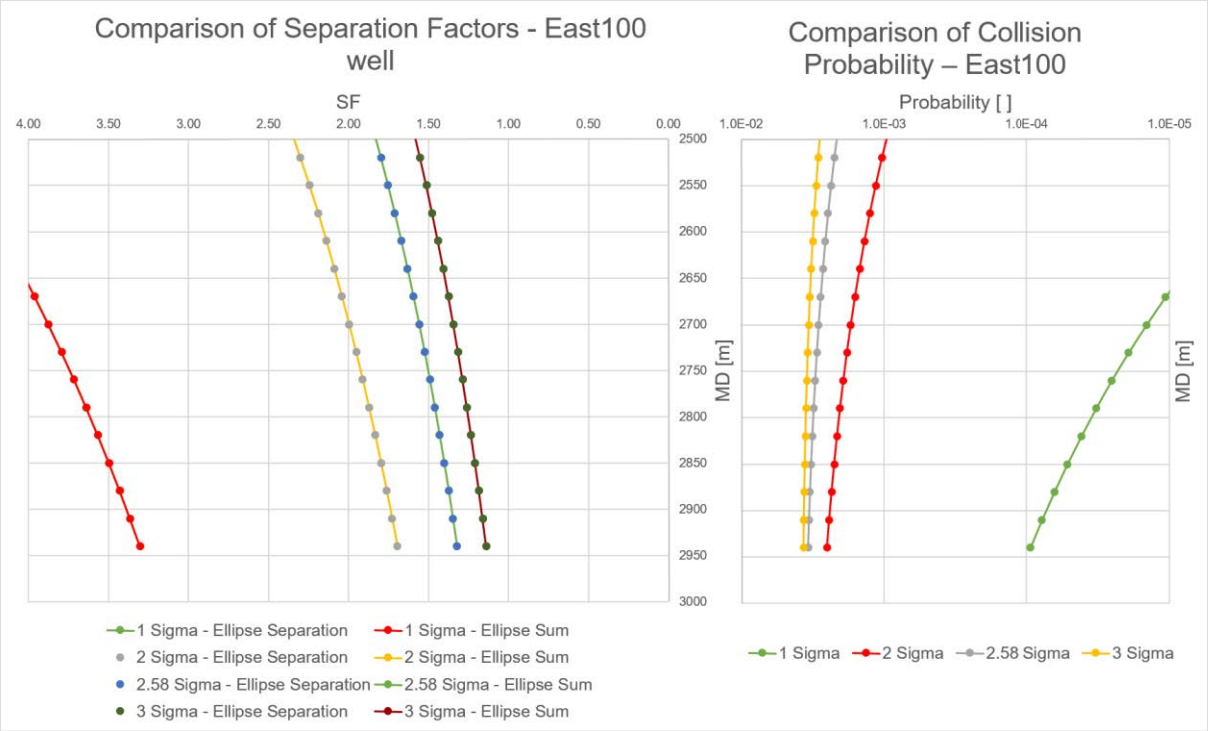

Figure 33: Results for East100 well. The results for a parallel well are predictable. A linear trend in both, the SF and probability, can be seen. The methods deliver equal outcomes due to the geometry of both EOUs.

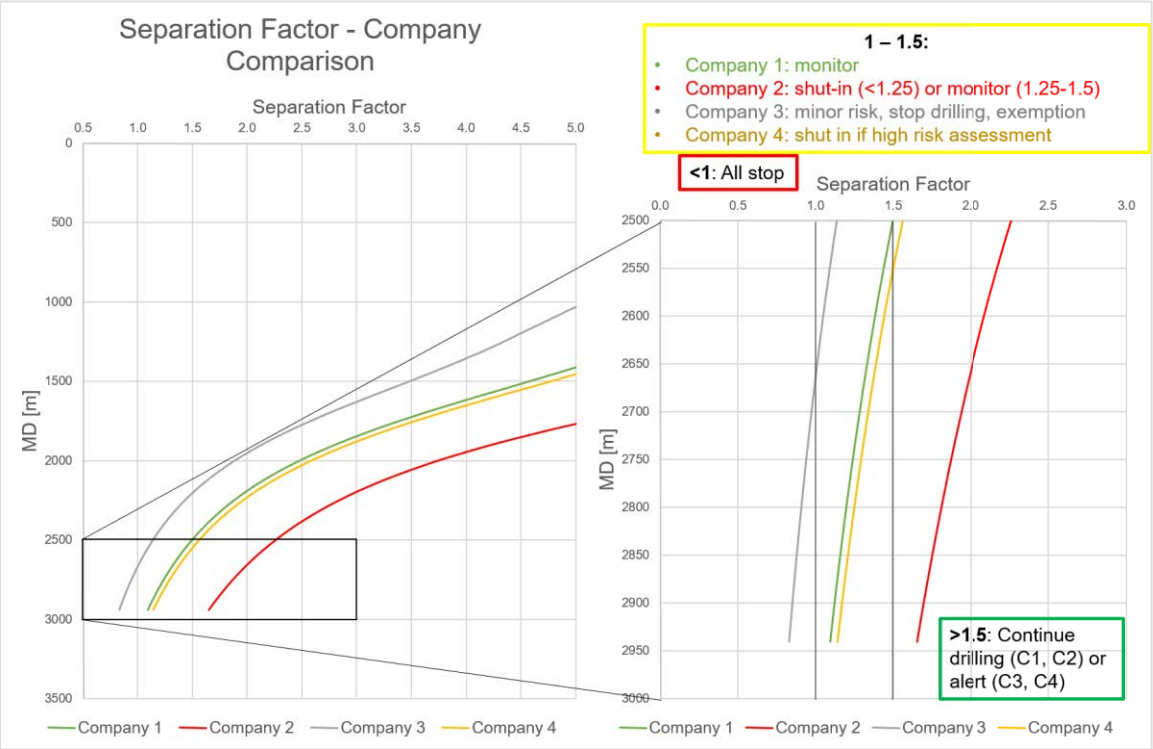

Figure 34: Separation Factor Comparison between Companies for East100 well.

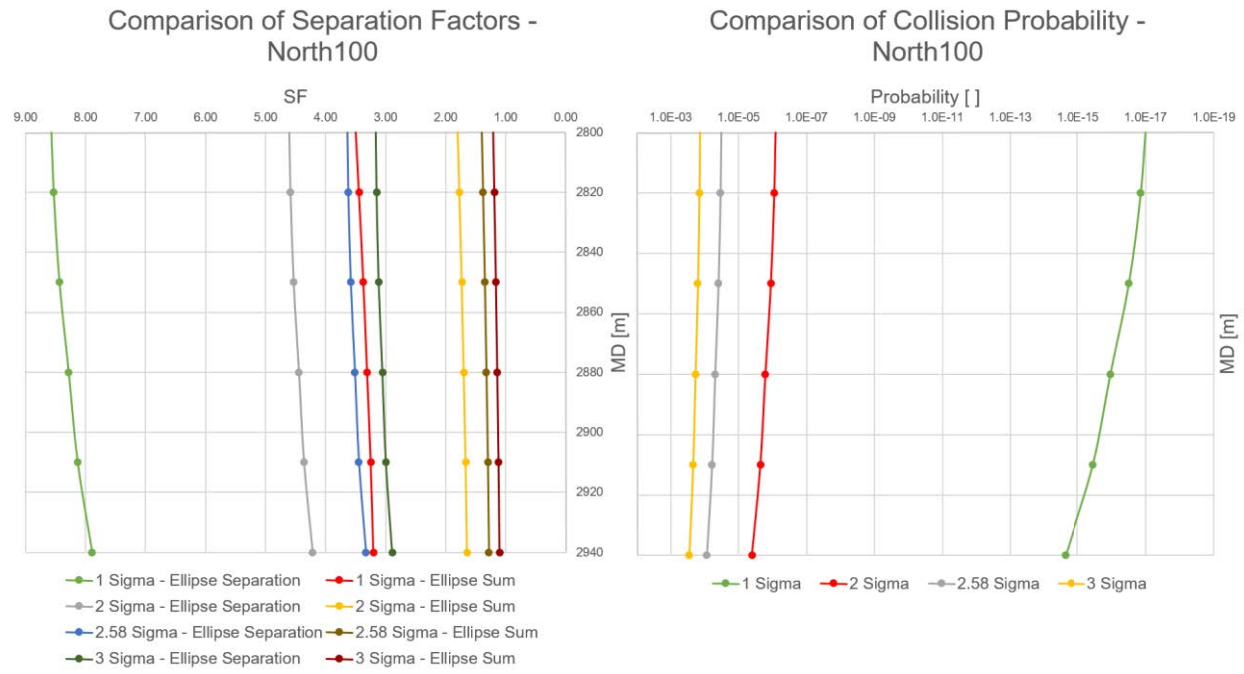

Figure 35: Results for North100 well. The two methods produce different results. While Ellipse Separation accounts for the individual position, Ellipse Sum does not and produces consequential wrong separation factors.

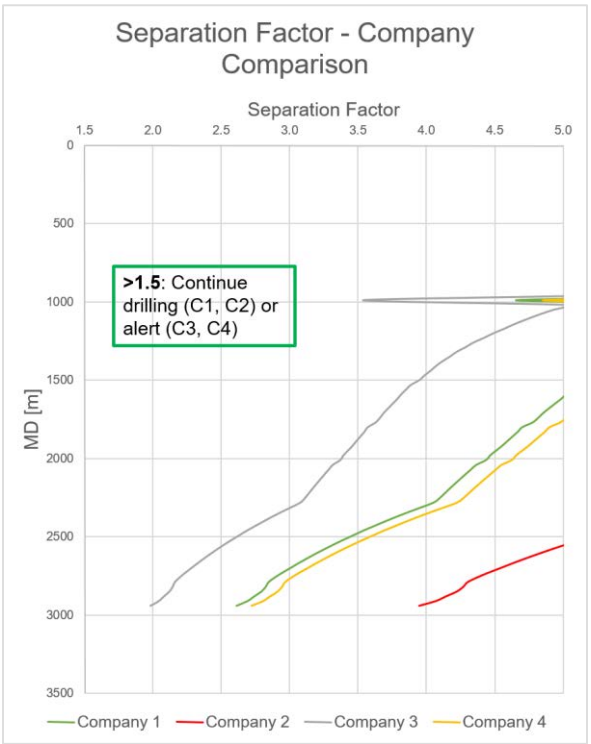

Figure 36 Separation Factor Comparison between Companies for North100 well. This well should be drillable by all software applications.

4.1.4. East20

East20 has the highest DDI (5.5) of the eleven wells. Comparison of the two methods is difficult, as a long interval of the RW has a close distance to the offset well, resulting in capped SF for the ellipse separation method. The angle of collision is 20° (difference between 180° azimuth angle of RW and 200° azimuth angle of East20, at approximately 2700 [m] MD RW), implying curves similar to Angular well. The deeper section (2600-2700 [m]) confirms this with varying outcomes in the two methods. A correct separation factor calculation should be consistent with the probability, and this is valid for the ellipse separation method and incorrect for the ellipse sum method.

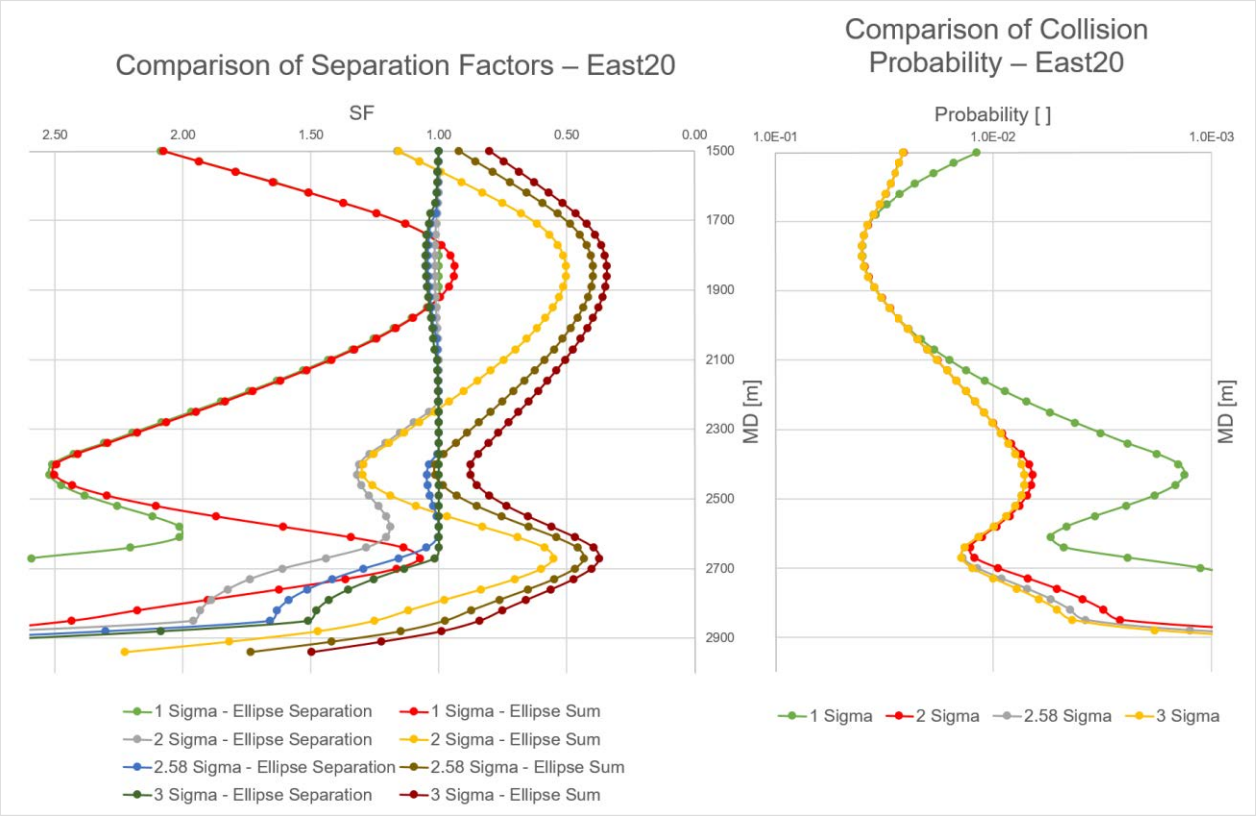

Figure 37: Results for East20 well. The SF decreases two times significantly.

The probability curve indicates that the first increase is more dangerous than the one in the deeper section. The scenario is very important for the validation process of a software, which can be recognized in the left diagram of Figure 37. The SFs of the ellipse separation method are approximately alike at the two positions, while the probability differs immensely.

The separation factor comparison within the industry supports this impression. The SF at the first section is clearly lower than the one in the deeper part. It is of most importance, that a software is capable of distinguishing this scenario.

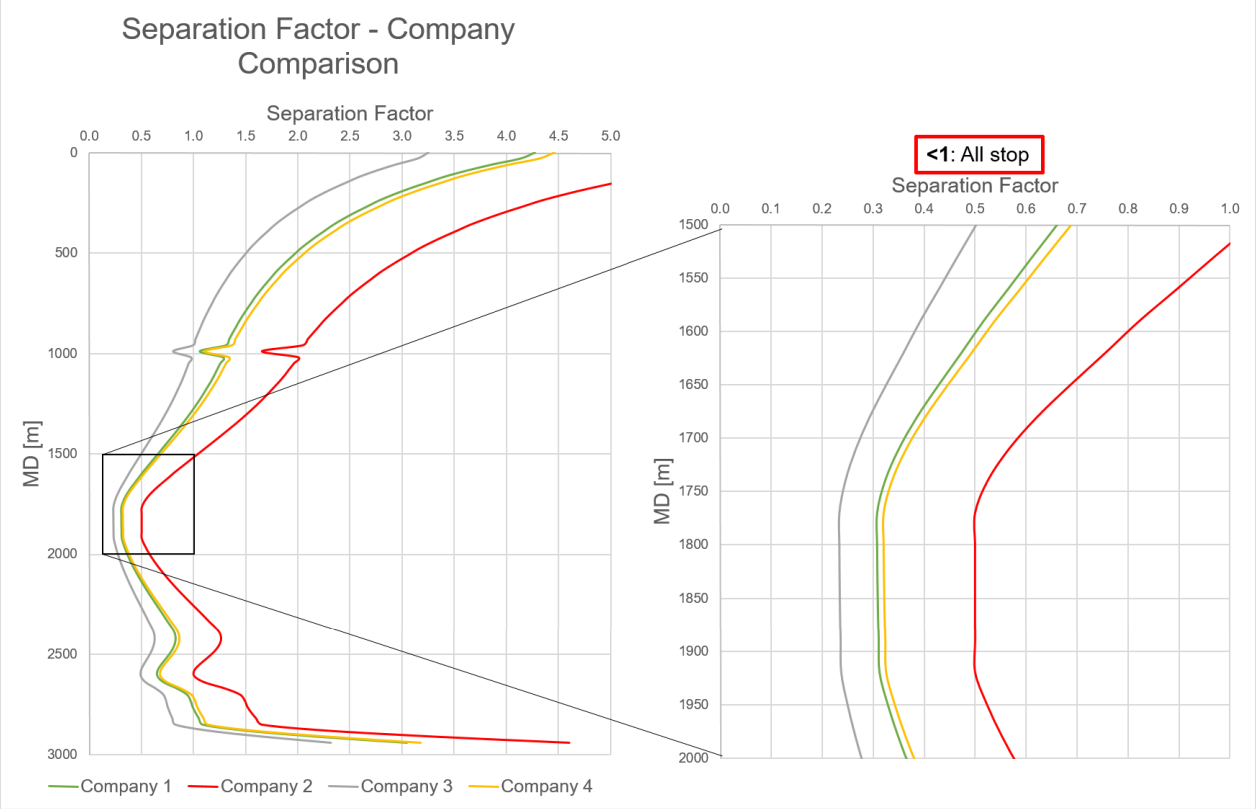

Figure 38: Separation Factor Comparison between Companies for East20 well

4.1.5. Horizontal and Perpendicular well

The two wells approach the RW at an azimuth of 90°. The RW hits the Horizontal well directly and misses the Perpendicular closely (12.73 and 45.18 [m] respectively). There are two recognizable points in Figure 39 and 40. Firstly, the program displays in Figure 29 an impossible value below 1 (SF calculated by ellipse separation method). The explanation is the drawing software interpolating between two points. Secondly, the collision probability is for the standard deviation of 1 the highest. This occurs each time the center to center distance is below 15 [m] (see upper section in East20, East10 and Sidetrack). All SF curves are not aligned, giving an indication for differences in the direction of the EOU axes.

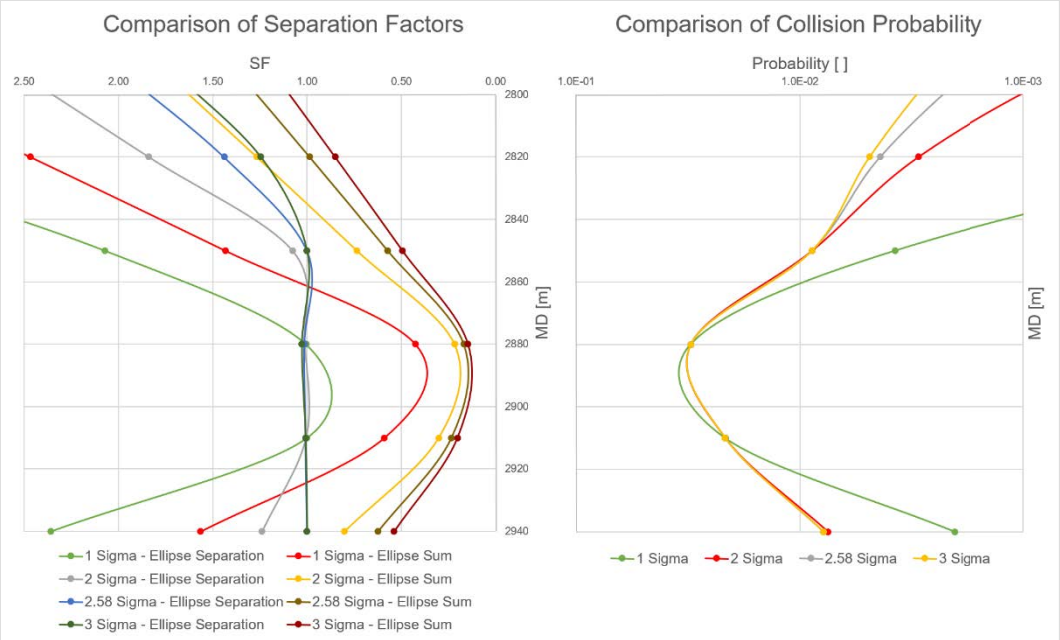

Figure 39: Results for Horizontal well. The RW hits the horizontal well closely. This can be confirmed with the two diagrams shown. The SF is extremely low (as it should be with such a close center to center distance) and the collision probability is very high.

The geometry of this situation is rather simple and leads to coherent results within all SF-variations. The four companies would all come to the same conclusion. The danger in this scenario is the strong decrease in the SF.

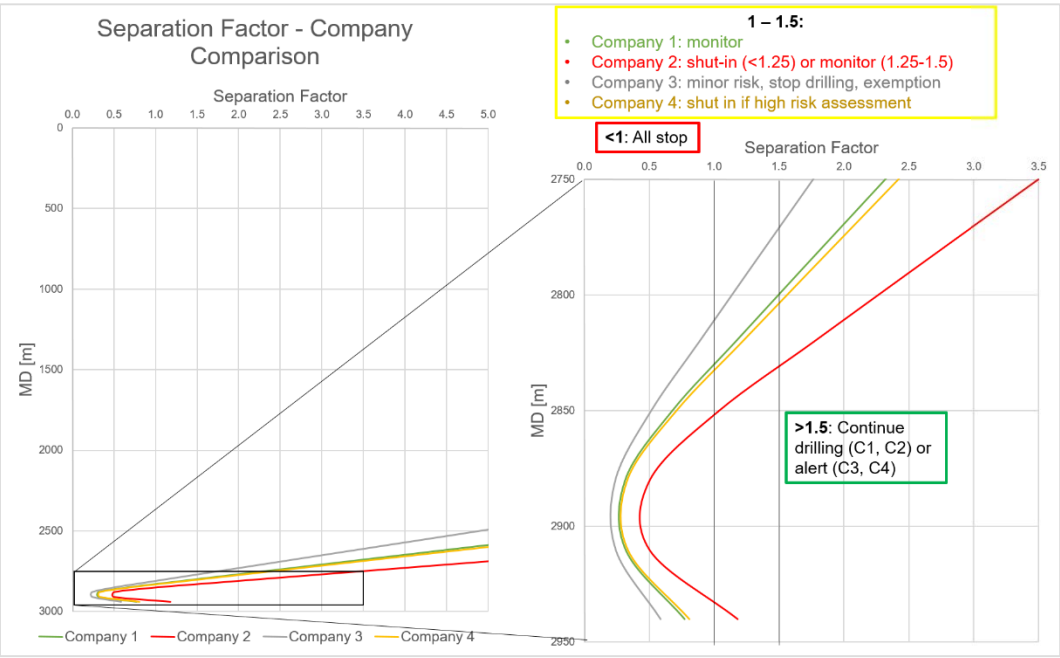

Figure 40: Separation Factor Comparison between Companies for Horizontal well.

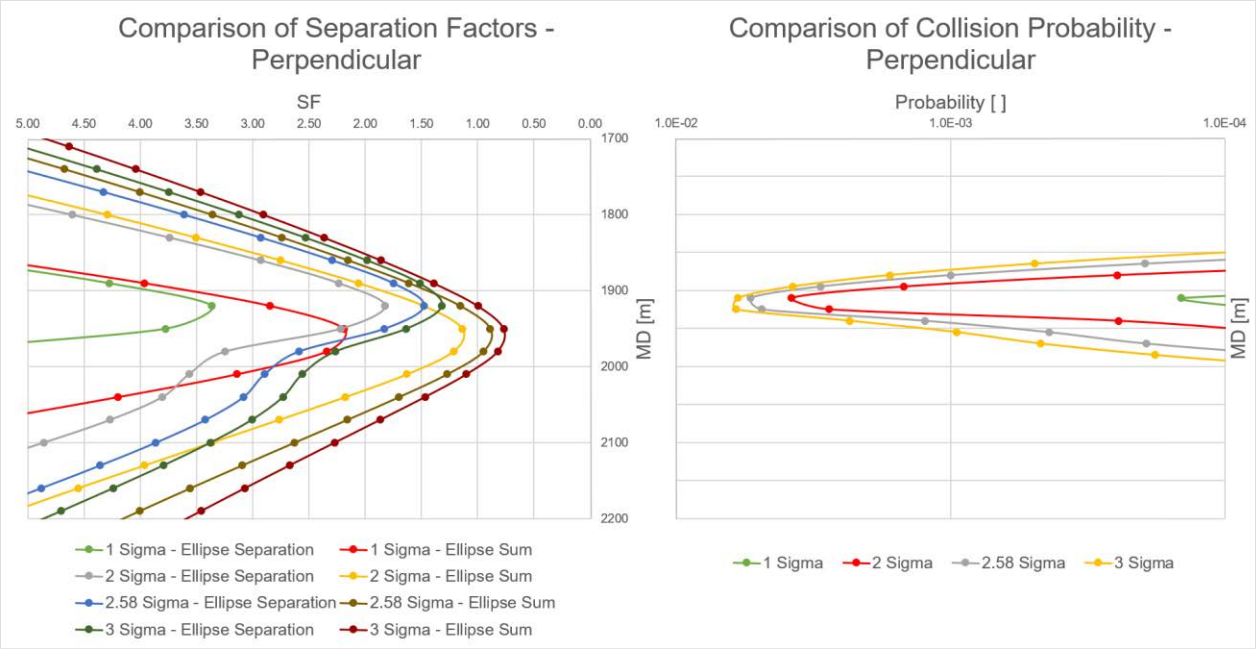

Figure 41: Results for Perpendicular well. A difference to Figure 39 can be noticed, as the SF based on ellipse separation start to increase before the SF based on ellipse sum. The probability is coherent with this and shows a high value in this section.

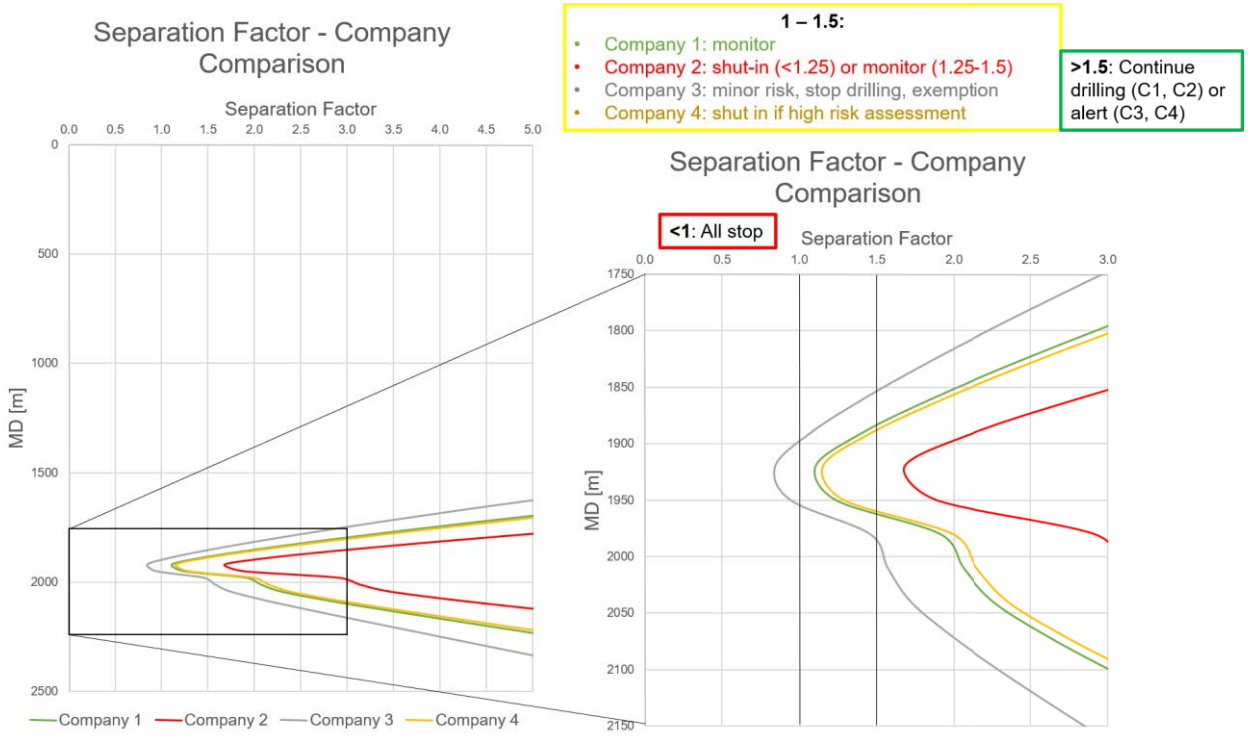

Figure 42: Separation Factor Comparison between Companies for PW The results for wells approaching the RW at perpendicular angles are similar. A small interval with low SF is characteristic and will lead to similar reactions along most companies.

4.1.6. Overlapping Opposite and Short Opposite

The main features of the two opposing wells are the high decline rates of the SF. This can be illustrated by a probability increase of a factor 1000 within 100 [m] MD (Figure 43).

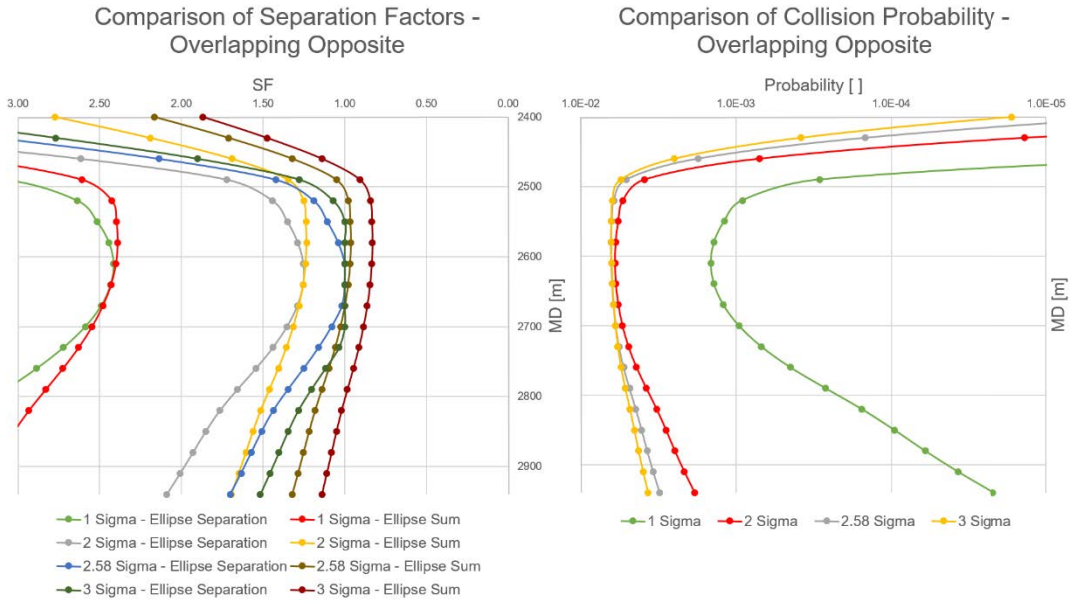

Figure 43: Results for Overlapping Opposite well. The curves behave similar. The variation is small and all methods produce reliable estimations.

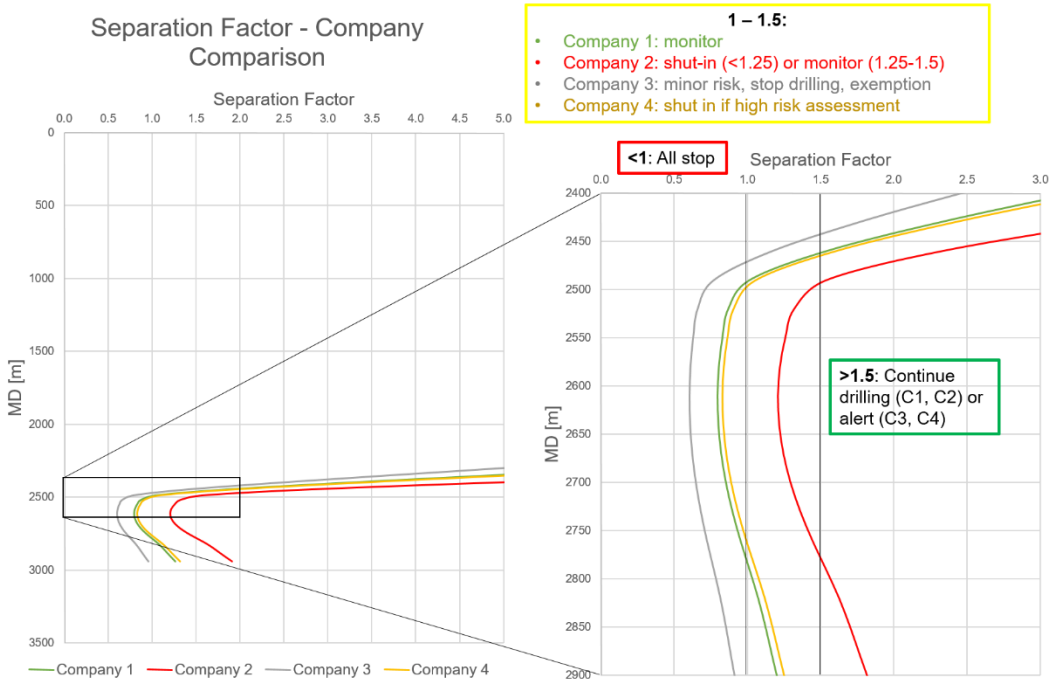

Figure 44: Separation Factor Comparison between Companies for PW.

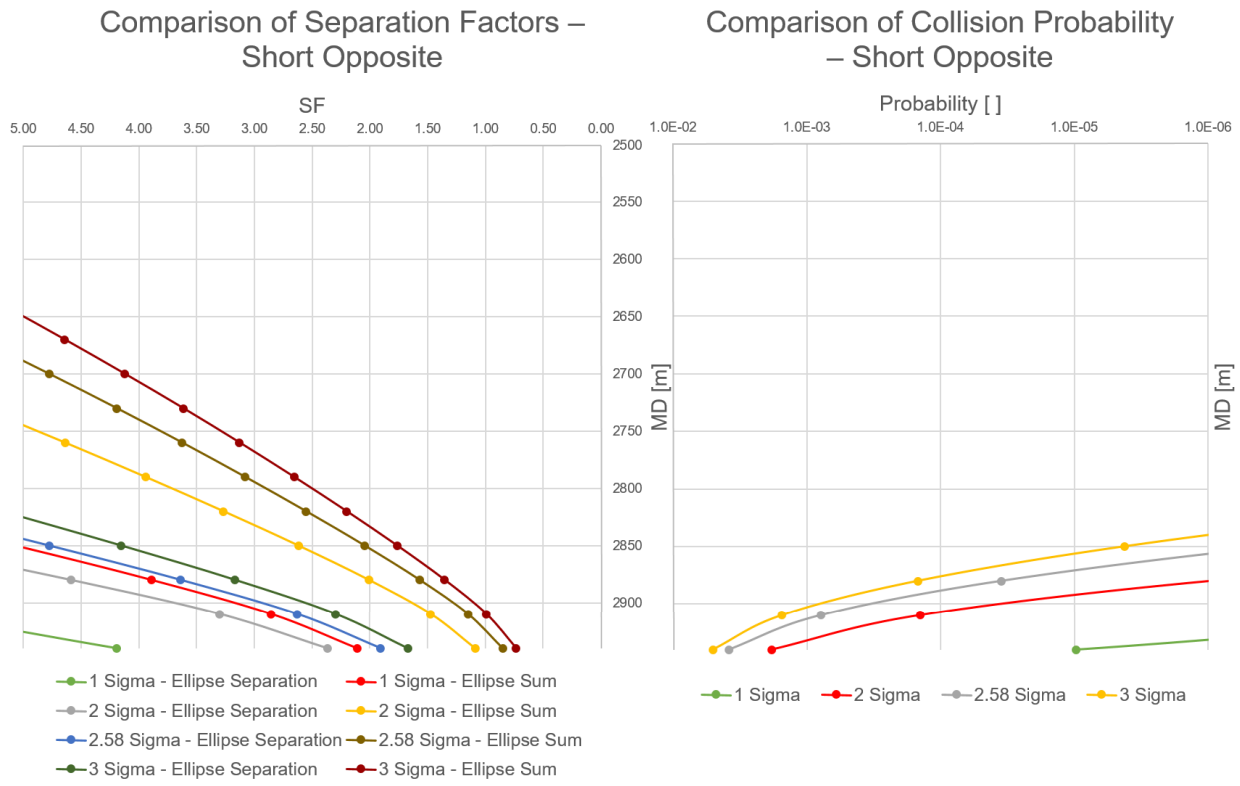

Figure 45: Results for Short Opposite well.

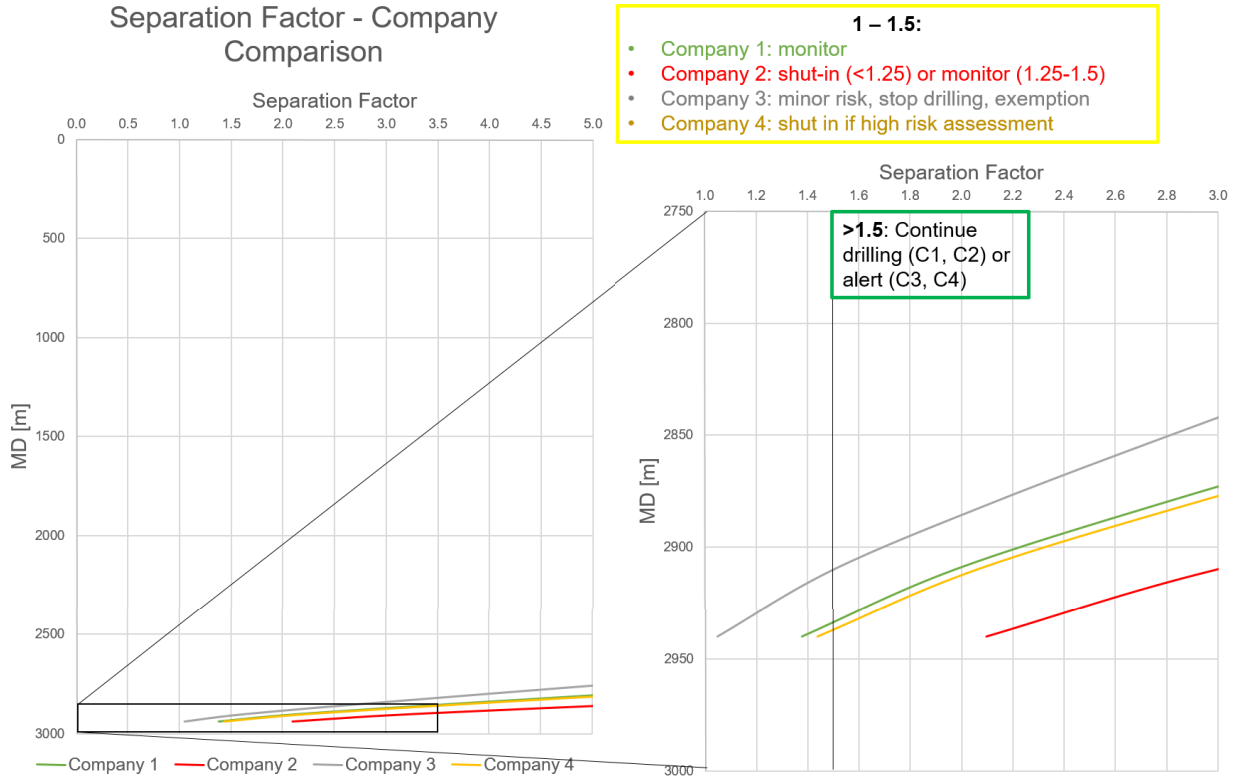

Figure 46: Separation Factor Comparison between Companies for SOW.

4.1.7. Sidetrack

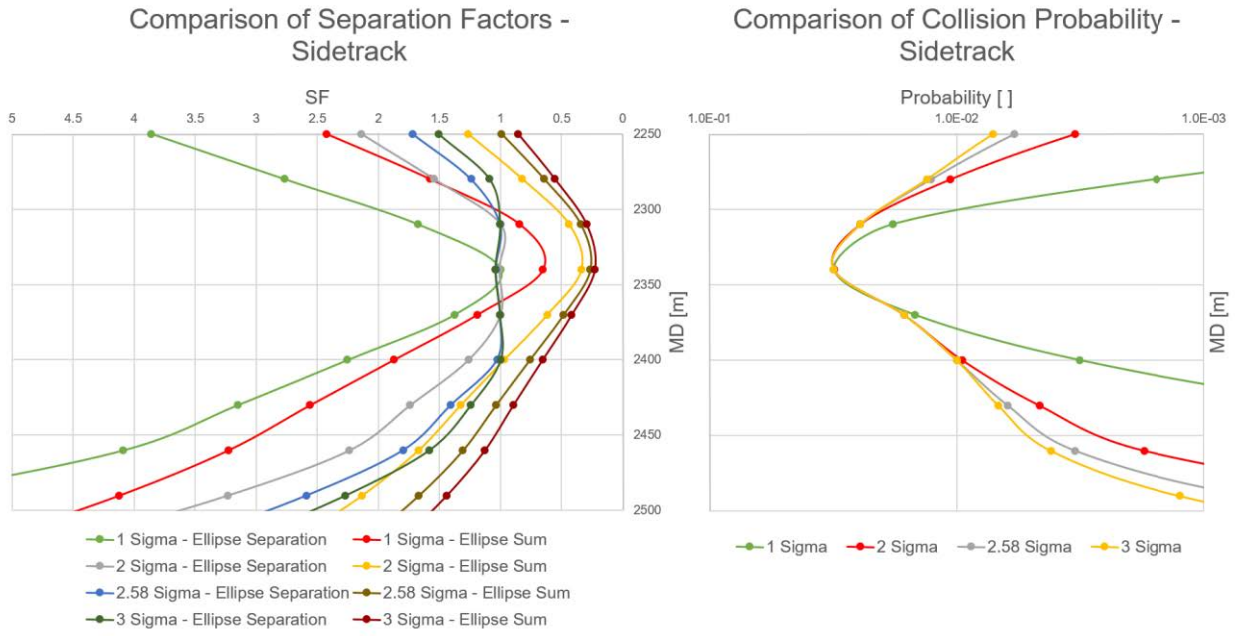

Figure 47: Results for Sidetrack well.

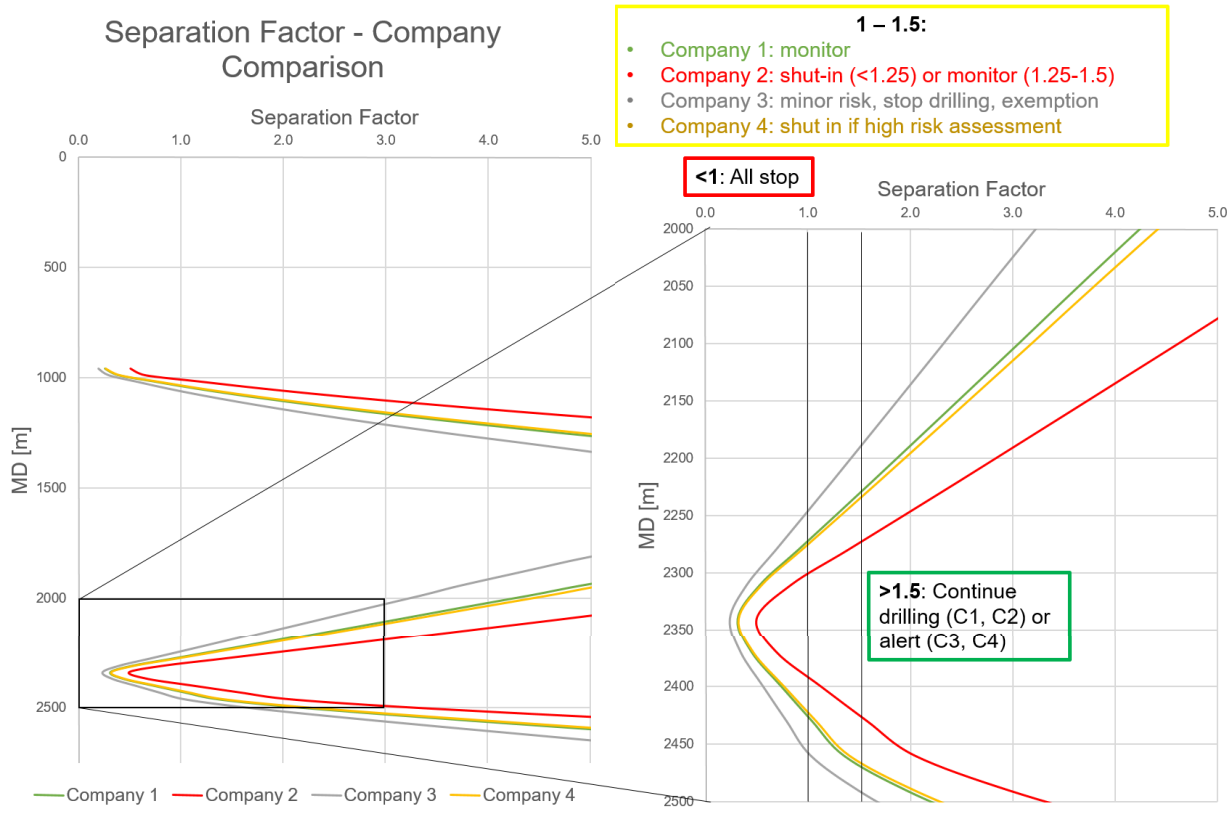

Figure 48: Separation Factor Comparison between Companies for Sidetrack well.

4.1.8. Vertical

The Vertical well is characterized by the highest probability and lowest separation factors throughout all offset wells. The center-to-center distance is by far the lowest, which is coherent with the results. In addition to that, Figure 16 indicates the low uncertainty magnitude for vertical wells. This feature can be seen in the probability estimate for the closest point. The probability is fairly high, confirming the small volume of the ellipsoid of uncertainty for the vertical well.

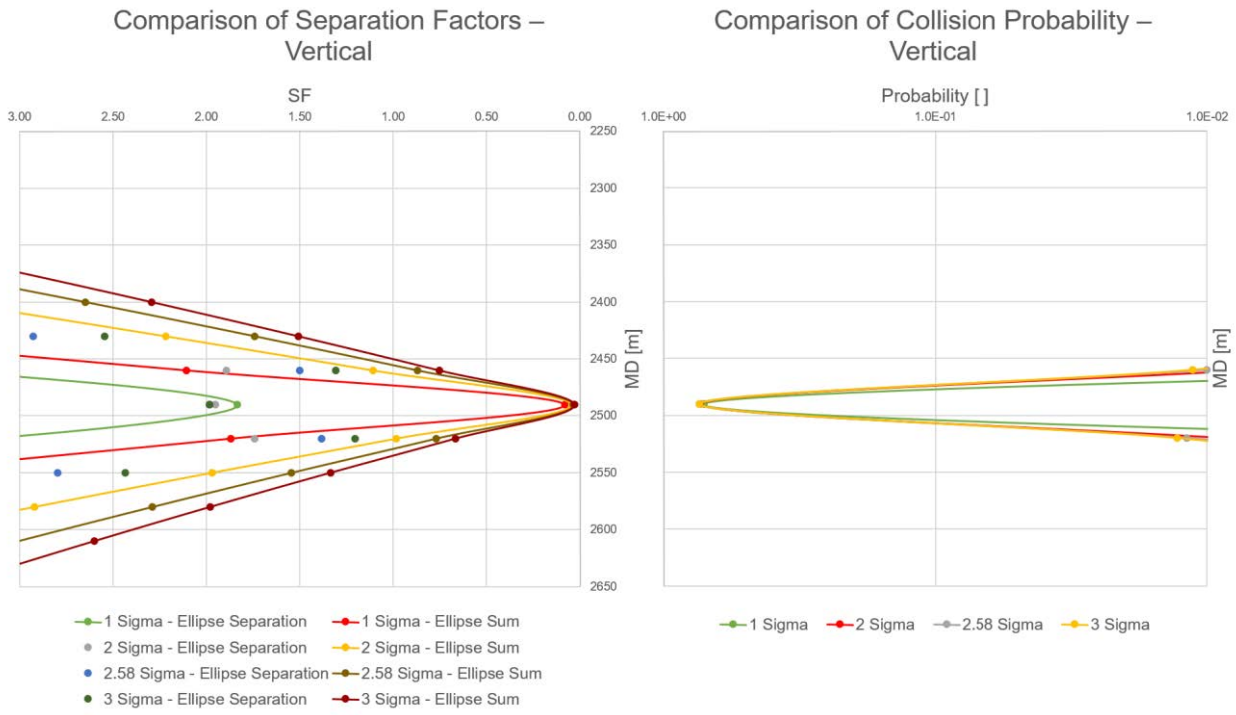

Figure 49: Results for Vertical well. The predictable result for a vertical well with a very low center to center distance. The collision probability is extremely high.

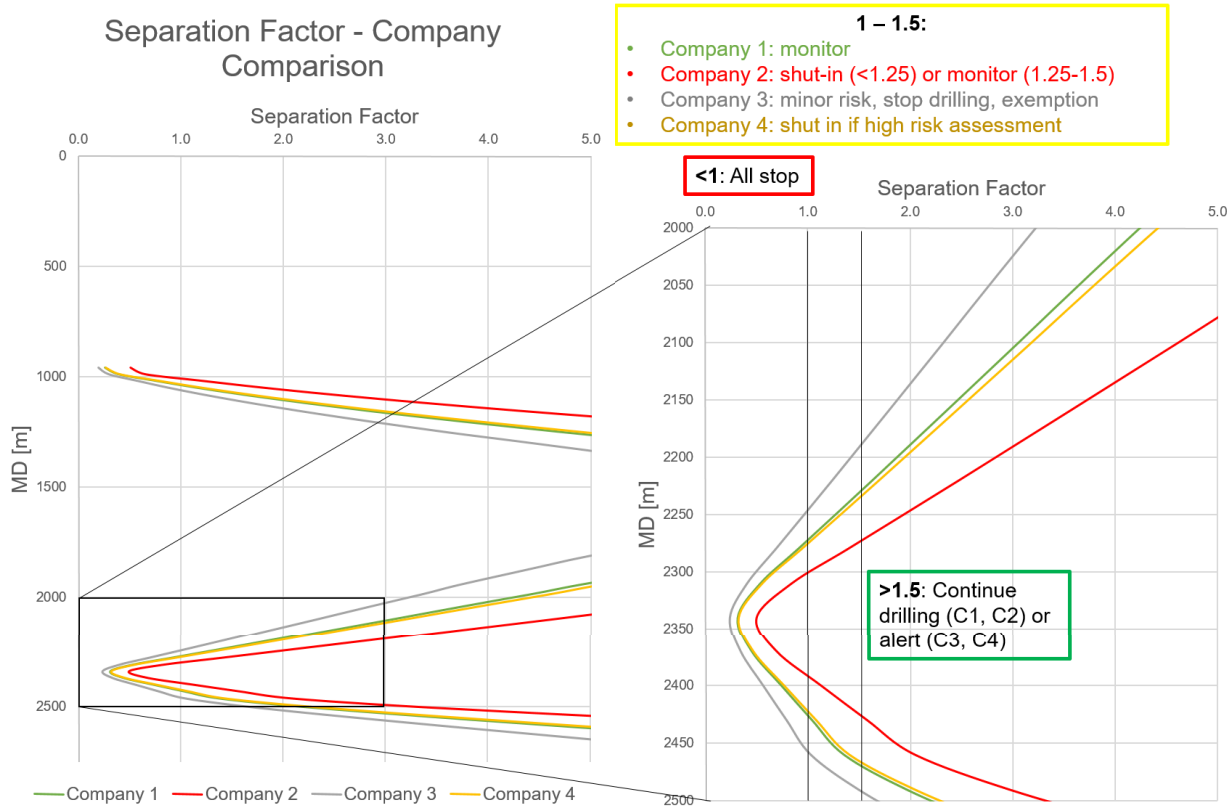

Figure 50: Separation Factor Comparison between Companies for Vertical well.

4.2. Summary

A meaningful summary was created in Figure 51 and 52. The eleven offset wells were summarized into five graphs, based on the similarity of the curves. A two-σ s.d. was used to calculate the curves. The safest wells are East100 and North100 (Figure 51, right diagram). The slope of both curves is alike and the two wells should not be categorized into risk-wells. East10 and East20 should both be major risk wells. Wells approaching from 90° azimuth are characterized by a sharp increase in SF, it should be mandatory to use geometry-based calculation methods for the two cases. The same accounts for the two wells reaching the RW at 180° azimuth. The SFs increase with a sharp slope. A further requirement is the usage of minimum distance calculation software, as a TC or horizontal scanning method will not detect the approaching well at all. The AW, SW and VW are intersected deep in the hole and have large collision probabilities. The vertical well in detail should be handled with caution, as the

uncertainty for this well is lower compared to the other wells, and thereby the collision probability is very high.

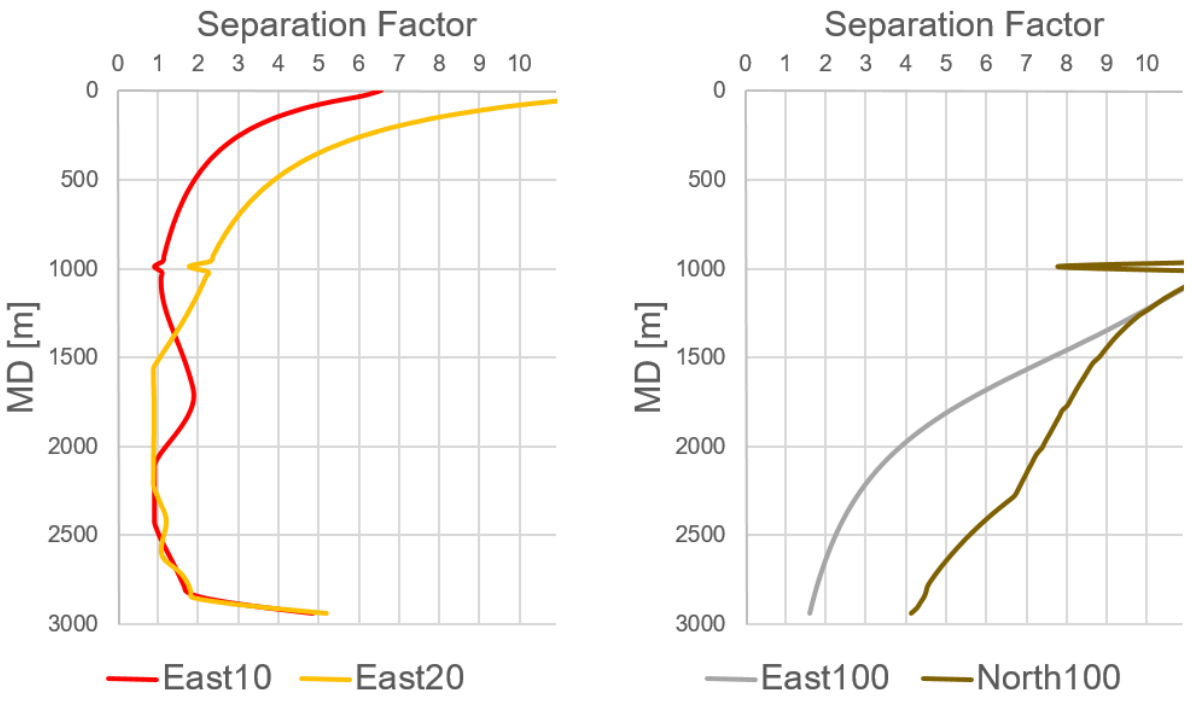

Figure 51: Summarized Wells (East10&East20 and East100&North100).

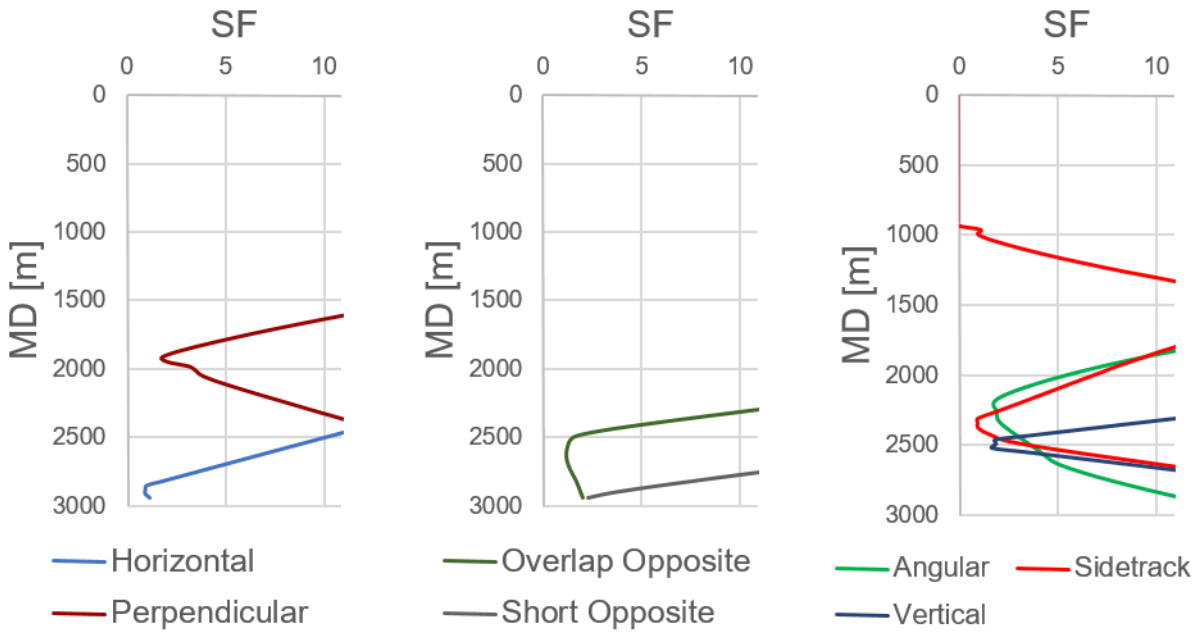

Figure 52: Summarized Wells (Horizontal&Perpendicular, Overlap Opposite&Short Opposite and Angular&Vertical&Sidetrack.

5. Discussion

Starting from the premise that directional drilling is one of the most important innovations introduced to the oil and gas industry, it is mandatory to have suitable tools to describe positional uncertainty. Under the rapid development of this technology, the methods to characterize became increasingly accurate. And with the growing dimensions of directional drilling applications, the multitude of software solutions increased similarly. The goal of this thesis was to deliver a procedure to analyze separation factor calculations and show the importance of geometries on the outcomes. Okewunmi & Brooks (2011) proved that inconsistency within the industry will inevitably lead to a wide range of separation factors for the same survey. This is also emphasized by the numerous results, showing significant differences within the calculation method and within the confidence interval. The relevance of the scope of this thesis can be evaluated, if consequences are included into the considerations. The whole process of delivering accurate survey measurements and calculating the most truthful wellbore position has to be justified to the resulting decision. Economic risk was quantified ranging from 10,000$ (for example a shorter gyro run) to several billion US dollars (in case of a blowout). On top of that, human life will be most likely at risk, which can compromise the reputation of a company (De Wardt et al. 2013).

Standardization of a separation factor is a complicated task in an industry with several hundred companies that perform collision-avoidance procedures and proximity scans. The complexity of the process adds up to that, as uncertainty calculations can be done with a large variety of survey tools. It is thereby feasible to standardize a model on which the different programs can be tested. The theoretical set of wellpaths was created by a group of surveying experts, but a comparison study has not been published yet. With this work, a procedure was presented that gives insight into the complete workflow of the validation process. The biggest influencing factors were explained and calculation methods compared, resulting in the setup of a state of the art protocol.

But it is absolutely necessary to understand the boundaries of this approach. The magnetic interference of an adjacent well will compromise the regularity of the MWD. The

model investigated is based on the assumption that the wells do not mutually interfere. This limitation can be justified with the requirement of ideal conditions. For example, high tortuosity might lead to incomparable results, hence the offset wells were set up rather simple. In reality, drilling should stop if the MWD records magnetic interference and fails quality checks. A gyroscopic tool will find remedy on this issue. But for the set of test wells, only MWD measurements for the entire length of the wellbores were considered.

Another remark of this thesis is the positive feedback for new methods in the different steps of the workflow. The minimum curvature method is already widely accepted as standard by the industry, but the minimum distance and expanding ellipsoid method are still under observation. The outcomes for the minimum distance method, compared to travelling cylinder or horizontal scanning, were by far more consistent and clearly indicated the benefits of this method. The ellipse expansion method was intensively discussed by the collision-avoidance group (ISCWSA) and the majority of experts voted for the Pedal-curve method (Sawaryn et al. 2015). It was argued that even though the PCM can give unrealistic results, it is still the most common method and an advantage is, that it can be converted to a probability. Kellydown™ proved in a two-well scenario better results for the ellipsoid expansion method (KellyDown 2013). A detailed comparison would exceed the scope of this thesis, but further investigation would be helpful to agree on a standard procedure.

The description of the eleven wellpath and the resulting estimations for separation factors and the collision probability led to the perception that a model with less wells could deliver sufficient outcomes.

A standard deviation recommendation cannot be declared with this thesis. A work capable to define a standard would have to include big amount of surveying data, combined with financial aspects and HSE-risk considerations. The deviations of this work strengthen the absolute necessity to create a standard.

In view of future work possibilities, this work could serve as the basis for an extended well testing model. More realistic scenarios with complex well trajectories could be included to characterize the separation factor behavior under special circumstances. In addition to that, implementation of the surface facilities and incorporation of, for example pressure

data of adjacent well could deliver more accurate results with respect to the possible outcomes and give the probability estimates more weight. Limitations incorporated in this thesis could be mitigated in a more sophisticated model. Such a model would also include geological uncertainties derived from the various disciplines on the rigsite.

6. References

Agilis Software Solutions, 2016. KellyDown User's Guide.

Bang, J. & Nyrnes, E., 2015. Collision Risk Analysis Pedal curve vs . Ellipse.

Bang, J. & Torkildsen, T., 2009. Targeting Challenges in Northern Areas Due to Degradation of Wellbore Positioning Accuracy. , pp.11–13.

Bourgoyne A. D., Chenevert M. E., Millhelm K. K., Y.F.S., 1986. *Applied Drilling Engineering*,

Brooks, a et al., 2005. Quantification of Depth Accuracy.

Brooks, A. & Wilson, H., 1996. An Improved Method for Computing Wellbore Position Uncertainty and its Application to Collision and Target Intersection Probability Analysis. , pp.411–420.

Caers, J., 2011. Modeling Uncertainty in the Earth Sciences.

Carden, R.S. & Grace, R.D., 2007. Horizontal and Directional Drilling.

Ekseth, R. et al., 2007. High-Integrity Wellbore Surveys : Methods for Eliminating Gross Errors. *Methods*, pp.1–17.

Ekseth, R. et al., 2006. The Reliability Problem Related to Directional Survey Data.

Gjerde, T., 2008. A heavy tailed statistical model applied in anti-collision calculations for petroleum wells. , (June).

Haarstad, I. et al., 2002. Target Design Based Upon Multidisciplinary Uncertainty Information.

ISCWSA, 2011. 11th Meeting Minutes Wellbore Positioning Technical Section - Collision Avoidance Work Group 11. , (November), pp.1–2. Available at: www.iscwsa.net.

ISCWSA, 2013a. 38th Meeting Minutes of the SPE Technical Section on Wellbore Surveying. *PhD Proposal*, 1. Available at: www.iscwsa.net.

ISCWSA, 2007. Collision Avoidance Work Group - 3rd Meeting (2007). , (November), pp.3–6.

ISCWSA, 2013b. Current Common Practice in Collision Avoidance Calculations.

ISCWSA, 2013c. Standard_set_of_wellpaths_for_evaluating_clearance_scenarios_5_Nov_13. Available at: www.iscwsa.net.

Jamieson, A., 2012. *Introduction to Wellbore Positioning*,

KellyDown, 2013. Ellipse Separation - Expanding Ellipsoid Method. , pp.1–5.

Mcnair, G.A. et al., 2005. SPE / IADC 92554 Implementation of a New Risk Based Well Collision Avoidance Method.

Mitchell, R.F. & Miska, S.Z., 2011. *Fundamentals of Drilling Engineering*,

Oag, A. & Williams, M., 2000a. The Directional Difficulty Index - A New Approach to Performance Benchmarking. *Proceedings of IADC/SPE Drilling Conference*. Available at: http://www.spe.org/elibrary/servlet/spepreview?id=00059196.

Oag, A. & Williams, M., 2000b. The Directional Difficulty Index - A New Approach to Performance Benchmarking. *Proceedings of IADC/SPE Drilling Conference*.

Okewunmi, S. & Brooks, A., 2011. A Comparison of Collision Avoidance Calculations. *Proceedings of SPE/IADC Drilling Conference and Exhibition*, (March), pp.1–3. Available at: http://www.onepetro.org/mslib/servlet/onepetropreview?id=SPE-140183-MS&soc=SPE.

Poedjono, B. et al., 2006. SPE 101719 Well-Collision Risk in Congested Environments.

Poedjono, B., Van, C.P., et al., 2009. SPE 121094 Anti-Collision Risk Management for Real-World Well Placement.

Poedjono, B., Lombardo, G.J. & Phillips, W., 2009. SPE 121040 Anti-Collision Risk Management Standard for Well Placement. , (March), pp.23–25.

Sawaryn, S. et al., 2015. ISCWSA / SPE Wellbore Positioning Technical Section Houston , Texas 30 th September 2015. , (September), pp.3–6.

Sawaryn, S.J. et al., 2013. Explicit Calculation of Expansion Factors for Collision Avoidance Between Two Coplanar Survey-Error Ellipses. , (October 2012), pp.8–10.

Sawaryn, S.J. & Thorogood, J.L., 2005. A Compendium of Directional Curvature Method. , (January 2004), pp.5–8.

Thorogood, J. & Sawaryn, S.J., 1990. The Traveling Cylinder - A Practical Tool for Collision Avoidance. , 1977(5), pp.653–664.

Thorogood, J.L. et al., 1990. SPE 20908 Quantitive Risk Assessment of Subsurface Well Collisions.

Torkildsen, T. et al., 2004. Prediction of Wellbore Position Accuracy When Surveyed With Gyroscopic Tools. *SPE Drilling & Completion*, 23(1).

Torkildsen, T. et al., 2008. Prediction of Wellbore Position Accuracy When Surveyed With Gyroscopic Tools. *SPE Drilling & Completion*, 23(1), pp.26–29.

Truex, J, N., 1971. Directional survey problems, East Wilmington oil field, California. *Am. Assoc. Petroleum Geologists Bull.*, 55, pp.621–628.

Walstrom, J.E., Brown, a. a. & Harvey, R.P., 1969. An Analysis of Uncertainty in Directional Surveying. *Journal of Petroleum Technology*, 21(4), pp.515–523.

De Wardt, J.P. et al., 2013. SPE / IADC 163411 Well Bore Collision Avoidance and Interceptions - State of the Art Summary of the SPE ATW Workshop Risk Factors Controlled by Wellbore Surveying Wellbore Collisions – An Escalating Risk for Operators.

Williamson, H.S., 2000. Accuracy Prediction for Directional Measurement While Drilling. *SPE Drilling & Completion*, 15(4).

Williamson, H.S., 1991. Supplement to SPE 23941: Mathematical Estimation of Collision and Post-Collision Outcome Probabilities.

Williamson, H.S., 1998. Towards Risk-Based Well Separation Rules. *SPE Drilling & Completion*, 13(1), pp.47–51.

Wolff, C.J.M. & De Wardt, J.P., 1981. Borehole Position Uncertainty - Analysis of Measuring Methods and Derivation of Systematic Error Model. *Journal of Petroleum Technology*, 33(12).

7. Appendix

Table 12: MWD Error Model Equations. Each error term has a specific equation which explains its influence on uncertainty magnitude of the respective axis.

#	Code	Term Description	Prop.	Depth Formula	Inclination Formula	Azimuth Formula
1	DRFR	Depth Reference - Random	R	1	0	0
2	DSFS	Depth Scale Factor - Systematic	S	MD	0	0
3	DSTG	Depth Stretch - Global	G	$MD * TVD$	0	0
4	ABXY-TI1S	MWD TF Ind: X and Y Accelerometer Bias	S	0	$-\frac{\cos(I)}{G}$	$\frac{\tan(\theta)\cos(\mathrm{I})\sin(\mathrm{A})}{G}$
5	ABXY-TI2S	MWD TF Ind: X and Y Accelerometer Bias	S	0	0	$\frac{\tan\left(\frac{\pi}{2}-I\right)-\tan(\theta)\cos(\mathrm{A})}{G}$
6	ABZ	MWD: Z-Accelerometer Bias	S	0	$-\frac{\sin(I)}{G}$	$\frac{\tan(\theta)\sin(I)\sin(\mathrm{A})}{G}$
7	ASXY-TI1S	MWD TF Ind: X and Y Accelerometer Scale Factor	S	0	$\frac{\sin(I)\cos(I)}{\sqrt{2}}$	$-\frac{\tan(\theta)\sin(I)\cos(\mathrm{I})\sin(\mathrm{A})}{\sqrt{2}}$
8	ASXY-TI2S	MWD TF Ind: X and Y Accelerometer Scale Factor	S	0	$\frac{\sin(I)\cos(I)}{2}$	$-\frac{\tan(\theta)\sin(I)\cos(\mathrm{I})\sin(\mathrm{A})}{2}$
9	ASXY-TI3S	MWD TF Ind: X and Y Accelerometer Scale Factor	S	0	0	$\frac{\tan(\theta)\sin(I)\cos(A)-\cos(\mathrm{I})}{2}$
10	ASZ	MWD: Z-Accelerometer Scale Factor	S	0	$-\sin(I)\cos(I)$	$\tan(\theta)\sin(I)\cos(I)\sin(\mathrm{A})$
11	MBXY-TI1S	MWD TF Ind: X and Y Magnetometer Bias	S	0	0	$-\frac{\cos(I)\sin(A)}{B*\cos(\theta)}$
12	MBXY-TI2S	MWD TF Ind: X and Y Magnetometer Bias	S	0	0	$\frac{\cos(A)}{B*\cos(\theta)}$
13	MBZ	MWD: Z-Magnetometer Bias	S	0	0	$-\frac{\sin(\mathrm{I})\sin(\mathrm{A})}{B*\cos(\theta)}$
14	MSXY-TI1S	MWD TF Ind: X and Y Magnetometer Scale Factor	S	0	0	$\frac{\sin(\mathrm{I})\sin(\mathrm{A})\tan(\theta)\cos(I)+\cos(A)}{\sqrt{2}}$

15	MSXY-TI2S	MWD TF Ind: X and Y Magnetometer Scale Factor	S	0	0	$\sin(A)(\frac{\tan(\theta)\sin(\mathrm{I})\cos(\mathrm{I})-\cos^2(I)\cos(A)}{2}$
16	MSXY-TI3S	MWD TF Ind: X and Y Magnetometer Scale Factor	S	0	0	$\frac{\cos(I)\cos^2(\mathrm{A})-\cos(\mathrm{I})\,sin^2(A)-}{2}$
17	MSZ	MWD: Z-Magnetometer Scale Factor	S	0	0	$-(\sin(I)\,cos(\mathrm{A})$ $+\tan(\theta)\cos(\mathrm{I}))\sin(\mathrm{I})\sin(A)$
18	DECG	MWD: Declination - Global	G	0	0	1
19	DECR	MWD: Declination - Random	R	0	0	1
20	DBHG	MWD: BH-Dependent Declination - Global	G	0	0	$\frac{1}{B*\cos(\theta)}$
21	DBHR	MWD: BH-Dependent Declination - Random	R	0	0	$\frac{1}{B*\cos(\theta)}$
22	AMIL	MWD: Axial Interference - SinI.SinA	S	0	0	$\frac{\sin(I)\sin(A)}{B*\cos(\theta)}$
23	SAG	MWD: Sag	S	0	$\sin(I)$	0
24	XYM1	Misalignment: XY Misalignment 1	S	0	$\lvert\sin(I)\rvert$	0
25	XYM2	Misalignment: XY Misalignment 2	S	0	0	-1
26	XYM3	Misalignment: XY Misalignment 3	S	0	$\lvert\cos(I)\cos(A)\rvert$	$-\lvert\frac{\cos(I)\sin(A)}{\sin(I)}\rvert$
27	XYM4	Misalignment: XY Misalignment 4	S	0	$\lvert\cos(I)\sin(A)\rvert$	$\lvert\frac{\cos(I)\cos(\mathrm{A})}{\sin(I)}\rvert$

Table 13: MWD Error Model Parameter including name, description, weighting function, source, type, magnitude, units and the propagation mode.

#	Code	Term Description	Wt.Fn.	Wt.Fn. Source	Type	Magnitude	Units	Prop.
1	DRFR	Depth Reference - Random	DREF	SPE 67616	Depth	0.35	m	R
2	DSFS	Depth Scale Factor - Systematic	DSF	SPE 67616	Depth	0.00056	-	S
3	DSTG	Depth Stretch - Global	DST	SPE 67616	Depth	2.5E-07	1/m	G

4	ABXY-TI1S	MWD TF Ind: X and Y Accelerometer Bias	ABXY-TI1	SPE 63275 + Andy Brooks	Sensor	0.004	m/s2	S
5	ABXY-TI2S	MWD TF Ind: X and Y Accelerometer Bias	ABXY-TI2	SPE 63275 + Andy Brooks	Sensor	0.004	m/s2	S
6	ABZ	MWD: Z-Accelerometer Bias	ABZ	SPE 67616 Table 1	Sensor	0.004	m/s2	S
7	ASXY-TI1S	MWD TF Ind: X and Y Accelerometer Scale Factor	ASXY-TI1	SPE 63275 + Andy Brooks	Sensor	0.0005	-	S
8	ASXY-TI2S	MWD TF Ind: X and Y Accelerometer Scale Factor	ASXY-TI2	SPE 63275 + Andy Brooks	Sensor	0.0005	-	S
9	ASXY-TI3S	MWD TF Ind: X and Y Accelerometer Scale Factor	ASXY-TI3	SPE 63275 + Andy Brooks	Sensor	0.0005	-	S
10	ASZ	MWD: Z-Accelerometer Scale Factor	ASZ	SPE 67616 Table 1	Sensor	0.0005	-	S
11	MBXY-TI1S	MWD TF Ind: X and Y Magnetometer Bias	MBXY-TI1	SPE 63275 + Andy Brooks	Sensor	70	nT	S
12	MBXY-TI2S	MWD TF Ind: X and Y Magnetometer Bias	MBXY-TI2	SPE 63275 + Andy Brooks	Sensor	70	nT	S
13	MBZ	MWD: Z-Magnetometer Bias	MBZ	SPE 67616 Table 1	Sensor	70	nT	S
14	MSXY-TI1S	MWD TF Ind: X and Y Magnetometer Scale Factor	MSXY-TI1	SPE 63275 + Andy Brooks	Sensor	0.0016	-	S
15	MSXY-TI2S	MWD TF Ind: X and Y Magnetometer Scale Factor	MSXY-TI2	SPE 63275 + Andy Brooks	Sensor	0.0016	-	S
16	MSXY-TI3S	MWD TF Ind: X and Y Magnetometer Scale Factor	MSXY-TI3	SPE 63275 + Andy Brooks	Sensor	0.0016	-	S
17	MSZ	MWD: Z-Magnetometer Scale Factor	MSZ	SPE 67616 Table 1	Sensor	0.0016	-	S
18	DECG	MWD: Declination - Global	AZ	SPE 67616	AziRef	0.36	deg	G
19	DECR	MWD: Declination - Random	AZ	SPE 67616	AziRef	0.1	deg	R

20	DBHG	MWD: BH-Dependent Declination - Global	DBH	SPE 67616	AziRef	5000	deg.nT	G
21	DBHR	MWD: BH-Dependent Declination - Random	DBH	SPE 67616	AziRef	3000	deg.nT	R
22	AMIL	MWD: Axial Interference - SinI.SinA	AMIL	Halliburton	Mgntcs	220	nT	S
23	SAG	MWD: Sag	SAG	SPE 67616	Align	0.2	deg	S
24	XYM1	Misalignment: XY Misalignment 1	XYM1	SPE 90408 Table 9 - Alt. 3	Align	0.1	deg	S
25	XYM2	Misalignment: XY Misalignment 2	XYM2	SPE 90408 Table 9 - Alt. 3	Align	0.1	deg	S
26	XYM3	Misalignment: XY Misalignment 3	XYM3	SPE 90408 Table 9 - Alt. 3	Align	0.1	deg	S
27	XYM4	Misalignment: XY Misalignment 4	XYM4	SPE 90408 Table 9 - Alt. 3	Align	0.1	deg	S

Probability of Collision (based on 2.7955Sigma)

SF	Probability
2.0	750599937895083
1.5	660669956
1.2	954910
1.1	146076
1.0	25959
0.8	669
0.5	42
0.3	9

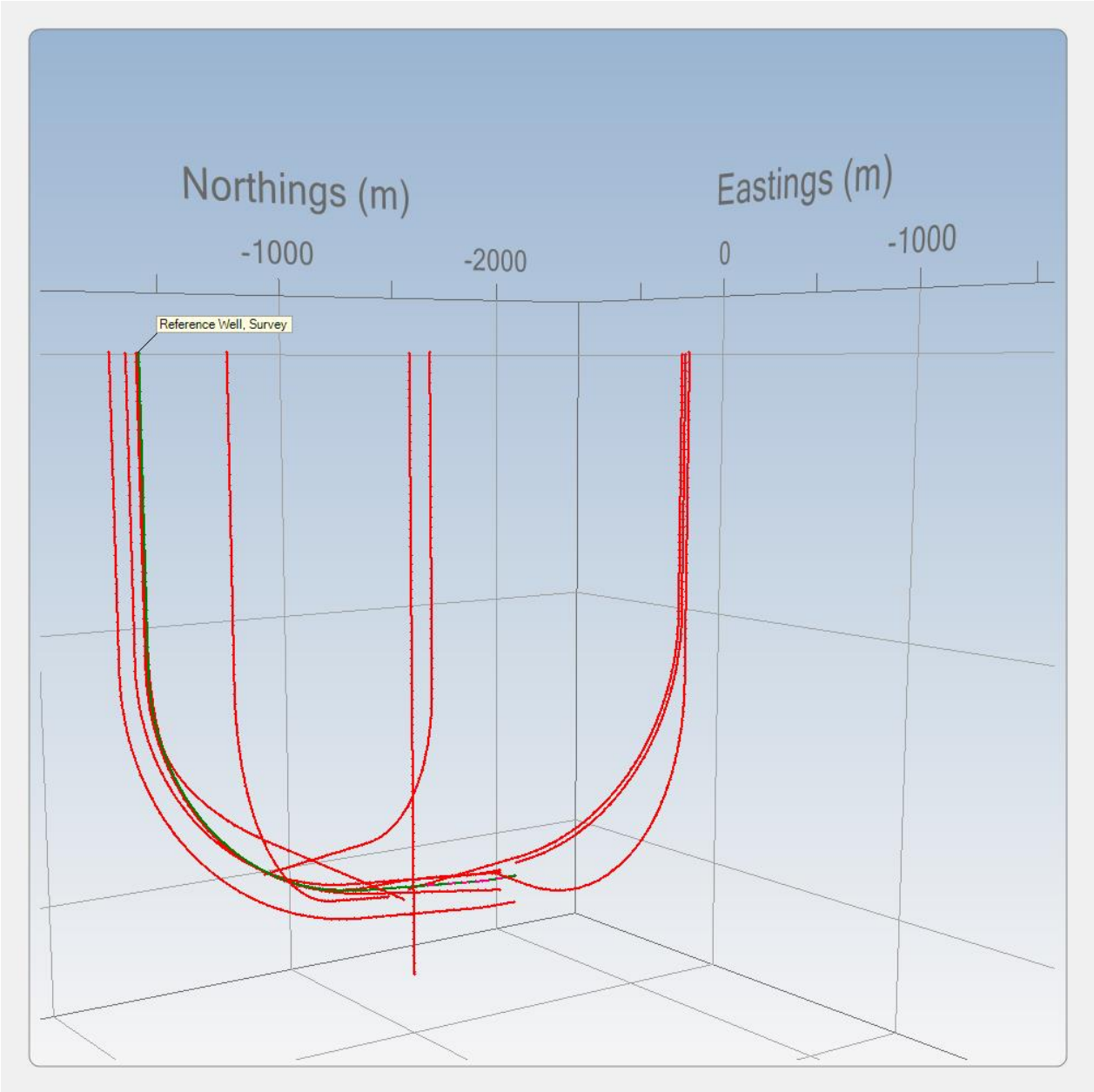

Figure 53: The Well Test Model. The complexity of the system can be recognized. Most possibilities, how a well can reach an adjacent one, are covered.